UNIVERSITÀ POLITECNICA DELLE MARCHE

DIPARTIMENTO SCIENZE DELLA VITA E DELL'AMBIENTE

Corso di Laurea Magistrale

Biologia Marina

"STYLASTERIDAE (CNIDARIA: HYDROZOA) DELL'ANTARTIDE E LORO SPUGNE ASSOCIATE"

"STYLASTERIDAE (CNIDARIA: HYDROZOA) FROM ANTARCTICA AND THEIR ASSOCIATED SPONGES"

Tesi di Laurea Magistrale di:

Carlo Vultaggio

Relatore

Chiar.mo Prof.

Stefania Puce

Correlatori

Prof. Barbara Calcinai

Dr. Camilla Roveta

Sessione Straordinaria Febbraio

Anno Accademico 2021/2022

CONTENTS

SUMMARY

La famiglia Stylasteridae Gray 1847 è una delle 112 famiglie di idrozoi appartenenti al phylum Cnidaria, che ad oggi include 328 specie e 33 generi distribuiti in tutto il mondo, fatta eccezione per l'Artico. Gli stylasteridi, comunemente conosciuti come "lace corals", sono organismi bentonici coloniali che necessitano di un substrato duro su cui stabilirsi e svilupparsi. Presentano uno scheletro calcareo, chiamato cenosteo, e colonie polimorfiche rappresentate da due differenti tipi di polipi: gastrozoidi e dattilozoidi.

Gli stylasteridi presentano un importante ruolo ecologico. Infatti, in molti ambienti, sono considerati specie strutturanti (*habitat-formers*) in quanto, grazie alla struttura tridimensionale del loro scheletro calcareo, contribuiscono ad aumentare la complessità dell'habitat, creando rifugi per una varietà di organismi, come ad esempio le spugne. Tuttavia, in letteratura, le informazioni sugli Stylasteridae e i loro epibionti sono relativamente scarse.

Scopo principale di questo lavoro è stato quello di dare un contributo per arricchire le conoscenze sulla tassonomia e l'ecologia di questi organismi. Le analisi si sono basate sull'osservazione di molteplici campioni di diverse specie di stylasteridi e dei loro epibionti, principalmente spugne, campionati in Antartide.

I campionamenti sono stati condotti nel Mare di Ross in 12 siti durante la XXXII campagna Antartica, tra Gennaio e Febbraio 2017, mediante l'utilizzo di una slitta epibentonica e un box corer, a profondità comprese tra i 432 e 1022 metri. I campioni di stylasteridi, già morti al momento del campionamento, e di spugne ad essi associate, sono stati poi trattati rispettivamente con perossido di idrogeno (35%) e acido nitrico e solforico, e successivamente identificati al minor livello tassonomico possibile attraverso osservazioni al miscroscopio elettronico a scansione (SEM), stereomicroscopio e microscopio ottico.

Lo studio tassonomico dei campioni raccolti ha condotto all'identificazione di quattro specie di stylasteridi: *Errina fissurata* (Gray, 1872)*, Errina laterorifa* Eguchi, 1964*, Errina (Errina) gracilis* von Marenzeller, 1903 e *Inferiolabiata labiata* (Moseley, 1879), e a 38 specie di spugne, di cui 9 probabilmente sono nuove specie, appartenenti a due classi di poriferi, Demospongiae Sollas, 1885 ed Hexactinellida Schmidt, 1870.

Attraverso confronti con dati di letteratura, è emerso che i nostri dati relativi alla distribuzione geografica delle specie di stylasteridi identificate, confermano quelle già osservate da altri autori, mentre per ciò che concerne le spugne, si ipotizza che i letti di stylasteridi, non siano il substrato secondario ideale per loro in quanto non rappresentano un substrato vivo o elevato, ma in

carenza di dati a riguardo, ulteriori studi necessitano per confermare le nostre ipotesi.

In conclusione, il presente studio mostra quanto poco le comunità bentoniche dell'Antartide siano studiate e quanto poco si sappia ancora sulle relazioni esistenti tra gli organismi dell'Oceano Antartico. Nel prossimo futuro, un aumento dello sforzo di campionamento e studi più approfonditi, dovrebbero essere condotti in sinergia, al fine di sostenere l'ipotesi secondo cui l'Oceano Meridionale rappresenti un hot-spot di biodiversità.

Chapter 1

1. INTRODUCTION

1.1. Stylasteridae

The family Stylasteridae Gray 1847 is one of the 112 hydrozoan families (Daly et al., 2007) including 328 species and 33 genera distributed world-wide (WoRMS, http://www.marinespecies.org/aphia.php?p=taxdetails&id=22805). Due to their hard calcareous skeleton Stylasteridae is included within the stony corals, and after scleractinians, they are the second most species-rich (15%) of calcified cnidarians (Lindner et al., 2008; Häussermann and Försterra, 2007). Because of this characteristic, they were previously inserted inside the Anthozoa, and only after detailed studies conducted by Moseley in 1881 on the soft tissues of several genera of Stylasteridae, it was definitively declared that Stylasteridae were hydrozoans and not anthozoans (Moseley, 1879; 1881). Although originally considered to be a hydroid family, lately they were classified as an order; however, after different molecular studies they are now reconsidered as a large and highly diverse family, belonging to the superfamily Hydractinoidea within the order Filifera (Cairns, 2011).

1.1.1. Biology

Stylasterids, commonly known as ‘‘lace corals’’, are fragile, usually small, uniplanar to slightly arborescent colonial hydrozoans of the phylum Cnidaria (Cairns, 2011). The Stylasteridae family specifically includes sessile, benthic organisms that need a hard substrate to develop and settle on (Cairns and Samimi Namin, 2015). Their calcareous skeleton, named coenosteum (Pica, 2012), is a synapomorphy of the family, but this feature is not unique as it is also present in the Hydroidolina: in fact, some genera of the Hydroidolina, have a calcareous skeleton (Cairns and Samimi-Namin, 2015). In addition, the colour of the coenosteum can be different: white, orange, red, pink, purple or brown (Brooke and Stone, 2007; Cairns, 2011). The surface of the coenosteum shows various textures depending on the species (figure 1): in most cases, there are microscopic bands on the surface called strips, that are separated by ridges, called slits (Cairns, 1983a). Moreover, on its surface, the coenosteum presents pores, that represent the exit of canals which run inside the skeleton and produce a complex network, linking all the peculiar structures of the colony (Ostarello, 1973; Puce et al., 2016).

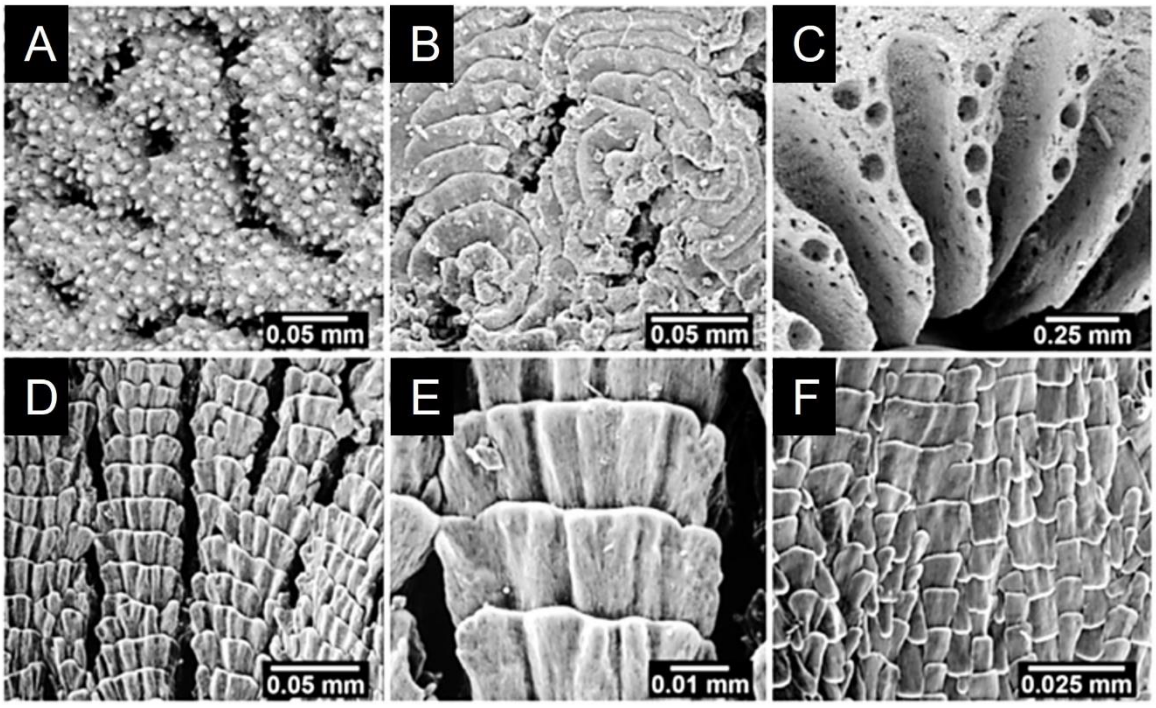

Figure 1. Aspects of Coenosteal Texture. **A**. *Stylaster verrillii*, USNM 1123299, reticulate granular coenosteal texture. **B**. *Errina sinuosa*, USNM 85131, radial-imbricate coenosteal texture. **C**. *Crypthelia trophostega*, USNM 1122887, nematopores. **D**–**E**. *Errina altispina*, USNM 71778, linear-imbricate coenosteal texture. **F**. *Systemapora ornata*, USNM 85117 contiguous alternating polarity of imbricating platelets (modified from Cairns, 2011).

The majority of stylasterid species have the coenosteum composed of aragonite, only a few species present a calcite skeleton (Broch, 1942; Cairns and Macintyre, 1992) while several species present a combination of both the two polymorphs (Pica, 2012). In this hydrozoan family the carbonatic composition of the skeleton is mostly related to the phylogenesis of the taxa rather than to the environmental conditions (Cairns and Macintyre, 1992). The general effect of temperature on the distribution of polymorphs was observed among genera. In fact, genera with a calcareous skeleton are restricted to cold

water (up to 13° C), while genera with an aragonitic coenosteum occur in waters with a wide range of temperatures (-1.5 to 30° C) (Cairns and Macintyre, 1992). Guinotte et al, in 2006, pointed out the importance of the Aragonitic Saturation Horizon (ASH) as a limiting factor in the distribution of deep-sea corals: few or no corals are present in water below the ASH because it is much more difficult to extract the calcium carbonate from the water to form the skeleton. Stylasterids have polymorphic colonies represented by two different types of polyps: gastrozooids and dactylozooids; they also include nematophores (Puce et al., 2011) and gonophores (Puce et al., 2016). Zooids generally have a small size, and they retract into tubes of different diameter, called gastropores and dactylopores. The gonophores develop inside spherical cavities named ampullae (figure 2) that are distributed on the colony surface or inside the coenosteum.

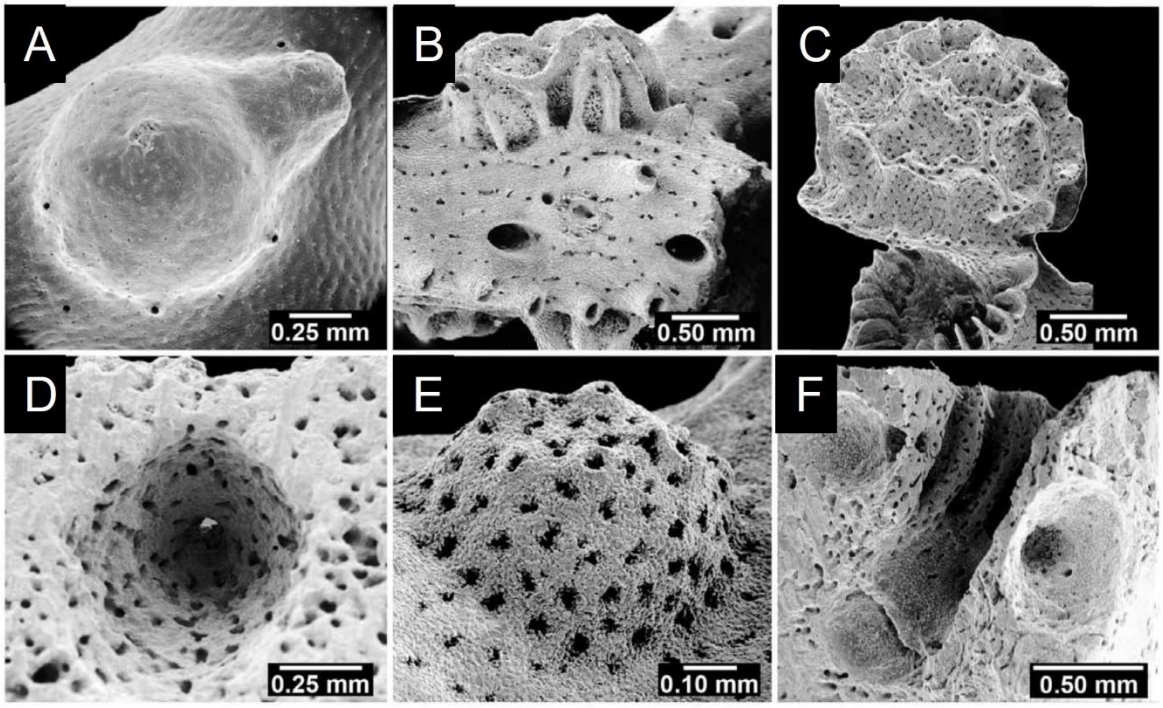

Figure 2. Aspects of Ampullae. **A**. Superficial female ampulla of *Adelopora pseudothyron*, USNM 60128, with a large lateral efferent tube. **B**. Stellate-ridged superficial female ampullae of *Distichopora anomala*, USNM 71813. **C**. Large female ampulla in cyclosistem lid of *Crypthelia lacunosa*, USNM 45684. **D**. Internal female ampulla of *Sporadopora dichotoma*, USNM 60100. **E**. Cluster of superficial male ampullae of *Stenohelia robusta*, USNM 21283. **F**. Internal male ampullae flanking a double-chambered gastropore tube of *Conopora pauciseptata*, USNM 52619 (modified from Cairns, 2011).

The coenosarcal canals usually permeate the entire skeleton linking together all these structures and forming a complex three-dimensional canal network. Gastrozooids are cylindrical polyps with a single whorl of a few short, filiform, and extensible tentacles around the apical hypostome; these polyps are specialized to feed the colony, but they are unable to catch prey by themself (Pica, 2012). On the contrary, dactylozooids are modified polyps, in which the mouth is missing, filled with nematocysts, through which they

defend the colony and catch preys: these zooids can extend their body 1-2 mm above dactylopores and, when they capture the prey, they give it to the gastrozooids that ingest and digest it (Ostarello, 1973; Brooke and Stone, 2007; Pica, 2012). Among the thirty-three stylasterid genera, gastrozooids and dactylozooids have three main types of distribution on the colony. The first type is characterized by a random distribution, in which polyps are usually dispersed in the cenosteum. The second type exhibits a distichoporin disposition which consists of an organization of the polyps in rows, usually a row of gastrozooids is flanked on both sides by a single row of dactylozooids and the row system is limited to the lateral edges of the branch. The third type shows the polyps organized into cyclosystems, where a central gastrozooid is surrounded by a single ring of dactylozooids. Sometimes the dactylozoid ring is incomplete and forms an adcauline diastema on the cenosteum (Pica, 2012). Gastropores and dactylopores have typical characteristics and structures within the various species (figure 3).

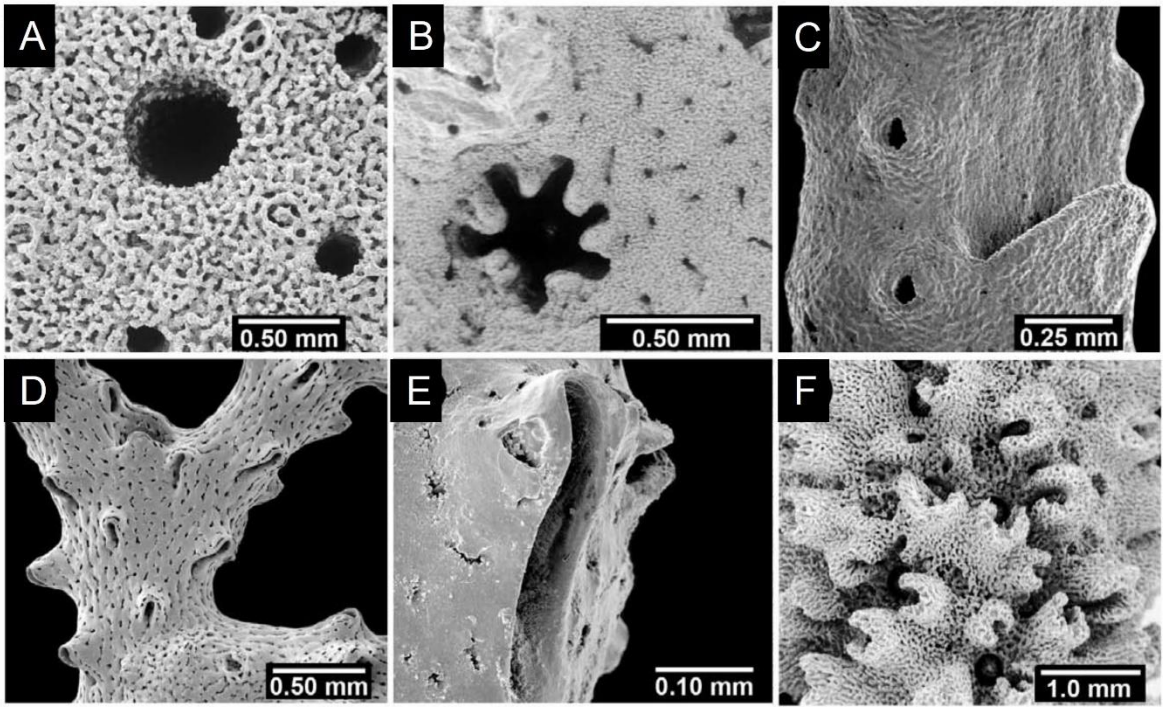

Figure 3. Aspects of Gastropores and Dactylopores. **A**. Flush gastropore of *Sporadopora dichotoma* USNM 52647, with several smaller flush dactylopores. **B**. A stellate gastropore of *Stellapora echinata*, USNM 59945. **C**. A broad abcauline gastropore lip of Lepidopora sp., BM 1890.4.11.24. **D**. Adcauline dactylopore spines of *Errina dendyi*, USNM 76302. **E**. Adcauline dactylopore spine of *Errina cheilopora*, USNM 85134. **F**. Compound dactylopore spines of *Errinopora pourtalesii*, USNM 52254, (modified from Cairns, 2011).

The gastropores in some cases have the gastrostyle inside, a vertical structure that arises from the base of the gastropore. The gastrostyle has variable forms: from lanceolate to massive and is decorated with simple or multiple spines sometimes arranged in ridges (Pica, 2012). It has been hypothesized that the gastrostyle carries a defensive function, allowing the gastrozooid to take refuge inside the tube in case of danger or presence of a predator (Cairns, 2015). Cairns (2015) observed that six genera of stylasterids do not possess

the gastrostyle in the centre of the gastropore tube. Three of these six genera have developed a double-chambered gastropore tube: chambers are separated by a constriction ring, which probably has the function of further protection from predators. Furthermore, two of these three genera have developed protective operculi, while the third genus (*Astya*) produces a protruding shelf, which protrudes into the lower gastropore tube. To cover its gastrozooids, the fourth genus, *Adelopora*, has developed movable lids. Only two genera (*Phalangopora* and *Pliobot hrus*) have no evident protective structures, and including only few species, one and six, respectively. In addition, two genera (*Leptohelia* and *Paraconopora*) have only rudimentary gastrostyles, but *Paraconopora* also has a double-chambered gastropore tube. The gastropore can have another structure, the ring palisade, that is, in the wall of the tube. It separates the lower part of the gastropore tube, with the gastrostyles, from the top which is in communication with the dactylopores and the surface (Pica, 2012; Cairns, 2015). Dactylopores may have different form, from circular to drop shape, and in some genera, they may be surrounded by well-defined spines. Dactylopore spines are of two types: conical shape with an apical opening and U-shape in cross section with a slit, called dactylotome. The dactylotome shows different orientations in different genera. It can be directed toward the apex of the colony, the abcauline dactylotomes, or toward

the base, the adcauline dactylotomes. In few species is present a dimorphism in the dactylopore spines with the presence of two kind of dactylopores. Sometimes the dactylopore spines are grouped and partially fused together forming composite dactylopore spines with multiple dactylotomes. In a cyclosystem the dactylotomes of the dactylopores are separated by pseudosepta, a little portion of coenosteum. In the genera showing a pore organisation, in cyclosystems or rows, it is also possible to detect the presence of solitary dactylopores along the colony (Pica, 2012). Exactly as the gastropores, also the dactylopores show small calcareous structures inside, named dactylostyle, usually distributed longitudinally along the dactylopore tube and they are composed by single and isolated or several partially fused elements (Ostarello, 1973). Cairns (2015) asserted that in addition to the dactylostyle, Stylasteridae can have other structures, such as dactyloridges, psudotabulae, dactyloglossae and dactylopore plugs. All these elements have the function to constrict the diameter of the dactylopore tube, being more difficult for the dactylozooids to emerge from their pores. Cairns also suggested that these structures, rather than having a protective function from possible attacks by predators, have the role of keeping the surface of the organism clean and therefore avoiding the proliferation of microscopic organisms such as coccolithophores. However, in some species, they are also

or only inside the coenosteum (internal ampullae). The external ampullae show a variety of morphology depending on the species and they usually show a sexual dimorphism between the male and female colonies of the same species. The dimorphism of the ampullae, in general, is evident not only in the morphology but also in the dimension; in fact, the female ampullae are usually larger than the male ones. The ampullae are often strictly grouped and they may be scattered along all the colony or preferentially localised in a portion of it, for example in the apex or only on one face of the colony. The gametes are released by efferent pores in the external ampullae or an efferent duct in the internal ones (Pica, 2012). Stylasteridae are gonochoric species with only two species known to be hermaphroditic, *Distichopora violacea* Pallas, 1766 (England, 1926) and *Stylaster roseus* (Pallas, 1766) (Goedbloed, 1962). The gonophores are fixed sporophores and develop within the ampullae. It is usually possible to see a dimorphism between male and female colonies, depending on the shape and size of the ampullae (Cairns, 1983b). Stylasteridae are characterized by an internal fertilization, then the egg will develop directly into a larva, called planula, which will not present the medusoid stage, and will exit from the ampullae through an efferent pore (Pica, 2012). In the male colony, within a single ampullary sac, one or many sperm cysts may be contained. The development of the gonophores of the

same colony is not synchronous as well as the cysts of the same gonophore, in fact, within an ampullary sac the cysts show a different stage of maturation. The formation of male gonophores begins when spermatozoa-morulae, traveling along the endodermis of the coenosarcal canals, occur at the end of the canal right between the ectoderm and the endoderm (England, 1926). The endodermal cells above the germ cells are modified by elongating, thus forming a supporting structure called a spadix (England, 1926; Goedbloed, 1962). This structure can be branched to support more than one sperm cyst (Pica, 2012). In some species, simultaneously with sperm maturation, the ectoderm at the apex of the cysts begins to enlarge, forming a seminal duct (Hickson, 1891; Broch, 1914; England, 1926; Goedbloed, 1962). When spermatozoa complete their development, they exit the seminal duct or cenasarcal ducts (Hickson, 1891; Broch, 1914; England, 1926; Ostarello, 1973; Goedbloed, 1962; Fritchman, 1974) but the way sperm enters the female ampulla remains unknown (Fritchman, 1974). Female gonophores contain a single egg. The oocyte migrates between the ectodermal and endodermal layers from the coenosteal canals. During the growth of the oocyte, the endoderm develops in favour of a structure called the trophodisc, which is necessary for the support and nourishment of the egg (Hickson, 1890, 1891, 1892). Initially, the trophodisc is cup-shaped positioned around

the oocyte. It then widens and divides into digitiform structures forming a more complex structure (Hickson, 1890; England,1926; Goedbloed, 1962). Inside the egg is the germinal vesicle (Hickson, 1890, 1891, 1892) in which many spherical yolk granules of different sizes are evident. When the egg is ready to be fertilized, the germinal vesicle is in the distal pole of the egg surrounded by several yolk granules much smaller than those on the other side of the egg (Hickson, 1890). After fertilization, the yolk granules lose their organization and the embryo begins to form a peripheral columnar cell layer that will form the ectoderm of the mature planula (Moseley, 1879; Hickson, 1890, 1891; England, 1926). At this stage, the trophodiscus begins to degenerate and planula growth is now supported only by internal yolk granules (Moseley, 1879). The ectoderm of the planula contains large glandular cells, it and the endoderm possess nematocysts (Fritchman, 1974). The planula exits through an opening on one side of the ampulla roof or through an opening in an adjacent gastropore (Ostarello, 1973; Fritchman, 1974). The ampulla left by the escaped planula is not wasted. They are probably used for several years and as the colony increases in diameter some are closed with calcium carbonate (Moseley, 1879; Broch, 1942; Ostarello, 1973; Fritchman, 1974). Fritchman (1974) studied the structure, metamorphosis, and development of the planula of the species *Stylantheca*

papillosa (Dall, 1884) (cited as *Allopora petrograpta*) and observed that the released planula was deposited on the substrate after a few hours (Fritchman, 1974). Ostarello (1973) observed that the planula of the species *Stylaster californicus* (Verrill, 1866) (cited as *Allopora californica*) generally wanders for a short time around the parent colony eventually settling near it. However, some new colonies arise well away from the female, demonstrating that some degree of larval dispersal prior to settlement is possible (Ostarello, 1976). The planula attaches to the substrate from the front perhaps using the secretion of glandular cells and quickly covers itself into a flat disk (Ostarello, 1973; Fritchman, 1974). However, traces of the depression where the first cyclosystem will form are also visible at this early phase (Ostarello, 1973; Fritchman, 1974). Within weeks the first cyclosystem forms and the new colony resembles a miniature volcano (Ostarello, 1973; Fritchman, 1974). Additional cyclosystems subsequently form near the first gastrozoan forming a young colony (Fritchman, 1974). In 2012 Puce et al., described the skeletal morphology of early stages of *Stylaster sp*. colonies established on artificial panels placed along a coral reef. They found that the first stage is represented by a well-developed primary cyclosystem that symmetrically buds two secondary cyclosystems at a very early stage of growth. Subsequently each cyclosystem begins its vertical growth producing new symmetrically arranged

cyclosystems. The base of the colony begins to expand producing sister colonies resulting in asexual reproduction of several colonies from a single settled planula (Puce et al, 2010). The study of the reproductive cycle of stylasterids was done by Ostarello (1973) for the species *Stylaster californicus*. This species shows a regular annual cycle of sperm and egg production, fertilization, development, and planula release. Ostarello (1973) also suggested dormancy of the gonophores, in fact small ampullae with undeveloped future sperm and eggs were found throughout the year. Brooke and Stone (2007) studied reproductive aspects of stylasterids from the Aleutian Islands. They found that all species are gonochoristic brooders with the gonophores containing mature embryos or planulae. The stage of gamete development within a single specimen are not highly synchronized; females contained both eggs and planulae, and males exhibited a range of gamete development (Brooke and Stone, 2007). These reproductive traits indicate that hydrocorals have limited potential to recolonize disturbed areas in the Aleutian Islands (Brooke and Stone, 2007).

1.1.2. Distribution and Ecology

The family Stylasteridae represents the second largest group of calcified cnidarians in terms of number of species, after the scleractinians (Cairns,

1999). Among the class Hydrozoa, Stylasteridae is the second most species-rich family distributed worldwide (Cairns, 2011), except for the Arctic region (figure 4). Stylasteridae are primarily established in deep waters where they are an important component of deep coral communities (Heifetz, 2002; Cairns, 2011). The western Pacific is the most diverse area for stylasterid corals, the western Atlantic is second in number of species, while the Mediterranean and southern Indian Ocean contain only one species of stylasterids. Stylasterids are found at various depths, from 0 to 2789 m, with a maximum concentration between 200-500 m. However, some species such as *Stylaster californicus* (Verrill, 1866) from California and *Errina antarctica* (Gray, 1872) from Chile form very dense populations even in shallow water (Ostarello, 1973; Häussermann and Försterra, 2007; Love et al, 2010). A recent phylogenetic analysis showed that stylasterid corals originated and diversified in deep water and only later invaded shallow water. Precisely four different invasions occurred, three in tropical areas, in the Caribbean and Indonesia, and one in temperate areas, in the California region (Lindner et al, 2008). The distribution pattern of stylasterids usually shows they are found primarily off small oceanic islands, seamounts, and oceanic ridges (Cairns, 1992). Based on what was said earlier, it might seem stylasterids are distributed homogeneously, but upon closer examination a general pattern

emerges. Indeed, it appears that their distribution follows plate boundaries, and they are associated with geologic hotspots (Cairns, 1978; Cairns, 1992; Rogers et al., 2007). Stylasterids have never been found in the Arctic and Mediterranean Seas, except for the Strait of Messina (Cairns, 1992; Giacobbe et al., 2007; Salvati et al., 2010; Cairns, 2011), where there is only one species, *Errina aspera* (Linnaeus, 1787), with an uneven distribution mainly due to seismic activity, strong currents, and coarse sediment deposition (Giacobbe et al., 2007; Salvati et al., 2010). Cairns (1986a; 1991; 1992) gave three possible explanations for their distribution:

1. High sensitivity to fluctuating salinity associated with fluvial discharge from large island and continental land masses;

2. High sedimentation and turbidity of water masses associated with river discharge. In fact, Stylasteridae do not occur off large rivers, such as the Amazon delta, or in basins where they discharge streams, such as the Gulf of Guinea and the Mediterranean;

3. Substrate in which these organisms develop. Generally, stylasterids prefer vertical surfaces or steep walls for settlement, however, stylasterids have also been observed on horizontal walls, such as in U-shaped channels (Häussermann and Försterra, 2007). They usually colonize hard substrates, not only rocks, but also secondary substrates, such as barnacles and dead

gorgonians (Ostarello, 1973; Häussermann and Försterra, 2007), or detritus, plastic, and glass (Gili and Hughes, 1995).

Today, the waters of the southwestern Pacific Ocean appear to have the greatest species diversity of Stylasteridae, with 57 species in the temperate portion and 45 in the tropical areas (Cairns, 2011; Cairns, 2015; Puce et al., 2016).

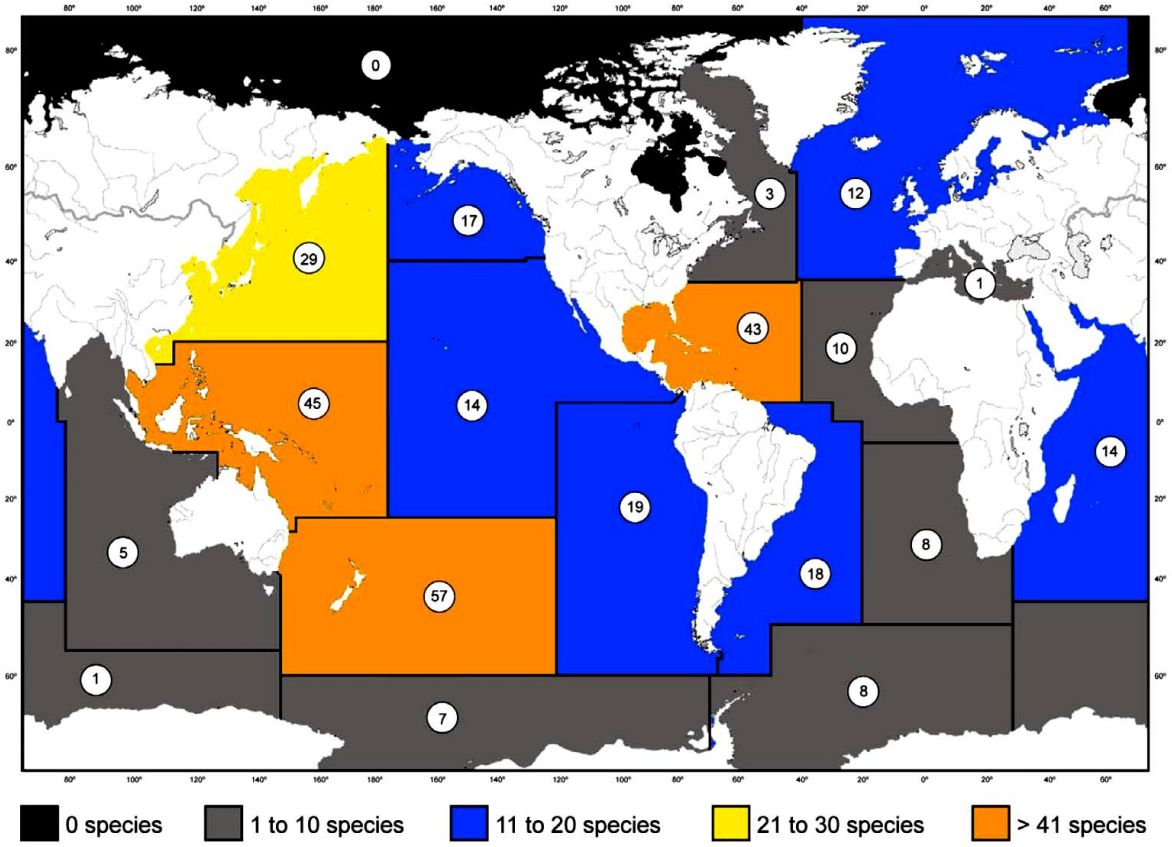

Figure 4: Number of stylasterid species present for each of the 19 FAO oceanic regions (modified from Cairns, 2011).

1.1.3. Southern Ocean distribution of stylasterid corals

Fourteen genera and thirty-three species of stylasterid corals are recorded in the Antarctic region, south of the Antarctic front at 54°S (Cairns, 1983; Cairns, 1991). There are no described stylasterids within the Arctic Circle (Cairns, 2011), and diversity in the Southern Ocean is relatively higher than in other oceans (Bax and Cairns, 2014). Stylasterids have been observed in Southern Ocean collections since the early 1800s (Stokes, 1847), and the last biogeographic summary was published in 1983 (Cairns, 1983). However, it is only in the last decade that modern remote sampling and video remote sampling techniques have allowed us to glimpse images of them in their natural habitat. The Census of Antarctic Marine Life (CAML), in collaboration with the Scientific Committee for Antarctic Research Marine Biodiversity Information Network (SCAR-MarBIN) conducted between 2005 and 2010, has provided new data on Antarctic biodiversity with new distribution records, in situ photographs, and environmental data to provide a broader view than ever before in Antarctic benthic biogeography. Despite their high occurrence in Antarctic collections, stylasterids remain a highly understudied group. A synthesis of recent records is lacking, many collections remain unidentified beyond family level, and the knowledge on stylasterid

distribution is superficial, with patchy and non-repetitive sampling across depths (Bax and Cairns, 2014).

Within the Antarctic region, four distribution patterns prevail for Antarctic stylasterids:

a. Circum-Antarctic field corals: *Errina fissurata* (Grey, 1872), *Errina laterorifa* (Eguchi, 1964), *Errina gracilis* (von Marenzeller, 1903), and *Inferiolabiata labiata* (Moseley, 1879). The recent discovery of field-like aggregations of *Errina fissurata* on the Antarctic continental shelf has emphasized the importance of the of stylasterid coral populations in the Southern Ocean (Post et al. 2010). Afterwards, an area of dense aggregations of *Errina* spp. in the Dumont d'Urville was listed as a vulnerable marine ecosystem (VME). *Errina* species are also listed as indicator taxa of VMEs through the Commission on the Conservation of Antarctic Marine Living Resources (CCAMLR 2012). These classifications recognise that the conservation of these species is crucial to maintaining regional biodiversity. *Errina fissurata* is listed by Cairns (1983) as collected in great abundance in the western Ross Sea. *E. fissurata* is normally the dominant coral component of the assemblage. However, it is invariably collected with another orange *Errina*, *Errina laterorifa*, and sometimes a white morphotype representing either

Inferiolabiata labiata, or *Errina gracilis* (Bax pers. obs.). Of these species, *E. fissurata*, *E. gracilis* and *E. laterorifa* are described as circum-Antarctic, and *E. fissurata* and *E. laterorifa* are morphologically similar and often occur in sympatry (Cairns, 1983). We now know from video transects and collections that this '*Errina* species' assortment is representative of stylasterid coral-fields in the Ross Sea and Dumont d'Urville Sea (Bax *et al.* unpublished). Although not circum-Antarctic, the coral *Errina antarctica* (Gray, 1872) from the Antarctic Peninsula, and Patagonian fjord region of South America is notable, as it has been found in extensive field-like aggregations in shallow waters (10–30 m) off the southern Chilean fjords between the Central Patagonian Zone (48°S) and Tierra del Fuego (55°S) (Häussermann & Försterra 2006).

b. Magellanic/Scotia Arc species: *Errina boschmai* (Cairns, 1983), *Crypthelia formosa* (Cairns, 1983), *Inferiolabiata lowei* (Cairns, 1983), *Lepidopora granulosa* (Cairns, 1983), *Sporadopora dichotoma* (Moseley, 1876), *Stellapora echinata* (Moseley, 1879), *Stylaster densicaulis* (Moseley, 1879), *Stylaster profundus* (Moseley, 1879), *Stylaster robustus* (Cairns, 1983). The Magellan region and adjacent areas immediately south of the of the polar front are the most species-

rich region in the Southern Ocean comprising 16 of the 33 described species. The regions of Burdwood Bank, Cape Horn, South Georgia, and Shag Rocks have particularly high levels of stylasterid diversity. The Cape Horn region examined by Waller & Robinson (2012), they found extensive aggregations of the coral *Stylaster densicaulis*. Recent collections and video surveys have also identified *Errinopsis reticulum* (Broch, 1951) in high abundance (Bax et al. unpublished, Fillinger pers. com., Waller pers. com.) at Burdwood Bank. *Errinopsis reticulum* is a large coral (up to 24 cm high and 14 cm in diameter) (Cairns 1983), which forms a three-dimensional, matrix-like sieve that often provides habitat for a diverse fauna. There are also new records of this coral near South Georgia and south of Cape Horn. However, the field-like cover appears to be limited to the Burdwood Bank, an area of high biodiversity for several Antarctic invertebrate groups Antarctic groups (Clarke & Johnson 2003). In contrast, there is only one new record for *Errina boschmai*, two new records for *Lepidopora granulosa* at Cape Horn, and no new records for *Crypthelia formosa*, *Inferiolabiata lowei*, *Stylaster robustus*, or *Stylaster profundus* after 1983. *Sporadopora dichotoma* and *Stellapora echinata* are sampled most frequently; however, no range extensions have been recorded since 1983. A new

species in the genus *Stellapora* from Burdwood Bank has been described by Bax and Cairns (Bax and Cairns, 2014).

c. Localised and potentially endemic species: *Adelopora pseudothyron* (Cairns, 1982), *Cheiloporidion pulvinatum* (Cairns, 1983), *Errina cyclopora* (Cairns, 1983), *Errinopora cestoporina* (Cairns, 1983), *Errinopsis fenestrata* (Cairns, 1983), *Errinopsis reticulum* (Broch, 1951) and *Lepidopora acrolophos* (Cairns, 1983). Seven Antarctic species are considered rare or endemic and are thus rarely sampled. *Errina cyclopora* and *Errinopora cestoporina*, are restricted to a small number of seamounts, and very few records exist for these species. *Lepidopora acrolophos* is only described from South Georgia, with new records at Burdwood Bank and Cape Horn. *Adelopora pseudothyron* has only been documented on four sub-Antarctic seamounts (Cairns 1983). *Errinopsis reticulum*, *Errinopsis fenestrata* and *Cheiloporidion pulvinatum* are also listed by Cairns (1983) as only known from their type localities. However, we now know that the range of these species is more widespread (Bax and Cairns, 2014).

d. Species endemic to or present in New Zealand waters extending into Antarctic territory include: *Calyptopora reticulata* (Boschma, 1968), *Crypthelia fragilis* (Cairns, 1983), *Crypthelia studeri* (Cairns, 1991),

Errina cheilopora (Cairns, 1983), *Errina laevigata* (Cairns, 1991), *Errina reticulata* (Cairns, 1991), *Lepidopora sarmentosa* (Boschma, 1968), *Lepidotheca inconsuta* (Cairns, 1991) and *Stylaster eguchii* (Boschma, 1966). Nine species are described from the sub-Antarctic region south of New Zealand, five are considered endemic (Cairns 1983, 1991). The Macquarie Ridge area appears to be a hot spot of stylasterid biodiversity, as all nine species are described from this Region. *Lepidopora sarmentosa* has been recorded on the Tasmanian Ridge, Macquarie Ridge, and South of the Polar Front. *Errina cheilopora* and *Stylaster eguchii* appear to form the dominant component of the Macquarie Ridge samples accounting for up to 70% of the National Institute of Water and Atmospheric Research (NIWA) stylasterid collection. *Calpytopora reticulata*, a large (~20 cm wide) fan-shaped coral has been documented in field-like accumulations off New Zealand (Schnabel pers. com.), with only a few colonies described further south along the Macquarie Ridge (Bax and Cairns, 2014).

1.1.4. Epibiosis

Many stylasterid corals, like their shallow-water largely scleractinian counterparts (e.g., Patton, 1994; Stella et al., 2011; Hoeksema et al., 2012),

are considered habitat-forming species because they contribute to the structuring of deep and shallow water coral banks (Roberts et al., 2006; Häussermann and Försterra, 2007). In this context the tridimensional structure of their calcareous skeleton should enhance the complexity of the habitat, by creating refuges for a variety of mobile and sessile organisms (Braga-Henriques et al., 2010). In fact they can be considered as basibionts for many other invertebrate such as annelids, anthozoans, cirripeds, copepods, cyanobacteria, echinoderms, gastropods, hydroids and sponges (Zibrowius, 1981; Braga-Henriques et al., 2010; Goud and Hoeksema, 2001; Pica et al., 2012; Puce et al., 2009). Species of the gastropod *Pedicularia*, considered obligate symbionts of Stylasteridae, usually assume the colour of the host colony and modify the branch coral surface where they reside (Zibrowius, 1981; Goud and Hoeksema, 2001; Cairns and Zibrowius, 2013). Other organisms induce changes in the coral morphology and growth, like copepods that induce the formation of a gall on the coral branches (Zibrowius, 1981; Buhl-Mortensen and Mortensen, 2004a), and balanomorphs or acorn barnacles (Zibrowius, 1981), which usually are completely covered by the coral coenosteum. The presence of polychaetes on stylasterid colonies seems to occur in about 30% of the stylasterid species and frequently induces pronounced changes in the growth form and branching pattern in many

species. For example, in *Inferiolabiata labiata* (Moseley, 1879) the polynoid *Polyeunoa laevis* McIntosh, 1885 induces modifications in the growing branches prior to the production of a reticulate tube in which the worm travels (Cairns, 1983a). Those epibionts probably receive protection from predators, and also access to food is increased due to the tridimensional shape of the colonies (Braga-Henriques et al., 2010). More recently, several invertebrates, such as sponges, were observed attached to both dead and living sections of *Errina dabneyi* skeletons (Braga-Henriques et al. 2010). Despite the local abundance of stylasterid corals and the wide number of species associated with them, until now no specific studies have been dedicated to the diversity of sponges etching their coenosteum (Pica et al., 2012). To date only five sponge species have been occasionally recorded in association with stylasterid hydrozoans. *Alectona microspiculata* (Bavestrello, Calcinai, Cerrano & Sarà, 1998) was found in the inner part of the stem of *Distichopora* sp. (Bavestrello et al., 1998), *Diplastrella spiniglobata* (Carter, 1879), *Alectona wallichii* (Carter, 1874) and *Samus anonyma* (Gray, 1867) over the stem of *Stylaster sanguineus* (Milne Edwards & Haime, 1850) and an unidentified hadromerid sponge was documented inside the basal portion of a colony of *E. dabneyi* (Wisshak et al., 2009).

Although several boring sponges can bore a large spectrum of carbonatic structures, in some cases more specific co-evolving relationships are recorded (Pica et al., 2012). For example, the association between the species belonging to the genus *Spiroxya* and precious corals (*Corallium* and *Paracorallium*) is particularly strong in six out of nine species of the genus excavating in this substratum. This relationship was probably established before the separation of the Tethys Sea, as demonstrated by the relic distribution that the genus *Corallium* shares with the genus *Spiroxya* (Calcinai et al., 2008). The specific relationships between boring sponges and these octocorals are probably driven by: (1) the peculiar size and shape of the calcite crystals building their skeleton, (2) the high amount of proteinaceous matrix mixed with the inorganic fraction of the skeleton, and (3) by the external living coenenchyma limiting the attack of the most boring sponge species (Allemand et al., 1994; Cortesogno et al., 1999; Calcinai et al., 2008). In the latter case the way of penetration of sponges is not completely clarified but it is believed that they are not able to penetrate through the living coenenchyme. It has been therefore hypothesised that the penetration of sponges in the precious coral scleraxis starts from dead portions of the colonies or from the underneath substratum (Calcinai et al. 2008).

Similarly to precious corals, stylasterid corals have a massive calcareous skeleton covered by a living epithelium but the coenosteum is also completely pervaded by a dense three-dimensional network of living stolons (Puce et al., 2011). Polyps (gastrozooids, dactylozooids and nematophores) are lodged in the larger canals, while the smaller ones contain the coenosarc. All these structures are visible, on the coral surface, as round pores of different size (Cairns, 2011). In this case, boring sponges attacking these organisms have not only to overcome the superficial living tissue, but also, to interact with the canal network of living tissue (Pica et al., 2012).

1.1.5. Threats

Anthropogenic impacts in the marine environment continue to increase when the risks of extinction and extirpation remain unknown for many species and populations. The vulnerability of stylasterid corals to human impacts is due to some of their characteristics, as patchy distributions, slow growth, long generation times, low natural mortality rates and short-distance dispersal of larvae (Miller et al., 2004; Brook and Stone, 2007; Cairns, 2011; Di Camillo et al., 2017).

Marine protected areas (MPAs) are an increasingly common tool used globally to protect marine environments and species (Agardy, 1994). They

can: (1) be effective harvest refugia for commercial species (Castilla and Duran, 1985; Roberts, 1995; Bohnsack, 1998; Babcock et al., 1999; Mosquera et al., 2000), (2) act as sources to re-seed impacted populations through spillover effects (Russ and Alcala, 1996; Cole et al., 2000; McClanahan and Mangi, 2000) and (3) conserve important biological and social resources (Bernal et al., 1999; Badalamenti et al., 2000). However, controversy surrounds the potential negative effects of MPAs, particularly where designation of reserves in biologically rich or unique areas may lead to accelerate environmental degradation of the very resource that the reserve was set up to protect (Jones et al., 1993). This disparity is particularly evident in the damaging effect of scuba diving on benthic communities, as divers are increasingly attracted to marine reserves that have high diversity, spectacular scenery, and abundant fish populations (Tilmant and Schmahl, 1981; Davis et al., 1995; Sala et al., 1996; Harriott et al., 1997; Rouphael and Inglis, 1997; Plathong et al., 2000; Zakai and Chadwick-Furman, 2002). For benthic, modular marine organisms such as corals, which are often the dominant habitat-forming species in marine ecosystems, even sub-lethal damage from divers may have profound impacts. In a worst-case scenario, if diver damage is biased towards the typically less-abundant large colonies (Grigg, 1977; Hughes and Jackson, 1980; Grange and Singleton, 1988; Babcock, 1991; Bak

and Meesters, 1998), then reproductive output of a population may decline dramatically, as observed by Miller et al. (2004) for *Errina novaezelandiae* Hickson, 1912 in the Te Awaatu Marine Reserve. Another important threat to their survival is the indiscriminate collection of colonies. In fact, all the species belonging to the Stylasteridae family, are placed in the CITES Appendix II since 1990, which regulates the trade of these taxa across international borders (CITES, 1975; Häussermann and Försterra, 2007; Cairns, 2011). An example is *Stylaster californicus* (Verrill,1866), known from relatively shallow water (0-110 m) from San Francisco to Baja California: in the early 1970's this species was collected and sold for up to $150 and manufactured into jewellery. While *S. californicus* has a rather porous corallum, which is not amenable to cutting, carving, and polishing, other stylasterids, such as *Stylaster corallium* (Cairns, 1986), which has a hard and colourful coenosteum like that of *Corallium* spp. (Cairns, 2011). Some of the South African stylasterids were once commercially harvested on a very limited scale to use as decorative objects, such as *Stylaster blatteus* (Boschma, 1961) from the tropical areas of West Africa, which was harvested as "akori" (typical ornamental object of the region). It is known that 382 kg of *Allopora* (probably *Stylaster nobilis*) was legally taken from Struis Bay to Quoia Point in 1991 (Cairns and Zibrowius, 2013).

In the Southern Ocean, both longline and bottom trawl fisheries are regulated by CCAMLR and the Protocol on Environmental Protection to the Antarctic Treaty (The Madrid Protocol), which allow mid-water trawls and long line fisheries to < 550 m, whilst the deep-sea bottom trawling is allowed only for scientific purposes. Nevertheless, trawl fishing was used till the '90s for the mackerel ice fishery (Bax, 2014). The main problem of trawl fishery is represented by the bycatch. A wide range of invertebrate taxa were recorded in the benthic bycatch, such as: crustaceans, polynoid polychaetes, bryozoans, fish, and cephalopods. However, the main invertebrate groups are represented by Asteroidea, Holothuroidea, Galatheidae, Ophiuroidea and corals, as Stylasteridae, Stolonifera, Gorgonacea, Scleractinia and Antipatharia (Probert et al., 1997). Regarding bottom drilling, the practice is mainly executed for the hydrocarbon extraction. This is dangerous for cold-water coral ecosystems because it can cause their suffocation, due to the great amount of sediment hoisted from the bottom, and the destruction of populations, determined by the multiple perforations of the area. Then, the extraction activity can cause local extinctions, mainly on seamounts, because they are characterized by a great number of endemic species (Roberts et al., 2006).

Perhaps, the most insidious threat is represented by ocean acidification, particularly for cold-water communities. An important role is played by the

increase of carbon dioxide (CO2) level in the atmosphere; this is due to anthropic and non-anthropic emissions, causing the ocean uptake (Guinotte et al., 2006; Thresher et al., 2011; Bax, 2014). The growth of CO_2 concentration into the water determines a reduction of carbonate ions (CO_3^{2-}), available for the formation of biogenic calcium carbonate, because they are necessary to plug the increasing of hydrogen ions (H^+), released by the previous reaction between CO_2 and water (Thresher et al., 2011). However, high CO_2 concentrations cannot be tamponed by the carbonate system, so an increasing of the oceanic H^+ concentration occurred, and it is still recorded, consequently determining a reduction of the general pH of the water (Guinotte and Fabry, 2008). Those changes have significant consequences for the various marine taxa, particularly for the organisms which build skeleton, shells, or other structures in biogenic calcium carbonate, both calcitic or aragonitic (Guinotte and Fabry, 2008; Thresher et al., 2011). Recent studies predicted that tropical corals calcification will be reduced more than the 54% if the CO_2 concentration should redouble (Roberts, 2006). The depth of aragonite and calcite saturation horizon (SH) are important for calcifying organisms, such as corals, because the horizons depth determine the limit at which the precipitation of biogenic calcium carbonate is promoted (shallower that the SH) and the limit at which the dissolution occurs (deeper than the SH)

(Guinotte et al., 2006; Guinotte and Fabry, 2008). The aragonite and calcite saturation horizons of the world's oceans are moving to shallower depths due to the rapid influx of anthropogenic CO_2 to the oceans. This process has been well documented and modelled at a global scale (Guinotte and Fabry, 2008). It is known that the 70% circa of deep-water coral reefs already is below the ASH, in fact the 15% of Scleractinia live at major depths (Guinotte et al., 2006), and around the 2100 the horizon will not exist anymore. Furthermore, it is estimated that, thanks to the higher solubility of CO_2 in cold waters, Antarctica will be the most affected region in the world by the acidification process (Guinotte and Fabry, 2008). In addition to human activities, in cold seas there are also natural causes which determine corals death, the main of them is the ice scour. In Antarctica, damages caused by this phenomenon are recorded at considerable depths (around 400 m), determining the destruction of entire communities. This kind of damage regulates the diversity of Antarctic benthos; however, global warming is expected to increase as already observed in recent years with the collapse of the Larson ice shelf in 1995 and 2002 and of the Mertz glacier calving in 2010 in the eastern part of the continent. Iceberg scour, and anthropogenic influences remove or damage fragile coral skeletons, eliminate substrate suitable for larval settlement and

allow more competitive taxa to colonise the available space, damaging less competitive species as Stylasteridae (Bax, 2014).

1.2. Aim of the study

In the literature, information on Stylasteridae and their epibionts is relatively scarce. The main purpose of this work is to give a contribution to enrich the knowledge on the taxonomy and ecology of these organisms. Analyses were based on the observation of several samples of different stylasterid species and their epibionts, mainly sponges, from the Antarctic Ocean with the aim of recognizing species and performing a taxonomic study. Species have been observed and analysed using the stereomicroscope, light microscope, and the Scanning Electron Microscope (SEM), that allowed a better view of the morphological characters of stylasterids and their sponges, fundamental for the recognition of species.

Chapter 2

2. MATERIALS AND METHODS

2.1. Study area

The study was carried out in January and February 2017 in the Ross Sea (75°S - 175°W Antarctica), between 432 and 1022 water, during the XXXII Antarctic campaign on board R/V Italica in the framework of the PNRA research program GRACEFUL (PNRA16_00069). Three sites, on the Western and Northern edge of the Ross Sea continental shelf, were carefully investigated and sampled: Iselin Bank, Cape Hallett Canyon and Hallett Ridge, together with various unknown stations, numbered from 1 to 9 (figure 5 and 6). The position of each site was recorded using a GPS.

2.2. Samples collection

Sampling of stylasterids was performed using an epibenthic sledge (width = 150 cm; depth =120 cm; height = 50 cm) equipped with a two-mesh net with different sizes: a 20 mm square mesh on the front, 5 mm on the back. Some of the specimens were opportunistically taken from a 52-l box-corer used by other research groups on-board the same research vessel, which were not interested in the benthos present on top of their sediment samples. All samples were then carefully described and documented photographically,

classified, preserved in ethanol, and stored at +4°C. At the end of the Antarctic campaign, they were routed to Italy and delivered to the Italian National Antarctic Museum (MNA, Genova Section, Italy), where they are now permanently preserved and cared for. All the specimens collected during the campaign were marked by the code GRC “number” and MNA “number”.

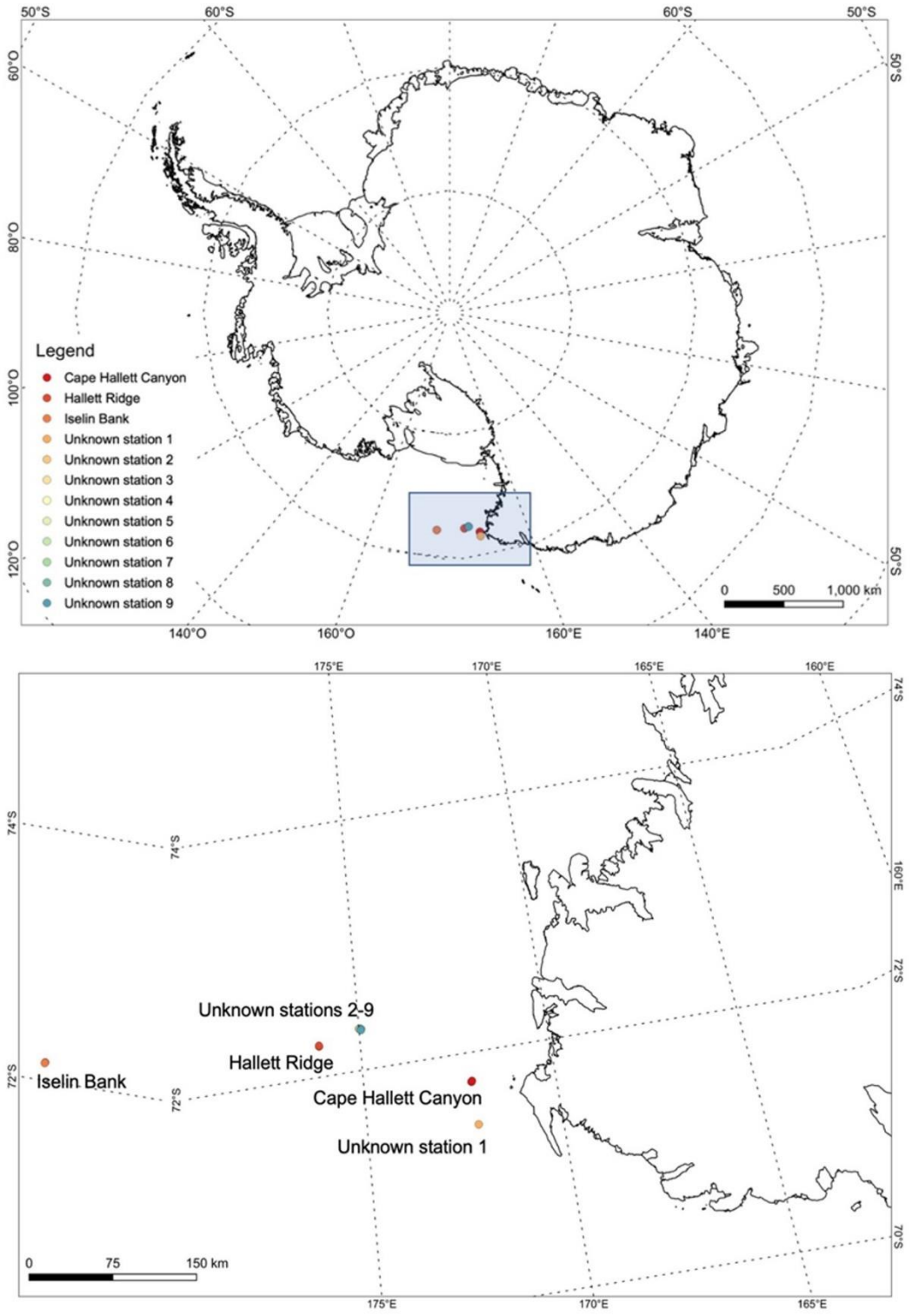

Figure 5: map of the 12 sampling sites in the Ross Sea.

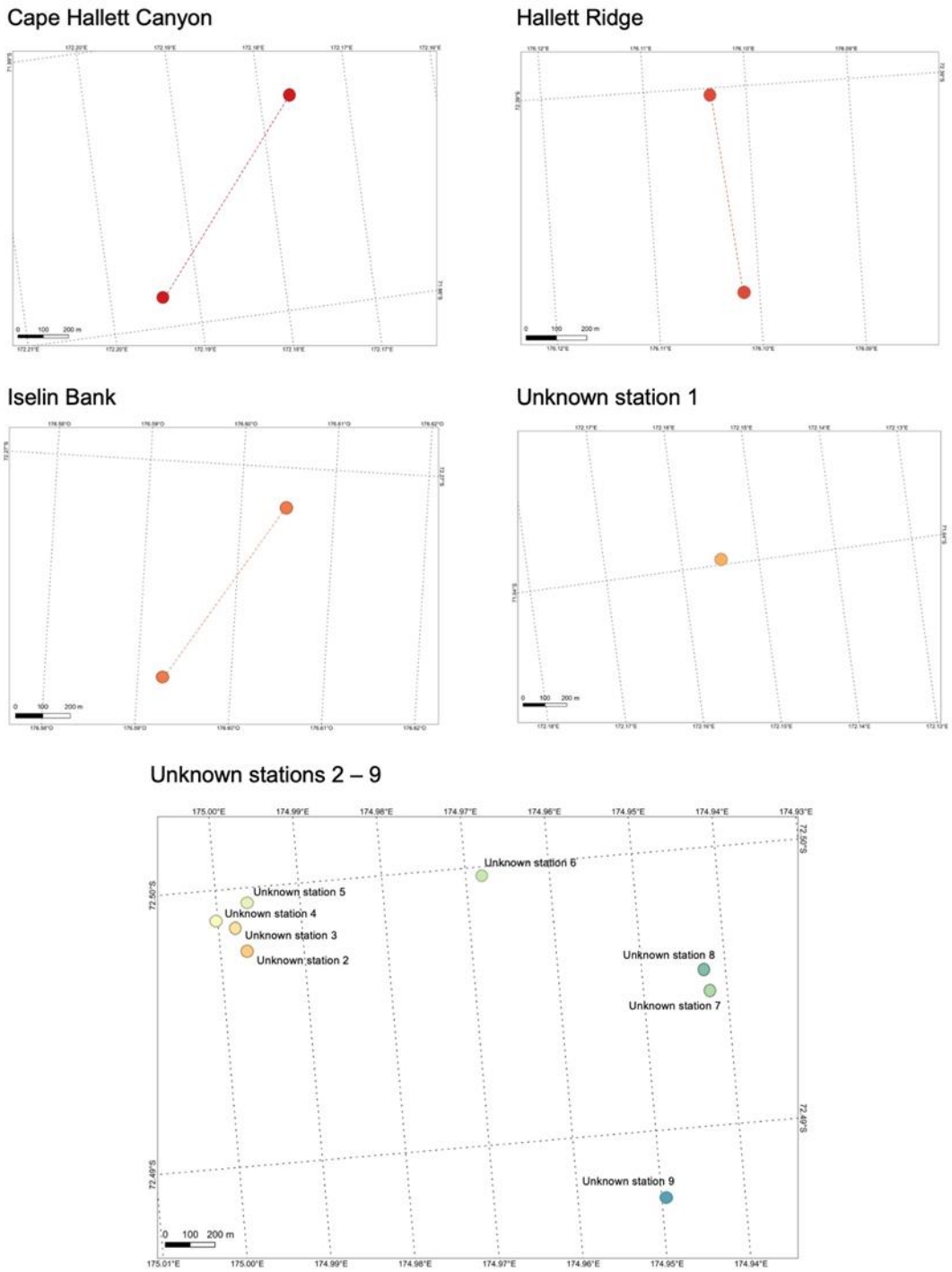

Figure 6: Sampling of stylasterids performed using an epibenthic sledge in Cape Hallett Canyon, Hallett Ridge and Iselin Bank, whereas sampling at unknown stations (1 - 9) were performed using a box-corer.

Video footage and images of the seabed were acquired with a depth camera attached to a Rosette system that was dragged for few minutes at 550 m water depth along the sites. From videos, it was possible to observe that the regions of the seabed analysed, are characterized by extensive deposits of skeletons of dead stylasterids lying on the muddy bottom, and by few living colonies, represented mainly by short branches. The massive presence of dead stylasterids deposited on the bottom gives rise to a thick and hard secondary substrate at all three sites, suggesting that this is a common bottom structure.

2.3. Laboratory analysis

Analysis of morphological characters of stylasterids

Stylasterid specimens were observed to assess their morphological characters in order to conduct a taxonomic study. A distinction between colonies and fragments was made: 'colonies' were considered the specimens where it was recognizable the basal part that was attached to the substrate, while specimens without basal part were considered 'fragments'. Subsequently, all the specimens were observed under the stereomicroscope to be sorted into different bags, on the basis of similar morphological characteristics. From each bag, the most representative samples were selected and photographed with a metric reference and a label with the corresponding code. The selected

samples were prepared for the observation at scanning electron microscope (SEM). Samples were washed under hood through the use of hydrogen peroxide (35%), to remove the organic matter present on their surface, rinsed with distilled water and left dry for about 24 hours. After the washing procedure, small portions were cut, filed with a grinder where necessary to study the internal structures, and placed on aluminium stubs. Specimens were then coated with gold–palladium in a Blazer Union evaporator and examined with a Philips XL20 SEM.

Measurements of morphological characters of SEM pictures were made using the free software ImageJ (Rasband, 1997-2011). Fifteen measurements were taken for each morphological character of taxonomic relevance and reported as: smallest measurement - (mean ± standard deviation) - largest measurement.

Morphological analysis of epibiotic sponge species

The taxonomic analysis of the spicules obtained from the sponge species identified on the samples of the stylasterid *Inferiolabiata labiata*, was carried out using four different protocols:

1. Temporary spicule preparation using glass slides with sodium hypochlorite for optical microscope study.

A small portion of the sample was taken and placed on a glass slide and then drops of sodium hypochlorite were added to dissolve the organic matter, for five minutes. With a needle the foam formed during the dissolution of the organic matter was removed. Distilled water was then added to better distribute the spicules and clean the preparation. Finally, the extracted spicules were placed on a glass slide and observed under the light of the optical microscope.

This procedure is ideal not to lose rare spicules and/or microscleres, considered as mandatory for calcareous sponges.

2. Permanent spicule preparation using glass slides with nitric acid for optical microscope study.

Ideal for not losing rare spicules and microscleres; only for siliceous sponges.

A small portion of the sample was taken and placed on a glass slide and then under an extractor hood, drops of nitric acid were added. Using a tong, the sample was allowed to boil under a flame to dissolve the organic matter. In some samples, this step was repeated several times to be sure to dissolve most or all the organic matter. Slides were allowed to cool and then drops of ethanol were added and passed over the flame again. Once the slides were

dry, drops of mounting medium were added and slides were covered with a cover glass.

Ideal not to lose rare spicules and/or microscleres, applied only for siliceous sponges.

Once slides were prepared following the two mentioned protocols, they were visualized under a Zeiss Axioplan 2 light microscope to identify the species and get morphometric data. To this purpose, measurements were obtained from 15 measurements for each spicule type and reported as: smallest length - (mean ± - standard deviation) - largest length x smallest width - (mean ± - standard deviation) - largest width.

3. A protocol for the preparation of the skeleton (mineral skeleton) was used in order to specifically analyse the organization of the spicules.

Using a scalpel, tangential and perpendicular sections were made as thin as possible. Sections were placed on a glass slide and then drops of tissue clearing agent were added. For very pigmented and dark samples, the sections were left on the slide for about half a day, covered by the clearing agent (Bio Clear, Bio-Optica). After this process was completed, the slide was closed with the cover glass and the mounting medium. In many cases it was not

possible to conduct a skeletal analysis due to the small size of the samples making impossible to obtain skeletal sections.

4. Permanent spicule preparation using test tubes with nitric and sulphuric acid for SEM study (von Stosch, 1974 modified).

A small portion of samples was taken and placed inside a glass test tube. Subsequently, under an extractor hood, nitric acid and sulphuric acid were added at a volume ratio of 1:4 respectively. Test tubes were filled for approximately three quarters of their volume with acids, then left in a bain-marie, in heated bath for about 24 hours, allowing the tissue to be digested and spicules to settle to the bottom. After removing the supernatant, distilled water was added, and tubes placed in a centrifuge for 5 minutes at 1000 *rpm*. At the end of the centrifugation, the supernatant was removed. This step was repeated about three times for each sample, in order to clean the spicules from the acids. After the last centrifugation, the supernatant was removed and, 90% ethanol added and left for approximately 30 minutes, to leave the time to spicules to settle to the bottom of the tube. At the end of this step, approximately three quarters of ethanol was removed from each test tube, leaving only one quarter at the bottom. The spicules deposited and the remaining ethanol were removed using a pasteur pipette and placed on a cover glass set on a dryer to accelerate the process of evaporation of the ethanol and

the fixing of the spicules on the cover glass. The latter was then placed on the stub and subsequently coated with gold–palladium in order to visualise the spicules through the scanning electron microscope (SEM).

This procedure is ideal for obtain clean preparations.

2.4. Sponge epibiosis

To assess the size, percentage of sponge cover and density of specimens present on the surface of stylasterids, each sample belonging to the species *Inferiolabiata labiata* (Moseley, 1879) was photographed together with the epibiontic sponges. Due to the uniplanar growth of these corals, both surfaces of each colony were photographed and measured using ImageJ software (Rasband, 1997-2011) (figure 7 A). In the same way, the size of each sponge sample was measured (figure 7 B). From the size data, it was then possible to assess the percentage of sponge coverage and also the sponge density, understood as individuals per cm^2 of *I. labiata*.

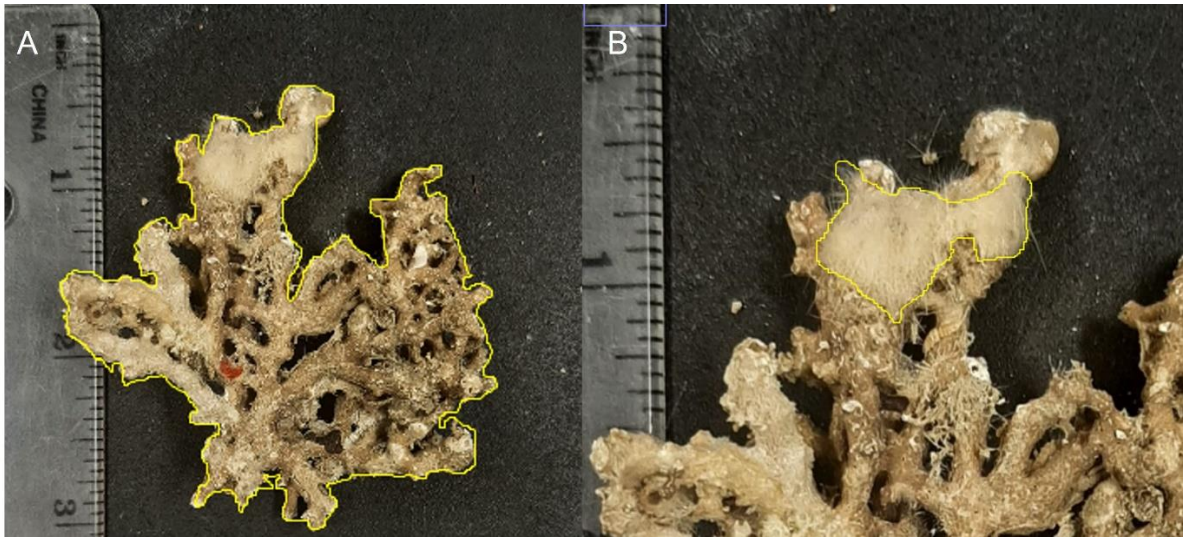

Figure 7. **A**: Measurement of an *Inferiolabiata labiata* fragment surface obtained using imageJ software (Rasband, 1997-2011). **B**: Measurement of a sponge surface obtained using imageJ software (Rasband, 1997-2011).

Chapter 3

3. RESULTS

3.1. Part 1. Stylasteridae

Out of a total of 2688 stylasterid samples analysed (table s. 1), 14 colonies and 2674 fragments were detected with a total of 4 species identified: *Errina fissurata* Gray, 1872, *Errina laterorifa* Eguchi, 1964, *Errina gracilis* von Marenzeller, 1903 and *Inferiolabiata labiata* (Moseley, 1879). Among samples, the most abundant species was *E. laterorifa* representing the 52% of the collected specimens (5 colonies and 1400 fragments) followed by *E. fissurata* representing the 32% (6 colonies and 847 fragments). *I. labiata* represented the 10% of the specimens (2 colonies and 276 fragments) while *E. gracilis* represented the 1% (1 colony and 20 fragments). Of the total fragments, 5% (136 broken branches) could not be classified as species due to the obvious damaged state and loss of taxonomic characters.

3.1.1. Systematic

Phylum Cnidaria

Class Hydrozoa Owen, 1843

Subclass Hydroidolina Collins & Marques, 2004

Order Anthoathecata Cornelius, 1992

Suborder Filifera Kühn, 1913

Family Stylasteridae Gray, 1847

Genus *Errina* Gray, 1835

Diagnosis. Gastropores and dactylopores randomly distributed in almost all species observed. Coenosteal texture reticulate-granular and linear-imbricate. Lower gastropore lip present in some specimens. Gastrostyles present but ring palisade usually absent. Dactylopore spines represented by up to two types and varying in shape and dimension. Dactylopore spines with a primarily adcauline dactylotome. Dactylostyles rarely present. Ampullae superficial and deep.

Discussion. The genus *Errina* includes 25 Recent species and one extinct species (Cairns 2014).

Type species. *Millepora aspera* Linnaeus, 1767.

Depth range. 6–1772 m.

Distribution. North Atlantic, Mediterranean Sea, Galápagos, South Africa,

Antarctica and Sub-Antarctic area, New Zealand, Japan, and Tristan da Cunha Archipelago.

Errina fissurata (Gray, 1872)

Madrepora fissurata Stokes 1847: 336
Errina fissurata Gray 1872: 745; Moseley 1879: 479; 1881: 84; Boschma 1957: 53; 1964: 284;
Boschma and Lowe 1969: 15; Cairns 1983a: 89.
Labiopora fissurata Hickson 1912: 878.
Errina (Eu-Errina) fissurata Broch 1942: 38.
Errina (Eu-Errina) antarctica Broch 1951: 35 (part of material from sta. 1948).
Errina (Errina) fissurata Boschma 1963: 337; Cairns 1983a: 89.
Errina antarctica Boschma 1966: 109 (part of material from sta. 30).

Material studied:

Table 1: list of observed specimens of *Errina fissurata* with additionally information.

Specimen code	Preservation	Station	Latitude	Longitude	Depth (m)
GRC-08-024 A	Dry	Cape Hallett Canyon	71° 58.8666' S 71° 59.2512' S	172° 11.6298' E 172° 10.6020' E	750
GRC-08-022 A	Dry	Cape Hallett Canyon	71° 58.8666' S 71° 59.2512' S	172° 11.6298' E 172° 10.6020' E	750
GRC-08-067	Dry	Cape Hallett Canyon	71° 58.8666' S 71° 59.2512' S	172° 11.6298' E 172° 10.6020' E	750
GRC-08-083	Dry	Cape Hallett Canyon	71° 58.8666' S 71° 59.2512' S	172° 11.6298' E 172° 10.6020' E	750
GRC-08-079	Dry	Cape Hallett Canyon	71° 58.8666' S 71° 59.2512' S	172° 11.6298' E 172° 10.6020' E	750
GRC-C2-T2-R2-008	Dry	\	72° 29.8692' S \	174° 59.7984' E \	434
GRC-08-092	Dry	Cape Hallett Canyon	71° 58.8666' S 71° 59.2512' S	172° 11.6298' E 172° 10.6020' E	750
GRC-02-109	Dry	Iselin Bank	72° 16.1196' S 72° 15.7728' S	176° 36.2814' W 176° 35.5638' W	670
GRC-C2-R4-003	Dry	\	72° 29.9826' S \	174° 58.0728' E \	434
GRC-02-036 MNA9276	Dry Alcohol	Iselin Bank	72° 16.1196' S 72° 15.7728' S	176° 36.2814' W 176° 35.5638' W	670

GRC-TR17-005	Dry	\	71° 38.4132' S \	172° 09.3048' E \	1022
GRC-C2-R4-011 A	Dry	\	72° 29.9826' S \	174° 58.0728' E \	434
GRC-C2-T2-R5-002	Dry	\	72° 29.9130' S \	174° 59.8812' E \	433
GRC-C2-R4-005 A	Dry	\	72° 29.9826' S \	174° 58.0728' E \	434
GRC-02-033 MNA9273	Dry Alcohol	Iselin Bank	72° 16.1196' S 72° 15.7728' S	176° 36.2814' W 176° 35.5638' W	670
GRC-C2-T2-R1-002	Dry	\	72° 29.9352' S \	175° 00.0018' E \	434
GRC-C2-R4-001 MNA9280	Dry Alcohol	\	72° 29.9826' S \	174° 58.0728' E \	434
GRC-08-050 MNA9214	Dry Alcohol	Cape Hallett Canyon	71° 58.8666' S 71° 59.2512' S	172° 11.6298' E 172° 10.6020' E	750
GRC-TR17-004	Dry	\	71° 38.4132' S \	172° 09.3048' E \	1022
GRC-02-032 MNA9275	Dry Alcohol	Iselin Bank	72° 16.1196' S 72° 15.7728' S	176° 36.2814' W 176° 35.5638' W	670
GRC-08-086	Dry	Cape Hallett Canyon	71° 58.8666' S 71° 59.2512' S	172° 11.6298' E 172° 10.6020' E	750
GRC-02-034 MNA9254	Dry Alcohol	Iselin Bank	72° 16.1196' S 72° 15.7728' S	176° 36.2814' W 176° 35.5638' W	670
GRC-02-030 MNA9253	Dry Alcohol	Iselin Bank	72° 16.1196' S 72° 15.7728' S	176° 36.2814' W 176° 35.5638' W	670
GRC-C2-R4-004 MNA9282	Dry Alcohol	\	72° 29.9826' S \	174° 58.0728' E \	434
GRC-C2-R1-003 MNA9279	Dry Alcohol	\	72° 29.9700' S \	174° 59.7822' E \	434
GRC-02-031 MNA9252	Dry Alcohol	Iselin Bank	72° 16.1196' S 72° 15.7728' S	176° 36.2814' W 176° 35.5638' W	670
GRC-02-029 MNA9272	Dry Alcohol	Iselin Bank	72° 16.1196' S 72° 15.7728' S	176° 36.2814' W 176° 35.5638' W	670
GRC-02-028 MNA9256	Dry Alcohol	Iselin Bank	72° 16.1196' S 72° 15.7728' S	176° 36.2814' W 176° 35.5638' W	670

GRC-08-004 MNA9222 A	Dry Alcohol	Cape Hallett Canyon	71° 58.8666' S 71° 59.2512' S	172° 11.6298' E 172° 10.6020' E	750
GRC-08-001 MNA9227 A	Dry Alcohol	Cape Hallett Canyon	71° 58.8666' S 71° 59.2512' S	172° 11.6298' E 172° 10.6020' E	750
GRC-02-128	Dry	Iselin Bank	72° 16.1196' S 72° 15.7728' S	176° 36.2814' W 176° 35.5638' W	670
GRC-02-184	Dry	Iselin Bank	72° 16.1196' S 72° 15.7728' S	176° 36.2814' W 176° 35.5638' W	670
GRC-C2-T2-R2-002	Dry	\	72° 29.8692' S \	174° 59.7984' E \	434
GRC-08-025 A	Dry	Cape Hallett Canyon	71° 58.8666' S 71° 59.2512' S	172° 11.6298' E 172° 10.6020' E	750
GRC-08-080	Dry	Cape Hallett Canyon	71° 58.8666' S 71° 59.2512' S	172° 11.6298' E 172° 10.6020' E	750
GRC-08-081	Dry	Cape Hallett Canyon	71° 58.8666' S 71° 59.2512' S	172° 11.6298' E 172° 10.6020' E	750
GRC-08-082	Dry	Cape Hallett Canyon	71° 58.8666' S 71° 59.2512' S	172° 11.6298' E 172° 10.6020' E	750
GRC-08-084	Dry	Cape Hallett Canyon	71° 58.8666' S 71° 59.2512' S	172° 11.6298' E 172° 10.6020' E	750
GRC-08-085	Dry	Cape Hallett Canyon	71° 58.8666' S 71° 59.2512' S	172° 11.6298' E 172° 10.6020' E	750
GRC-08-088 A	Dry	Cape Hallett Canyon	71° 58.8666' S 71° 59.2512' S	172° 11.6298' E 172° 10.6020' E	750
GRC-TR17-001 A	Dry	\	71° 38.4132' S \	172° 09.3048' E \	1022
GRC-TR17-006	Dry	\	71° 38.4132' S \	172° 09.3048' E \	1022
GRC-02-107	Dry	Iselin Bank	72° 16.1196' S 72° 15.7728' S	176° 36.2814' W 176° 35.5638' W	670

Description: Specimens consist of colonies and fragments up to 12.9 cm and 9 cm tall respectively (table 1; figure 8 A). Both colonies and fragments are

uniplanar. The branching pattern is irregular and dichotomous. Branches are oval in cross-section and up to 6 mm in diameter. The blunt tips (figure 8 B) are 3–5 mm in diameter. The colour of the coenosteum varies from orange to pale pink with the core of the branches white. The texture is reticulate-granular (figure 8 C) with small granules 3 (8 ± 3) 18 μm in diameter. On the surface of the coenosteum, the strips are 23 (57 ± 15) 101 μm wide and there are non-linear slits 8 (20 ± 7) 53 μm wide and provided with teeth projecting inward.

Gastropores and dactylopores are scattered over the coenosteum (figure 8 D) and their abundance decreases as one approaches the base. Round gastropores are 73 (280 ± 146) 745 μm in diameter, not lipped and the tips of the gastrostyle are visible from the surface. The gastrostyles are robust and lanceolate without ridges and have bifurcated spines 6 (18 ± 8) 38 μm in lenght with several tips (figure 8 E). They are 302 (449 ± 210) 821 μm long and 100 (107 ± 9) 113 μm in diameter. Ring palisades and tabulae are not recorded.

The surface of the coenosteum shows two kinds of dactylopores, with either large or small spines, which protrude perpendicularly from it (figure 8 F). The large spines are U-shaped in cross-section and have an adcauline opening and in most cases show an orderly arrangement in rows along the branches. They

are 127 (488 ± 199) 1131 µm long with a diameter of 226 (379 ± 74) 541 µm and are characterised by a thick, porous wall. Laterally they are composed of smooth overlapping platelets which give a strongly imbricated texture to dactylospines (figure 8 G), while the internal wall is characterised by the typical reticulate texture. The dactylopore slit is 131 (336 ± 112) 610 µm long and 42 (37 ± 24) 160 µm wide. The small spines are scattered between the large ones. Their external wall is smooth or reticulate and measures135 (214 ± 60) 315 µm in length. Most dactylospines have their slits oriented proximally.

Several round pores, 27 (60 ± 17) 111 µm in diameter, are scattered on the coral surface and among the dactylospines (figure 8 H).

The presence of raised or buried ampullae could be noted in many specimens (figure 8 I).

The female specimens have round ampullae 550 µm protruding from the coenosteum surface while, male specimens have smaller elliptical ampullae up to 360 µm, which are partially embedded in the coenosteum.

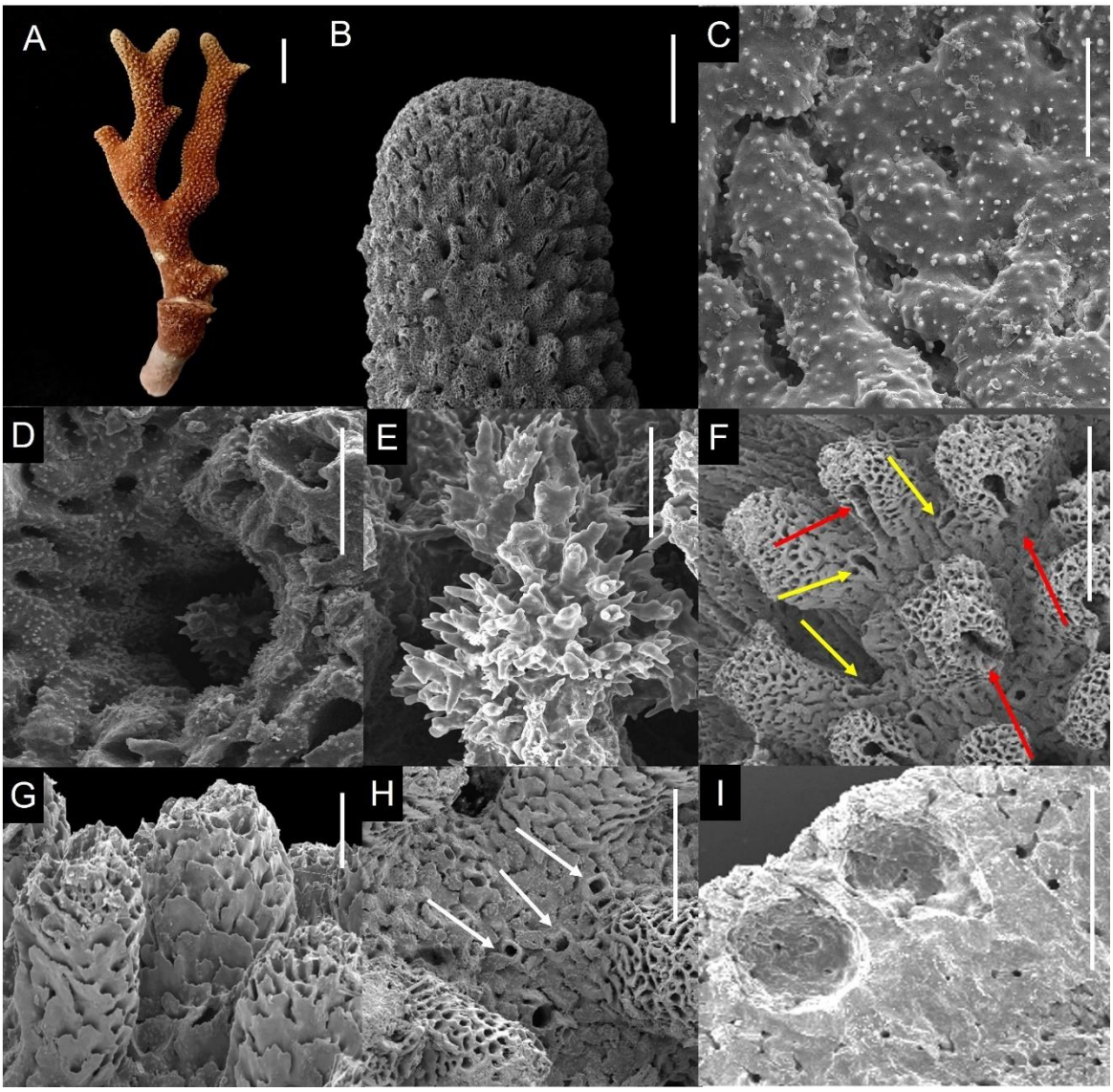

Figure 8: *Errina fissurata* (Gray, 1872). **A**. Fragment. SEM micrographs of: **B**. Apex of a branch. **C**. Reticulate-granular texture. **D**. Gastropore. **E**. Gastrostyle. **F**. Large (red arrows) and small spines (yellow arrows). **G**. Imbricated texture of dactylospines. **H**. Round pores on the coral surface (white arrows). **I**. Ampullae. **Scale bars**: **A**: 1 cm, **B-D-F-I**: 1 mm, **C**: 100 µm, **E**: 10 µm, **G**: 200 µm, **H**: 500 µm.

Remarks. In the Antarctic and Sub-Antarctic region 11 *Errina* species have been recorded (Cairns 1983b, 1991). Among them, *E. fissurata* is very similar to our specimens in various characters such as coenosteum colour and texture, non-lipped gastropores, and in having two kinds of dactylopores. The typical

shape of the large dactylopore spines, the shape of the gastrostyles and the dimorphism of the ampullae reported in *E. fissurata* clearly match our Antarctic specimens. Although most our samples were obviously damaged due to their fragile nature and possible to the method of sampling, they appear very similar to the specimens of *E. fissurata* described by Cairns (1983a). However, our colonies show clearly visible coenosteal pores and the presence of large round pores. These morphological characters have already been described by Pica et al., 2015. During the SEM observations of our specimens, a similarity with the dactylospines described by Cairns (1983a) for the species *E. kerguelensis* was noted several times. In fact, the sides of some dactylospines were characterised by the presence of coenosteal stripes arranged in a parallel, vertical orientation (Cairns, 1983a). This similarity prompted us to further investigate the dactylospines present in our samples and we noted that the dactylospines with parallel and vertical stripes are usually localized on the apices of the branches (figure 9 A); moving even a few centimetres towards the base, it was possible to observe that the dactylospines show the imbricate platelets, typical of *E. fissurata*.

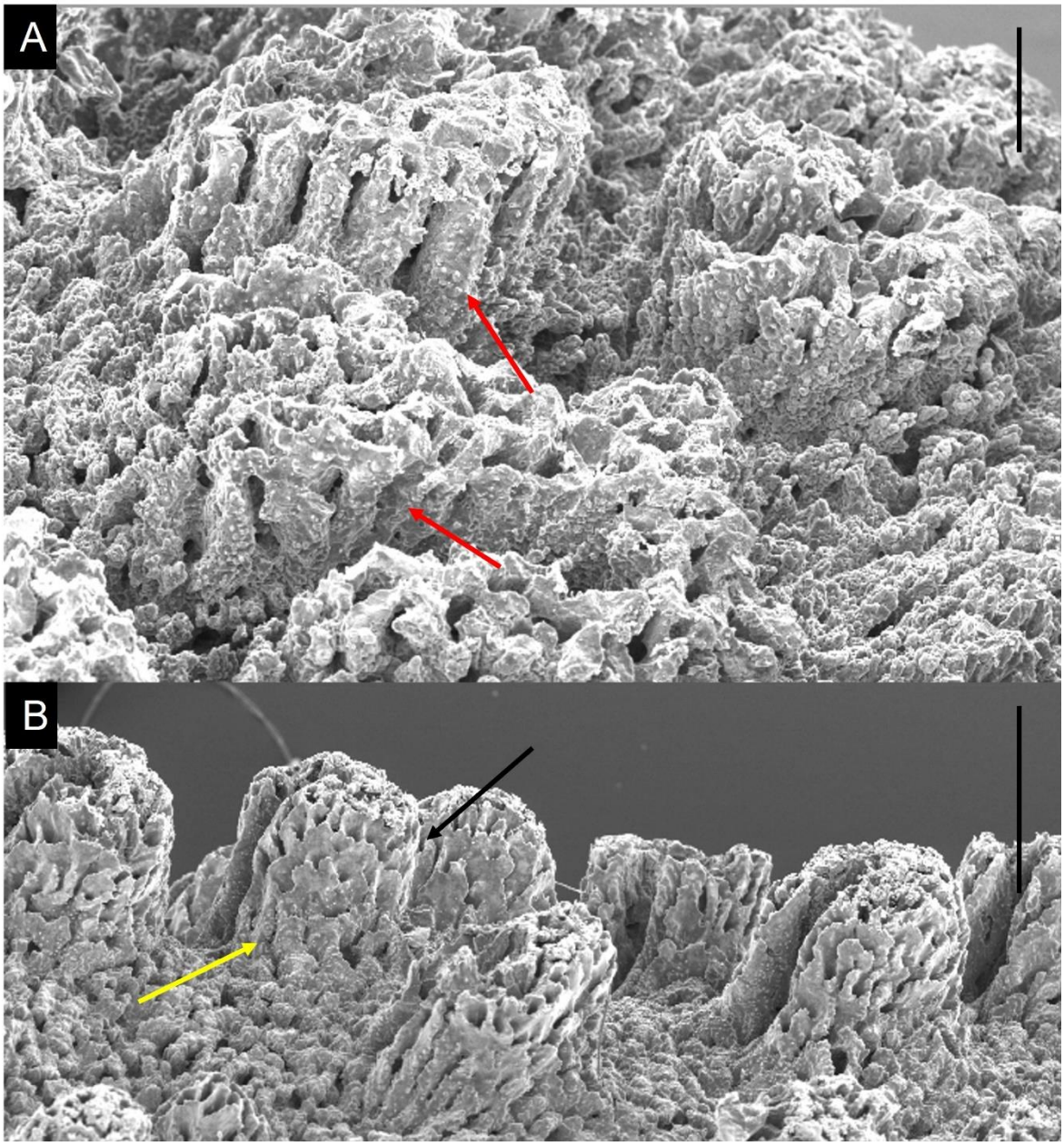

Figure 9: SEM micrographs of **A**: dactylospines of *E. fissurata* with parallel and vertical stripes. **B**: dactylospines of *E. fissurata* provided with parallel vertical stripes in their proximal portion (yellow arrow) but with imbricate platelets in their distal part (black arrow). **Scale bars**: **A-B**: 500 µm.

Sometimes we also observed dactylospines provided with parallel vertical stripes in their proximal portion but with imbricate platelets in their distal part

(figure 9 B). The presence of these vertical stripes on the dactylospines make difficult to distinguish *E. fissurata* from *E. kerguelensis* when it is not possible to investigate large fragments and different parts of the colony. An additional information that suggests the identification of our specimens as *E. fissurata* is the geographic distribution. In fact, *E. fissurata* has an Antarctic circumpolar in distribution, whereas *E. kerguelensis* is known only from off islands in the Southern Ocean (Cairns, 1983a).

Errina laterorifa Eguchi, 1964

Errina laterorifa Eguchi, 1964, pp. 5, 6, pl. 2, figs, 1-5. -- Lowe, 1967, pp. 72-78, pl. 5, figs, c-d, text figs. 10a-10g. -- Boschma, 1966b, pp. 109, 117. -- Boschma and Lowe, 1969, p. 15, pl. 5, map 1.
Errina (Errina) carnea Boschma, 1965b, pp. 21-24, pl. 1, figs. 1-2, text figs. 1a-1k.
Errina antárctica, Boschma, 1966b, p. 109 (most of BANZARE sta. 30).

Material studied:

Table 2: list of observed samples of *Errina laterorifa* with additionally information.

Specimen code	**Preservation**	**Station**	**Latitude**	**Longitude**	**Depth (m)**
GRC-08-024 B	Dry	Cape Hallett Canyon	71° 58.8666' S 71° 59.2512' S	172° 11.6298' E 172° 10.6020' E	750
GRC-08-022 B	Dry	Cape Hallett Canyon	71° 58.8666' S 71° 59.2512' S	172° 11.6298' E 172° 10.6020' E	750
GRC-02-038 MNA9250	Dry Alcohol	Iselin Bank	72° 16.1196' S 72° 15.7728' S	176° 36.2814' W 176° 35.5638' W	670
GRC-C2-T2-R2-007	Dry	\	72° 29.8692' S \	174° 59.7984' E \	434

GRC-02-035 MNA9274	Dry Alcohol	Iselin Bank	72° 16.1196' S 72° 15.7728' S	176° 36.2814' W 176° 35.5638' W	670
GRC-02-104	Dry	Iselin Bank	72° 16.1196' S 72° 15.7728' S	176° 36.2814' W 176° 35.5638' W	670
GRC-02-102	Dry	Iselin Bank	72° 16.1196' S 72° 15.7728' S	176° 36.2814' W 176° 35.5638' W	670
GRC-02-101	Dry	Iselin Bank	72° 16.1196' S 72° 15.7728' S	176° 36.2814' W 176° 35.5638' W	670
GRC-02-080 MNA9263	Dry Alcohol	Iselin Bank	72° 16.1196' S 72° 15.7728' S	176° 36.2814' W 176° 35.5638' W	670
GRC-C2-R4-011 B	Dry	\	72° 29.9826' S \	174° 58.0728' E \	434
GRC-C2-R4-005 B	Dry	\	72° 29.9826' S \	174° 58.0728' E \	434
GRC-08-087	Dry	Cape Hallett Canyon	71° 58.8666' S 71° 59.2512' S	172° 11.6298' E 172° 10.6020' E	750
GRC-C2-T2-R1-003	Dry	\	72° 29.9352' S \	175° 00.0018' E \	434
GRC-08-049 MNA9216	Dry Alcohol	Cape Hallett Canyon	71° 58.8666' S 71° 59.2512' S	172° 11.6298' E 172° 10.6020' E	750
GRC-02-081 MNA9260	Dry Alcohol	Iselin Bank	72° 16.1196' S 72° 15.7728' S	176° 36.2814' W 176° 35.5638' W	670
GRC-02-129	Dry	Iselin Bank	72° 16.1196' S 72° 15.7728' S	176° 36.2814' W 176° 35.5638' W	670
GRC-02-106	Dry	Iselin Bank	72° 16.1196' S 72° 15.7728' S	176° 36.2814' W 176° 35.5638' W	670
GRC-02-103	Dry	Iselin Bank	72° 16.1196' S 72° 15.7728' S	176° 36.2814' W 176° 35.5638' W	670
GRC-02-082 MNA9261	Dry Alcohol	Iselin Bank	72° 16.1196' S 72° 15.7728' S	176° 36.2814' W 176° 35.5638' W	670
GRC-C1-T2-R2-002	Dry	\	72° 29.6882' S \	174° 56.5272' E \	433
GRC-02-074 MNA9266	Dry Alcohol	Iselin Bank	72° 16.1196' S 72° 15.7728' S	176° 36.2814' W 176° 35.5638' W	670
GRC-C1-T2-R3-002	Dry	\	72° 29.7360' S \	174° 56.5602' E \	432

GRC-02-077 MNA9264	Dry Alcohol	Iselin Bank	72° 16.1196' S 72° 15.7728' S	176° 36.2814' W 176° 35.5638' W	670
GRC-02-083 MNA9262	Dry Alcohol	Iselin Bank	72° 16.1196' S 72° 15.7728' S	176° 36.2814' W 176° 35.5638' W	670
GRC-02-078 MNA9268	Dry Alcohol	Iselin Bank	72° 16.1196' S 72° 15.7728' S	176° 36.2814' W 176° 35.5638' W	670
GRC-02-079 MNA9269	Dry Alcohol	Iselin Bank	72° 16.1196' S 72° 15.7728' S	176° 36.2814' W 176° 35.5638' W	670
GRC-02-057 MNA10226	Dry Alcohol	Iselin Bank	72° 16.1196' S 72° 15.7728' S	176° 36.2814' W 176° 35.5638' W	670
GRC-02-037 MNA9277	Dry Alcohol	Iselin Bank	72° 16.1196' S 72° 15.7728' S	176° 36.2814' W \	670
GRC-02-076 MNA9265	Dry Alcohol	Iselin Bank	72° 16.1196' S 72° 15.7728' S	176° 36.2814' W 176° 35.5638' W	670
GRC-08-004 MNA9222 B	Dry Alcohol	Cape Hallett Canyon	71° 58.8666' S 71° 59.2512' S	172° 11.6298' E 172° 10.6020' E	750
GRC-08-006 MNA9226	Dry Alcohol	Cape Hallett Canyon	71° 58.8666' S 71° 59.2512' S	172° 11.6298' E 172° 10.6020' E	750
GRC-08-003 MNA9229	Dry Alcohol	Cape Hallett Canyon	71° 58.8666' S 71° 59.2512' S	172° 11.6298' E 172° 10.6020' E	750
GRC-08-001 MNA9227 B	Dry Alcohol	Cape Hallett Canyon	71° 58.8666' S 71° 59.2512' S	172° 11.6298' E 172° 10.6020' E	750
GRC-02-100	Dry	Iselin Bank	72° 16.1196' S 72° 15.7728' S	176° 36.2814' W 176° 35.5638' W	670
GRC-02-105	Dry	Iselin Bank	72° 16.1196' S 72° 15.7728' S	176° 36.2814' W 176° 35.5638' W	670
GRC-08-025 B	Dry	Cape Hallett Canyon	71° 58.8666' S 71° 59.2512' S	172° 11.6298' E 172° 10.6020' E	750
GRC-08-088 B	Dry	Cape Hallett Canyon	71° 58.8666' S 71° 59.2512' S	172° 11.6298' E 172° 10.6020' E	750
GRC-TR17-001 B	Dry	\	71° 38.4132' S \	172° 09.3048' E \	1022
GRC-02-075	Dry	Iselin Bank	72° 16.1196' S 72° 15.7728' S	176° 36.2814' W 176° 35.5638' W	670

Description: Colonies and fragments are usually flabellate with dense branching (table 2; figure 10 A). At the basal level the branches usually tend to anastomose, forming small plates. The largest colony examined measures 6.3 cm in length and 3 cm in width and the largest fragment measures 9.5 cm in length and 2.9 cm in width. Among the specimens of this species, it was possible to notice that the difference between the two surfaces of the branches, anterior and posterior, is very marked: the anterior surface shows a massive presence of dactylospines and gastropores (figure 10 B), while the posterior surface is almost completely devoid of these characters.

The coenosteum appears dense and porcelaneous (figure 10 C). There are also small fractures longitudinally proceeding along the coenosteum indicating the fragile nature of the corallum. Analysing the coenosteum at the apical level of the branches, it appears porous and reticulate, which is very close to the coenosteum typically presented by *Errina fissurata*, but away from the apical region of the branches, the coenosteum appears denser. Small, slightly elevated, round pores 13 (52 ± 21) 115 µm in diameter (figure 10 D), are scattered between the coenosteal pores and slits. The coenosteum of our specimens is pale pink or pinkish orange.

Gastropores (figure 10 E) are round to elliptical in shape, 115 (263 ± 72) 532 µm in diameter. Gastrostyles (figure 10 F) tips are easily visible from the

exterior. A typical gastrostyle is 260 (599 ± 281) 1305 µm tall and 20 (160 ± 74) 345 µm wide at the base, with blunt spines reaching a length of 11 (26 ± 8) 56 µm, sparsely distributed making the entire main shaft visible.

The orientation and size of the dactylopore spines are extremely variable; the largest dactylospines, occur on the lateral sides of branches. Some of them are hooded and have similar imbricated texture to those of *E. fissurata* but with greater fusion of the platelets (figure 10 G). Dactylopore spines, however, are much smaller, 73 (269 ± 89) 592 µm in height and about 67 (269 ± 69) 478 µm wide. They resemble low horseshoe shaped rims with narrow slits on one side, the slits being about 24 (68 ± 21) 151 µm wide. The slits of the dactylopore spines are usually abcauline, but different branches of the same colony may have both abcauline and adcauline slits. Frequently the dactylospines are grouped in clusters all along the branches, especially near the gastropores. It is common to find several dactylopore spines arranged in an irregular circle around the gastropore, resembling a pseudocyclosystem (figure 10 H).

Ampullae are observed either as hemispherical bulges near the tips of branches or as buried cavities (figure 10 I), without surface relief. Superficial ampullae of two sizes are observed: 803 (842 ± 67) 968 µm and 403 (545 ± 90) 718 µm in diameter and they are presumptively identified as female and

male respectively. Ampullae with a circular opening presumably caused by the exit of the planula were noted in some specimens.

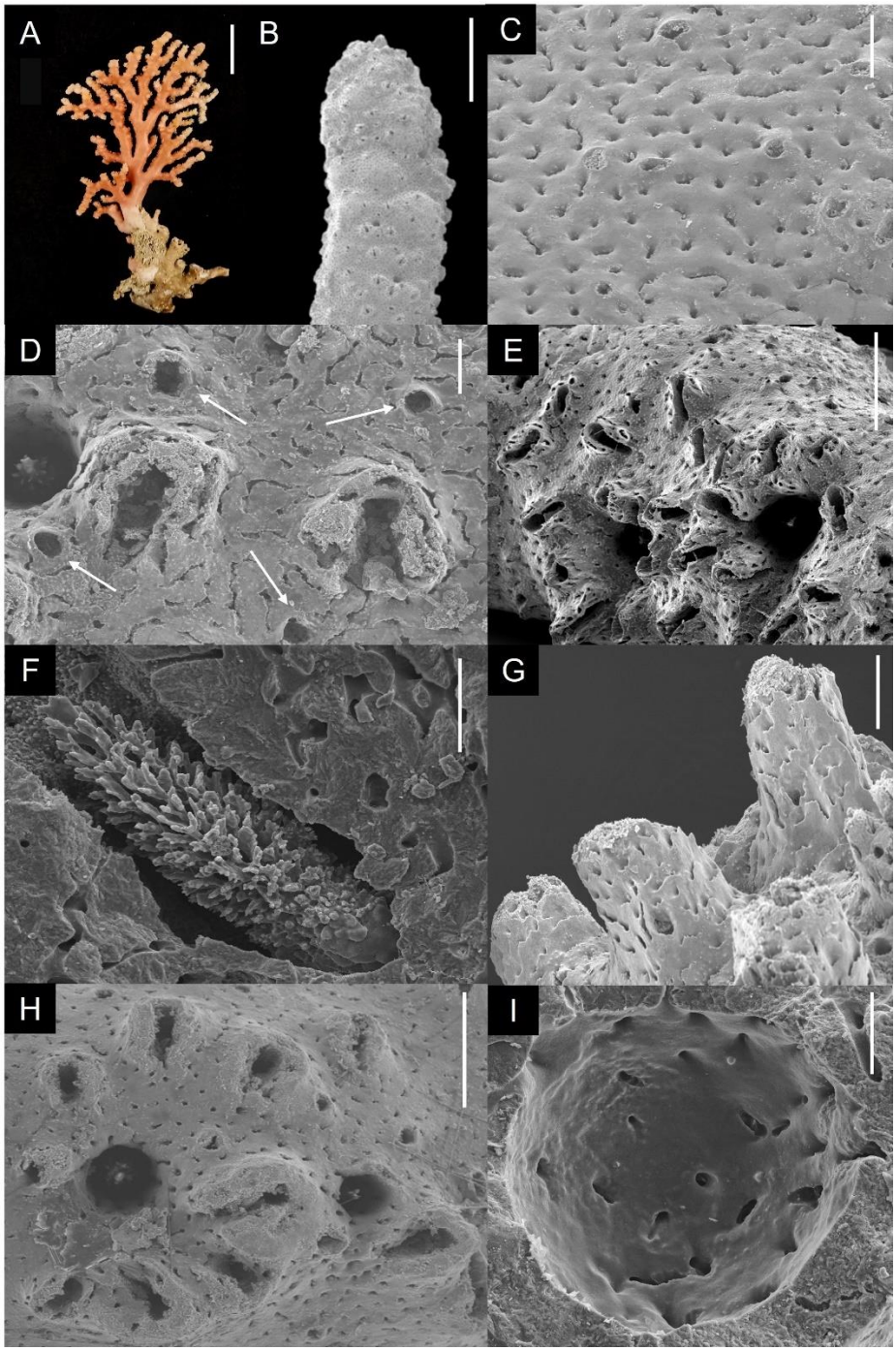

Figure 10: *Errina laterorifa* Eguchi, 1964. **A**. Colony. SEM micrographs of: **B**. Apex of a branch. **C**. Dense and porcelaneous texture. **D**. Round pores (white arrows). **E**. Gastropores. **F**. Gastrostyle. **G**. Imbricated texture of dactylospines. **H**. Dactylopore spines

arranged in an irregular circle around the gastropore, resembling a pseudocyclosystem. **I**. Ampulla. **Scale bars**: **A**: 1 cm, **B**: 2 mm, **C-D-F-G-I**: 200 µm, **E-H**: 500 µm.

Remarks. *Errina laterorifa* is similar to *E. fissurata* in terms of gross morphology and colour and they are often collected together (Cairns, 1983a). The specimens probably belonging to this species show several differences if compared with the description reported by Cairns in 1983. In particular, we observed a great dimensional heterogeneity in our fragments and colonies. In fact, they show differences in general shape, height, and diameter of both the main axis and the branches. The observation of the fragments of small size and diameter (1.4 cm in length and 0.1 cm in width for the smallest fragment and 8.5 cm in length and 0.7 cm in width for the biggest one) turned out to be even more difficult as it was not possible to know for certain which part of a colony they represented. These observations prompted us to group, according to morphological and dimensional criteria, the different samples for further investigations (figure 11 A-F).

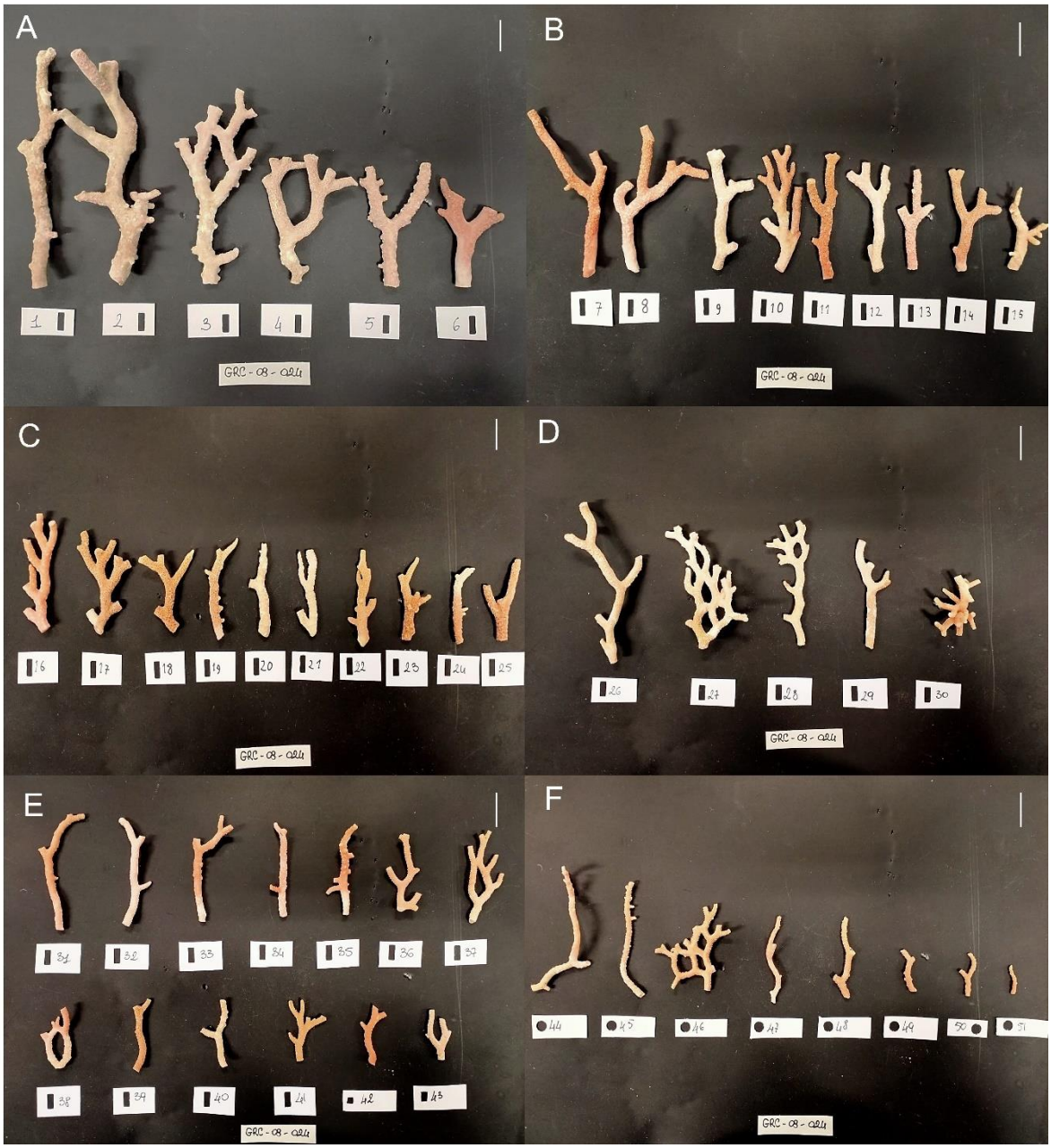

Figure 11: **A-F**, grouping of *Errina laterorifa* fragments according to similar morphological and size criteria. **Scale bars**: **A-F**: 1 cm.

Regardless the size and shape of fragments, in the vast majority of cases, our samples show a dense, porcelain-like coenosteum, as already described by Cairns in 1983. However, some specimens show a dense and porcelaneous

coenosteum flanked with areas showing a wrinkled and granular coenosteum. In agreement with Cairns (1983a), many of our specimens are also characterised by the presence of a longitudinal fracture in the coenosteum, that he recognized as evidence of the brittle nature of the coral. Moreover, Cairns (1983a) also noticed the presence of "an anterior and a posterior branch surface, the posterior one having many fewer or no gastropores and dactylopore spines" and we observed the same pattern. Small round, slightly elevated or flat pores are distributed on the coenosteum of many of our specimens with measurements that slightly differ from those reported by Cairns (1983a) in its species description, as the size range of our specimens appears to be slightly wider. Considering the gastropores of our specimens, the measurements are similar regardless the size and shape of the observed colonies/fragments; moreover, comparing these measurements with those reported by Cairns (1983a) and in the original description of the species published by Eguchi (1964), no differences were noticed. Their distribution along the corals is quite variable: in several our samples they are distributed along the entire surface of one of the two coral sides, while in other samples an evident lateral distribution pattern can be observed, where the gastropores run longitudinally along the branch sides. The gastrostyles of our samples show variable shapes and sizes. Nevertheless, as described by Cairns (1983a),

they are invariably characterized by blunt spines arranged in vertical rows, sometimes on ridges, extending from the base to the tip. Moreover, the spination results sparse, and the entire main shaft is visible (Cairns, 1983a). Due to the poor condition of many samples, it was difficult to make reliable measurements of the dactylopore spines and this also prevented comparisons of this character with previous descriptions. Length and width measurements, in fact, were not provided for all those dactylopore spines that appeared eroded, and we focussed on their texture and arrangement only. The texture of the dactylopore spines of *E. laterorifa* was described by Cairns (1983a) as similar to the texture of *E. fissurata* dactylopore spines but with greater fusion of the platelets. The dactylopore spine texture of our specimens resulted in agreement with this description. Differently from *E. fissurata*, the slits of dactylopore spines of *E. laterorifa* are reported as either abcauline and adcauline (Eguchi, 1964; Cairns, 1983a). Cairns (1983a) reported that "the orientation and size of the dactylopore spines are extremely variable. The largest spines, up to 1 mm tall, occur on the lateral sides of branches that are closely adjacent to other branches". In our specimens the spines have a variable orientation abcauline or adcauline even along the same branch. Moreover, the dactylopore spines are arranged around the gastropores producing pseudocyclosystems rarely distributed on the anterior/posterior

faces of branches but frequently on the side of the branches. This pattern is in accord with previous descriptions as Cairns (1983a) reported pseudocyclosystems on the posterior side of branches and older branches, while Eguchi (1964) reported them on the lateral sides of the branches. Thus, despite the differences in macroscopic morphology, the microscopic morphology supports the identification of our specimens with *E. laterorifa*, which therefore shows great morphological plasticity.

Errina (Errina) gracilis von Marenzeller, 1903

Errina gracilis von Marenzeller, 1903, pp. 4-7 figs. 1-4. -- Boschma, 1957: p. 54;
1966b, pp. 109, 117 (part: BANZARE sta. 98 and part of BANZARE sta. 30).
Errina (Labiopora) gracilis; Hickson, 1912a, pp. 889, 890.
Errina (Eu-Errina) gracilis; Broch, 1942, p. 38.
Errina (Errina) gracilis; Boschma, 1963a, p. 337.
Not Errina gracilis; Boschma, 1964d, pp. 298, 299, figs. 4b-4e (actual identity uncertain); Boschma and Lowe, 1969, p. 15, pl. 5, map 2 (= *E. boschmai*).
? Errina cfr. antárctica; Eguchi, 1964, pp. 4, 5, pl. 1, figs. 2, 3.
Errina (Errina) áspera; Lowe, 1967, pp. 58-63, pl. 3, figs, c, d, text figs. 7a-7f.
Not Errina (Errina) gracilis; Lowe, 1967, pp. 64-68, pi. 4, figs, a-c (= *S. boschmai*).
Errina áspera; Boschma and Lowe, 1969, p. 15, pl. 5, map 2.
? Errina gracilis; Fenninger and Flajs, 1974, pp. 71, 76.

Material studied:

Table 3: list of observed samples of *Errina gracilis* with additionally information.

Specimen code	Preservation	Station	Latitude	Longitude	Depth (m)
GRC-02-118	Dry	Iselin Bank	72° 16.1196' S 72° 15.7728' S	176° 36.2814' W 176° 35.5638' W	670

GRC-02-119	Dry	Iselin Bank	72° 16.1196' S 72° 15.7728' S	176° 36.2814' W 176° 35.5638' W	670
GRC-02-120	Dry	Iselin Bank	72° 16.1196' S 72° 15.7728' S	176° 36.2814' W 176° 35.5638' W	670
GRC-02-123	Dry	Iselin Bank	72° 16.1196' S 72° 15.7728' S	176° 36.2814' W 176° 35.5638' W	670
GRC-02-124	Dry	Iselin Bank	72° 16.1196' S 72° 15.7728' S	176° 36.2814' W 176° 35.5638' W	670
GRC-C2-R4-012	Dry	\	72° 29.9826' S \	174° 58.0728' E \	434
GRC-08-093	Dry	Cape Hallett Canyon	71° 58.8666' S 71° 59.2512' S	172° 11.6298' E 172° 10.6020' E	750
GRC-C2-T2-R2-006	Dry	\	72° 29.8692' S \	174° 59.7984' E \	434
GRC-C2-T2-R6-003	Dry	\	72° 29.9130' S \	174° 59.8812' E \	433
GRC-02-057 MNA10226	Dry Alcohol	Iselin Bank	72° 16.1196' S 72° 15.7728' S	176° 36.2814' W 176° 35.5638' W	670
GRC-C1-R3-003 MNA9278	Dry Alcohol	\	72° 29.2538' S \	174° 56.9598' E \	432
GRC-C2-R4-002 MNA9281	Dry Alcohol	\	72° 29.9826' S \	174° 58.0728' E \	434
GRC-02-117	Dry	Iselin Bank	72° 16.1196' S 72° 15.7728' S	176° 36.2814' W 176° 35.5638' W	670
GRC-02-122	Dry	Iselin Bank	72° 16.1196' S 72° 15.7728' S	176° 36.2814' W 176° 35.5638' W	670

Description: Colonies and fragments are uniplanar, with dense, irregular branching (table 3; figure 12 A). Terminal branch diameters, range from 0.2 cm to 1.2 cm (figure 12 B). The largest fragment is 2.5 cm tall with a basal branch diameter of 0.5 cm. The coenosteum is coarse, nonporcelaneous, and always white. Strips, delimited by short and discontinuous slits, are 23 (56 ±

13) 102 µm wide arranged in a reticulate pattern (figure 12 C). Scattered over the surface are numerous round pores 19 (36 ± 8) 58 µm in diameter (figure 12 D). The function of these pores is unknown, but perhaps they serve as reduced dactylopores. Granules 4 (8 ± 3) 15 µm in diameter cover the coenosteum.

Gastropores are round to elliptical (figure 12 E), 115 (218 ± 69) 408 µm in diameter. There is often a single dactylopore spine or cluster of spines directly proximal to each gastropore. Sometimes the pore is bordered by a broad, triangular lip 138 (184 ± 41) 215 µm in length (figure 12 E). Gastrostyles, 434 (515 ± 29) 535 µm in length, are elongated with a clearly visible base and provided with spines, µm in length, having gradually pointed tips (figure 12 F).

Dactylospines are large, 140 (267 ± 69) 382 µm in height and 133 (279 ± 94) 563 µm in width, and often clustered (figure 12 G), with several spines fused together. When spines are clustered, the dactylopore slits are oriented in various directions, but individual dactylopore spines invariably have their slits oriented proximally.

No ampullae were observed among our specimens.

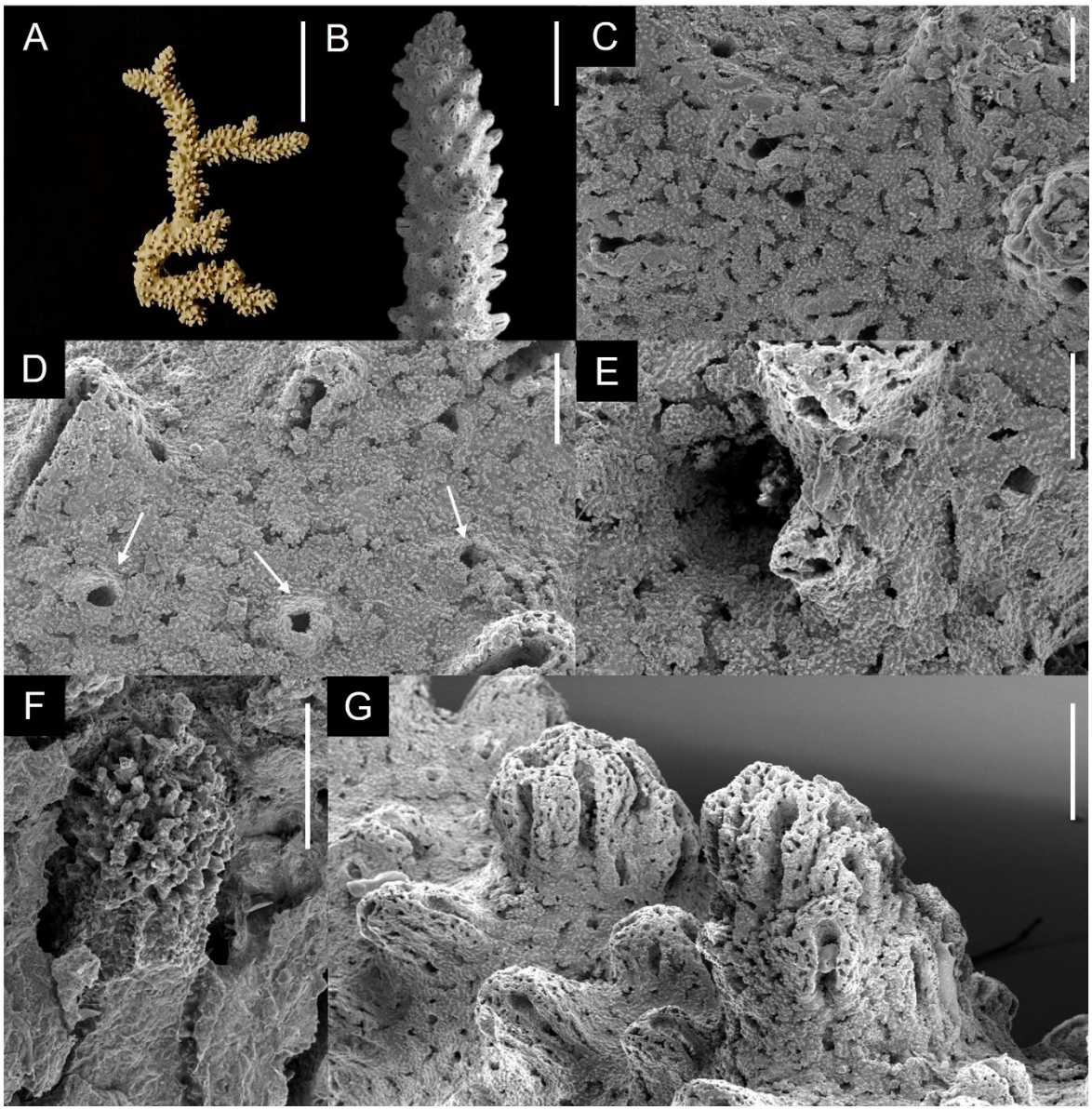

Figure 12: *Errina (Errina) gracilis* von Marenzeller, 1903. **A**. Fragment. SEM micrographs of: **B**. Apex of a branch. **C**. Coarse, nonporcelaneous texture. **D**. Round pores (white arrows). **E**. Gastropores bordered by a triangular lip. **F**. Gastrostyle. **G**. Clustered large dactylospines and individual dactylopore spines. **Scale bars**: **A**: 1 cm, **B**: 2 mm, **C-D-E-F**: 200 µm, **G**: 500 µm.

Remarks: Comparing our measurements with those reported by Cairn (1983), it appears that some of our values are slightly larger. In particular, the strips in

our samples show a larger size than those described by Cairns (1983), where the largest size reported is 85 µm. Regarding granules, Cairns reports sizes ranging from 5 to 7 µm, while in our specimens, the diameters of the measured granules present a larger size range. The sizes of the gastropore relative to our samples are also high, measuring almost twice as large as those described by Cairns (1983), where the maximum size reported is 250 µm. Despite this, our specimens closely match the species description of Cairns (1983).

Genus *Inferiolabiata* Broch, 1951

Diagnosis. Colonies commonly associated with a commensal polychaete. Gastropores and dactylopores randomly distributed. Coenosteal texture linear- or reticulate-imbricate. Gastrostyles are present but a ring palisade is usually absent. Tabulae often present. Dactylopore spines with a primarily abcauline dactylotome. Dactylostyles present. Ampullae superficial.

Discussion. The genus *Inferiolabiata* includes four species (Cairns and Zibrowius 2013).

Type species. *Errina labiata* Moseley, 1879.

Depth range. 80–2100 m.

Distribution. Tristan da Cunha Archipelago, South Africa, Antarctica and Sub-Antarctic area, New Zealand.

Inferiolabiata labiata (Moseley, 1879)

Errina labiata Moseley, 1879, pp. 443-447, pl. 34, fig. 7, pl. 37, pl. 44, figs. 9-11; 1881, pp. 50-55,
80, pl. 1, fig. 7, pl. 4, pl. 11, figs. 9-11 (part: not Challenger sta. 135). -- Hickson, 1892, p. 238. -- Boschma, 1957, p. 55; 1964d, pp. 287-299, pl. 1, text figs. 1-3; 1966b, pp. 109, 117. -- Boschma and Lowe, 1969, p. 15, pl. 5, map 2 (part: mixture of *E. labiata* and *E. lowei*).
Errina (Errina) labiata; Hickson, 1912a, p. 880.
Errina (Labiata) labiata; Broch, 1942, p. 39.
Errina (Inferiolabiata) labiata; Broch, 1951b, p. 125. -- Boschma, 1963a, pp. 337, 338.
Not Errina (Inferiolabiata) labiata; Lowe, 1967, pp. 68-72, pl. 5, figs, a-b (description and figures
based on *E. lowei*).

Material studied:

Table 4: list of observed samples *Inferiolabiata labiata* with additionally information.

Specimen code	Preservation	Station	Latitude	Longitude	Depth (m)
GRC-08-023	Dry	Cape Hallett Canyon	71° 58.8666' S 71° 59.2512' S	172° 11.6298' E 172° 10.6020' E	750
GRC-02-127	Dry	Iselin Bank	72° 16.1196' S 72° 15.7728' S	176° 36.2814' W 176° 35.5638' W	670
GRC-08-024 C	Dry	Cape Hallett Canyon	71° 58.8666' S 71° 59.2512' S	172° 11.6298' E 172° 10.6020' E	750
GRC-08-087	Dry	Cape Hallett Canyon	71° 58.8666' S 71° 59.2512' S	172° 11.6298' E 172° 10.6020' E	750
GRC-02-144 MNA 10231	Dry	Iselin Bank	72° 16.1196' S 72° 15.7728' S	176° 36.2814' W 176° 35.5638' W	670

GRC-07-030 MNA10230	Dry	Hallett Ridge	72° 23.0340' S 72° 23.3868' S	176° 06.1020' E 176° 06.2094' E	910
GRC-08-005 MNA9223	Dry	Cape Hallett Canyon	71° 58.8666' S 71° 59.2512' S	172° 11.6298' E 172° 10.6020' E	750
GRC-02-027 MNA9251	Dry Alcohol	Iselin Bank	72° 16.1196' S 72° 15.7728' S	176° 36.2814' W 176° 35.5638' W	670
GRC-02-046 MNA9259	Dry Alcohol	Iselin Bank	72° 16.1196' S 72° 15.7728' S	176° 36.2814' W 176° 35.5638' W	670
GRC-08-048 MNA9215	Dry Alcohol	Cape Hallett Canyon	71° 58.8666' S 71° 59.2512' S	172° 11.6298' E 172° 10.6020' E	750
GRC-02-049 MNA92	Dry Alcohol	Iselin Bank	72° 16.1196' S 72° 15.7728' S	176° 36.2814' W 176° 35.5638' W	670
GRC-02-041 MNA9258	Dry Alcohol	Iselin Bank	72° 16.1196' S 72° 15.7728' S	176° 36.2814' W 176° 35.5638' W	670
GRC-02-040 MNA9271	Dry Alcohol	Iselin Bank	72° 16.1196' S 72° 15.7728' S	176° 36.2814' W 176° 35.5638' W	670
GRC-02-223	Dry	Iselin Bank	72° 16.1196' S 72° 15.7728' S	176° 36.2814' W 176° 35.5638' W	670
GRC-02-114	Dry	Iselin Bank	72° 16.1196' S 72° 15.7728' S	176° 36.2814' W 176° 35.5638' W	670
GRC-08-065	Dry	Cape Hallett Canyon	71° 58.8666' S 71° 59.2512' S	172° 11.6298' E 172° 10.6020' E	750
GRC-08-077	Dry	Cape Hallett Canyon	71° 58.8666' S 71° 59.2512' S	172° 11.6298' E 172° 10.6020' E	750
GRC-TR17-007	Dry	\	71° 38.4132' S \	172° 09.3048' E \	1022
GRC-02-113	Dry	Iselin Bank	72° 16.1196' S 72° 15.7728' S	176° 36.2814' W 176° 35.5638' W	670
GRC-02-092	Dry	Iselin Bank	72° 16.1196' S 72° 15.7728' S	176° 36.2814' W 176° 35.5638' W	670
GRC-02-093	Dry	Iselin Bank	72° 16.1196' S 72° 15.7728' S	176° 36.2814' W 176° 35.5638' W	670

GRC-02-133	Dry	Iselin Bank	72° 16.1196' S 72° 15.7728' S	176° 36.2814' W 176° 35.5638' W	670
GRC-02-091	Dry	Iselin Bank	72° 16.1196' S 72° 15.7728' S	176° 36.2814' W 176° 35.5638' W	670
GRC-07-028	Dry	Hallett Ridge	72° 23.0340' S 72° 23.3868' S	176° 06.1020' E 176° 06.2094' E	910
GRC-08-002 MNA9228	Dry Alcohol	Cape Hallett Canyon	71° 58.8666' S 71° 59.2512' S	172° 11.6298' E 172° 10.6020' E	750
GRC-02-108	Dry	Iselin Bank	72° 16.1196' S 72° 15.7728' S	176° 36.2814' W 176° 35.5638' W	670
GRC-02-121	Dry	Iselin Bank	72° 16.1196' S 72° 15.7728' S	176° 36.2814' W 176° 35.5638' W	670
GRC-02-125	Dry	Iselin Bank	72° 16.1196' S 72° 15.7728' S	176° 36.2814' W 176° 35.5638' W	670
GRC-02-126	Dry	Iselin Bank	72° 16.1196' S 72° 15.7728' S	176° 36.2814' W 176° 35.5638' W	670
GRC-TR17-001 C	Dry	\	71° 38.4132' S \	172° 09.3048' E \	1022
GRC-02-115	Dry	Iselin Bank	72° 16.1196' S 72° 15.7728' S	176° 36.2814' W 176° 35.5638' W	670

Description. The shape of the colonies and fragments is variable, ranging from flabellate to bushy to columnar (table 4; figure 13 A), the latter form resulting from envelopment of a large commensal polychaete followed by little or no subsequent lateral branching. The presence of the commensal worm induces branches to elongate, and anastomose, forming a reticulate tube. Branches do not otherwise anastomose. Branches are round in cross section, tapering gradually to a blunt tip 0.3 cm in diameter (figure 13 B). The

largest colony examined is 5.1 cm tall with a basal diameter of 0.8 cm while the largest fragment is 20.1 cm tall and 11.3 cm wide. Colonies are attached by a broad, thin, encrusting base, 2.1 cm in width.

The coenosteum is characterized by rectangular spaces delimited by thin canals. Closely spaced along the canals, there are round coenosteal pores of 16 (23 ± 3) 29 µm in diameter (figure 13 C). This reticulate canal structure is slightly modified on the sides of the dactylopore spines where the coenosteum between canals becomes slightly ridged (figure 13 D), giving the spine a ribbed texture. When viewed in greater detail, the coenosteum is seen to be composed of imbricated platelets (figure 13 E).

Gastropores are round (figure 13 F), 166 (190 ± 23) 221 µm in diameter and often surrounded by a series of dactylospines with the slit facing the pore.

The dactylospines have a thin wall and are U-shaped. They are directed distally and often joined at their edges, forming a row of two to five fused spines surrounding part of the branch. The spines are 324 (0.458 ± 0.077) 573 µm high and 251 (305 ± 46) 379 µm wide, the highest spines being found on the most distal branches. Ampullae are very common and produce large craters 730 (750 ± 17) 761 µm in diameter (figure 13 G).

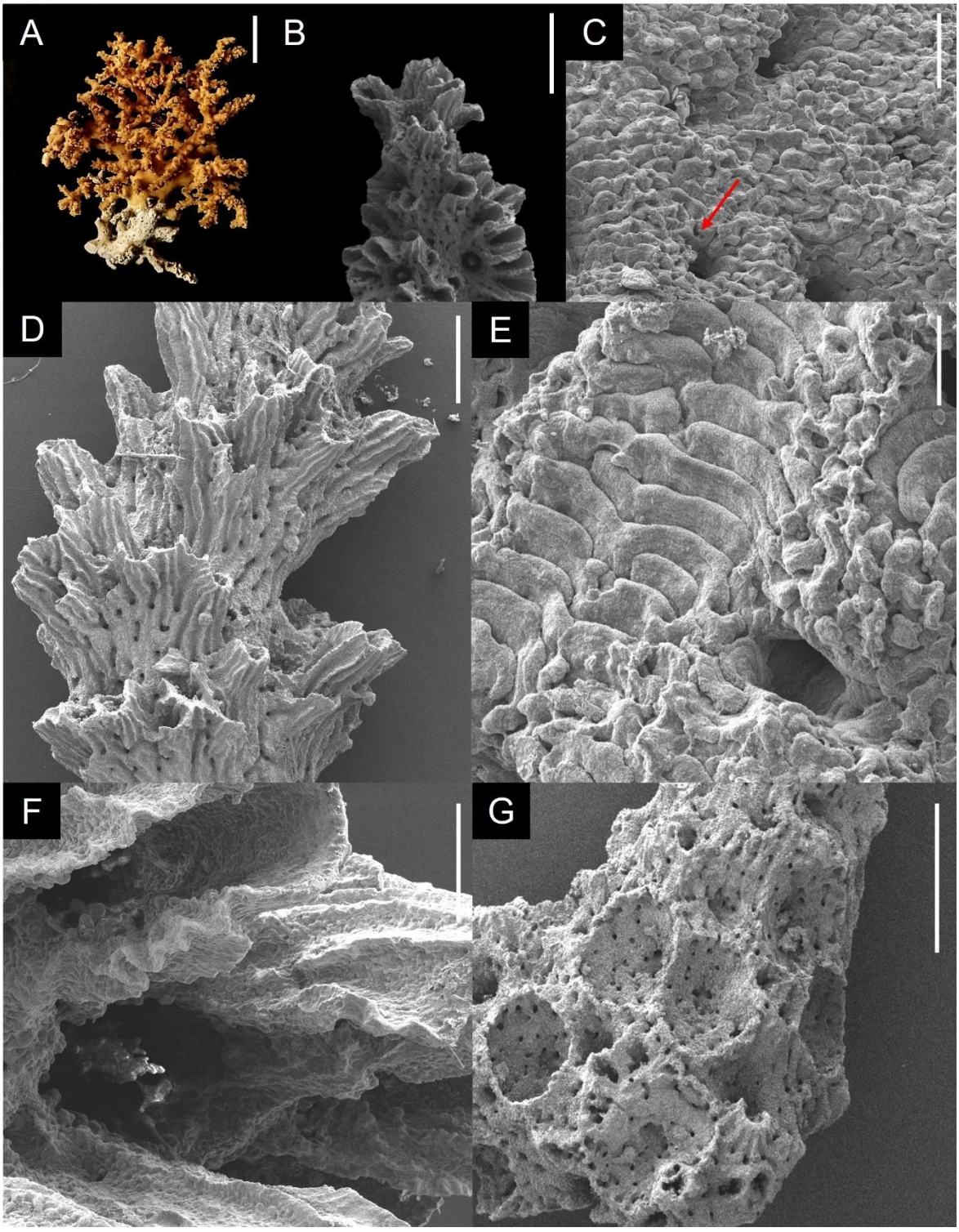

Figure 13: *Inferiolabiata labiata* (Moseley, 1879). **A**. Fragment. SEM micrographs of: **B**. Apex of a branch. **C**. Coenosteal pores (red arrow). **D**. Sides of the dactylopore spines where the coenosteum becomes slightly ridged. **E**. Texture. **F**. Gastropore.

G.Ampullae. **Scale bars**: **A**: 1 cm, **B-G**: 1 mm, **C**: 100 µm, **D**: 50 µm. **E**: 500 µm, **F**: 200 µm.

Remarks: Our data on the sizes of the characters considered are slightly different from those reported in the species description by Cairns (1983). In fact, the sizes of the samples described by Cairns (1983) appear slightly higher than those presented by our samples. More specifically, the author reports, regarding gastropores, a diameter between 280 and 330 µm, which when compared to our sizes, reach almost twice the size. The sizes of the dactylospines measured by Cairns (1983), also appear larger in that his specimens have dactylospines as high as 700 µm. Nevertheless, the samples we analyzed match the author's description.

3.1.2. Geographical distribution

Among the 12 sampling sites, the presence of *E. fissurata* was detected at 9 of them including: Iselin Bank, Cape Hallett Canyon and at 7 of the 9 unknown stations (figure 14 – 15 A). No samples were found from Hallett Ridge. *E. laterorifa* occurred at 8 of the 12 total sites, including Iselin Bank, Cape Hallett Canyon, and at 6 of the 9 unknown stations (figure 14 – 15 B). Specimens of *E. gracilis*, occurred in Iselin Bank and Cape Hallett Canyon and at 4 of the 9 unknown stations (figure 14 – 15 C). As with *E. fissurata*

and *E. laterorifa* no specimens from Hallett Ridge were found for this species *I. labiata* occurred in Iselin Bank, Cape Hallett Canyon, and Hallett Ridge and at one unknown station (figure 14 – 15 D).

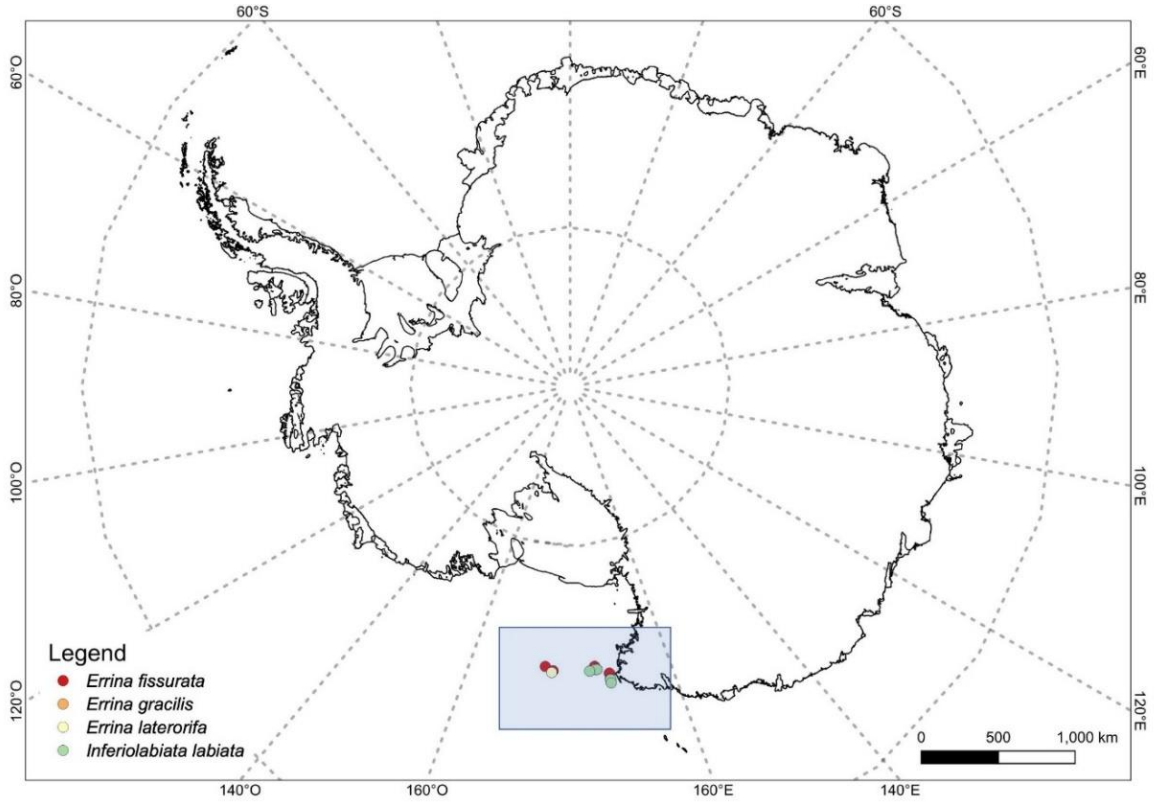

Figure 14: map showing the distribution of specimens identified in the Ross Sea.

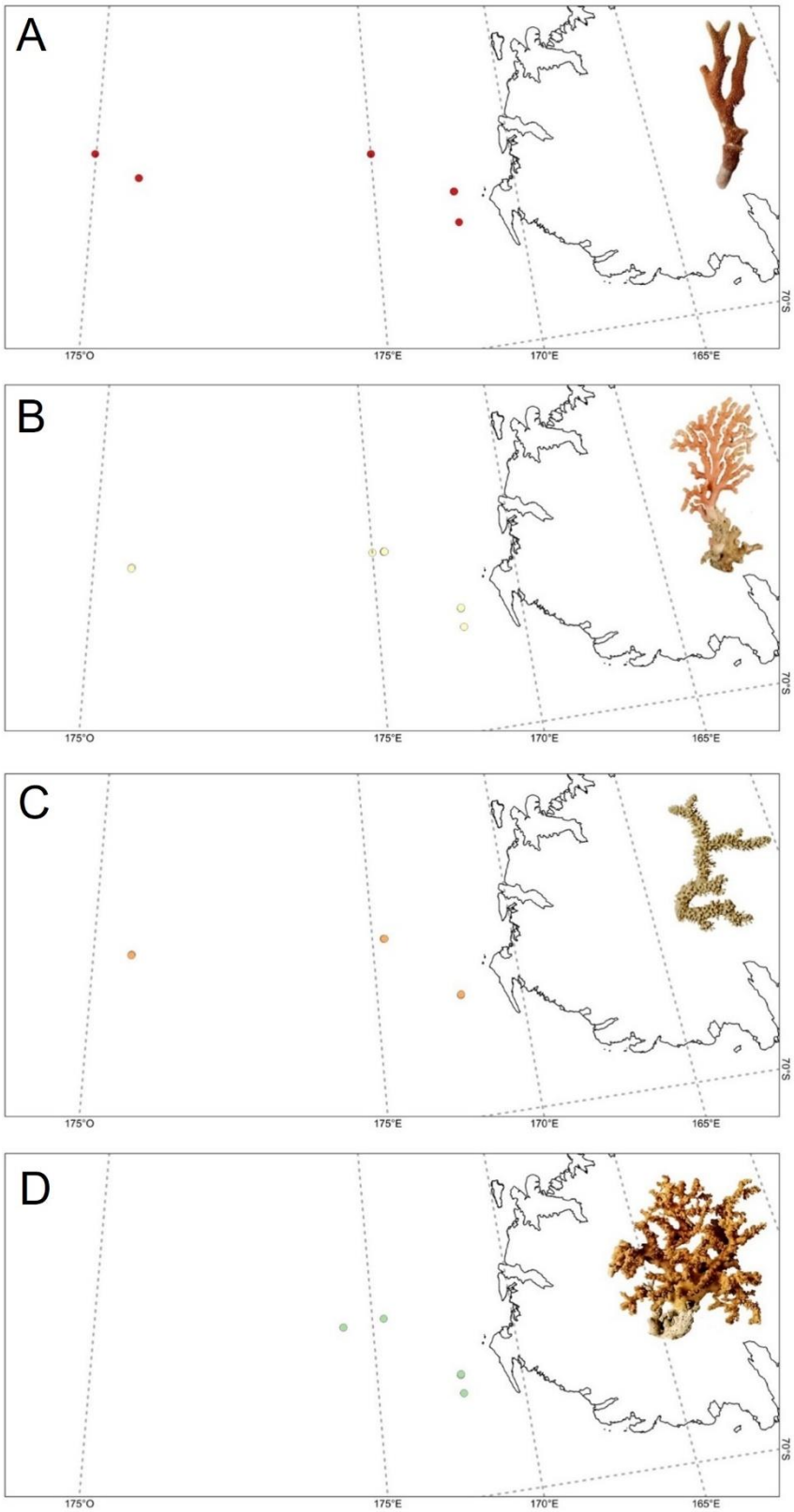

Figure 25: Maps showing distributions of each species identified in the Ross Sea: **A**. *Errina fissurata*, **B**. *Errina laterorifa*, **C**. *Errina gracilis*, **D**. *Inferiolabiata labiata*.

Therefore, among the four species in question, *E. fissurata* shows a wider distribution than the other species, being present in 9 sites, followed afterwards by *E. laterorifa* and *E. gracilis*. On the other hand, the species *I. labiata* shows a significantly smaller distribution being present in only 4 sites out of the total 12.

3.2. Part 2: Porifera

From the *Inferiolabiata labiata* samples, a total of 228 sponges were analysed (table s. 2), belonging to 2 classes, 7 orders and 19 families for a total of 38 species (table 5). Among the 228 sponges, a total of 61 individuals (27%) could not be classified taxonomically due to the presence of foreign spicules, as a result of contamination, and because of the small amount of available material, which did not allow us any further replication for possible confirmation. The most abundant species, in terms of number of specimens, is *Iophon radiatum* Topsent, 1901, with 47 specimens, followed by *Clathrochone* cf. *clathroclada* (Lévi & Lévi, 1982) with 24 specimens and *Clathria paucispicula* (Burton, 1932) with 17. Of great interest is the discovery of 10 species, out of 38, that are first records in the Ross Sea, and one species *Halichondria (Halichondria) cristata* Sarà, 1978 that represents a first record in the Antarctic continent, while 9 are probably new species (table 5).

Table 5: List of sponge species recordered associated to *I. labiata* with sponges' size, locality, number of specimens and growth habits. **Ec**: Encrusting; **ME**: Massive erect.

IB: Iselin Bank; **CHC**: Cape Hallett Canyon; **HR**: Hallett Ridge; **US**: Unknown station.

° Probably new species; * first record in Antarctica; ^ first record in the Ross Sea.

Sponge species	Growth habit	Sponge size (min – max)	Locality	Tot specimens
Class				
Demospongiae Sollas, 1885				
Haliclona (Flagellia) cf. *flagellifera* (Ridley & Dendy, 1886)	ME	0.482 cm^2	IB	1
Haliclona (Gellius) rudis (Topsent, 1901)	Ec	0.447-1.079 cm^2	IB CHC	3
Haliclona cf. *virens* (Topsent, 1901)	Ec	0.085-0.596 cm^2	IB	5
Haliclona sp.1	Ec	0.350-0.665 cm^2	IB HR	3
Haliclona sp. 2	Ec	0.115 cm^2	IB	1
Biemna chilensis Thiele, 1905	ME	0.027-1.407 cm^2	IB	2
Iophon abnormalis Ridley & Dendy, 1886 ^	Ec	0.061-0.234 cm^2	IB	2
Iophon radiatum Topsent, 1901	Ec	0.006-1.692 cm^2	IB CHC HR	47
Iophon unicorne Topsent, 1907	Ec	0.017-3.611 cm^2	IB CHC	2
Asbestopluma (Asbestopluma) sp. °	ME	0.01 cm^2	IB	1
Lissodendoryx (Lissodendoryx) complicata (Hansen, 1885) *sensu* Boury-Esnault & Van Beveren (1982) °	Ec	0.027-0.132 cm^2	IB	3
Lissodendoryx (Lissodendoryx) styloderma Hentschel, 1914 ^	Ec	0.045-0.564 cm^2	IB CHC	2
Lissondendoryx (Ectyodoryx) nobilis (Ridley & Dendy, 1886)	Ec	0.105 cm^2	IB	1
Lissondendoryx (Ectyodoryx) sp. °	Ec	1.483 cm^2	IB	1

Amphilectus rugosus (Thiele, 1905) ^	Ec	0.037-0.178 cm^2	IB	3
Esperiopsis villosa (Carter, 1874), *sensu* Koltun (1964) °	Ec	0.037-0.464 cm^2	IB	3
Isodictya setifera (Topsent, 1901)	Ec	0.003 cm^2	IB	1
Crella (Crella) tubifex (Hentschel, 1914) ^	Ec	0.084-0.103 cm^2	IB	2
Inflatella belli (Kirkpatrick, 1907)	ME	0.034 cm^2	IB	1
Artemisina plumosa Hentschel, 1914 ^	ME	0.031-0.188 cm^2	IB HR	5
Clathria (Clathria) paucispicula (Burton, 1932) ^	ME/Ec	0.01-1.794 cm^2	IB CHC	17
Clathria sp. °	Ec	0.078 cm^2	IB	1
Clathria (Microciona) sp. 1 °	Ec	0.193 cm^2	HR	1
Clathria (Microciona) sp. 2 °	Ec	0.086-0.125 cm^2	IB HR	2
Mycale (Anomomycale) titubans (Schmidt, 1870) *sensu* Boury-Esnault & Van Beveren (1982) °	Ec	0.07-1.615 cm^2	IB CHC	3
Myxilla (Myxilla) elongata Topsent, 1916	Ec	0.005-0.440 cm^2	IB CHC	3
Myxilla (Myxilla) mollis Ridley & Dendy, 1886	Ec	0.179-0.757 cm^2	IB CHC HR	7
Tedania (Tedaniopsis) oxeata Topsent, 1916	Ec	1.463 cm^2	IB	1
Tedania (Tedaniopsis) tantula (Kirkpatrick, 1907)	Ec	0.004-0.192 cm^2	IB	2
Polymastia invaginata Kirkpatrick, 1907	Ec	0.039-0.279 cm^2	IB	6
Plicatellopsis fragilis Koltun, 1964 ^	ME/Ec	0.051 cm^2	IB	1
Pseudosuberites sulcatus (Thiele, 1905) ^	Ec	0.072 cm^2	IB	1
Halichondria (Halichondria) cristata Sarà, 1978 *	Ec	0.212 cm^2	HR	1
Halichondria (Halichondria) prostrata Thiele, 1905	ME	0.400 cm^2	CHC	1

	Poecillastra compressa antarctica Koltun, 1964 ^	ME	0.015-0.315 cm^2	IB	3
	Tetilla coronida Sollas, 1888	ME	0.300 cm^2	US	1
Class Hexactinellida Schmidt, 1870					
	Clathrochone cf. *clathroclada* (Lévi & Lévi, 1982) °	ME	0.008-3.563 cm^2	IB HR	24
	Rhabdocalyptus australis Topsent, 1901 ^	ME	0.109-0.234 cm^2	IB	2
	Tot species: 38				**Tot specimens:** 228

3.2.1. Systematic

Class Demospongiae Sollas, 1885

Order Haplosclerida Topsent, 1928

Family Chalinidae Gray, 1867

Genus *Haliclona* Grant, 1841

Subgenus *Haliclona (Flagellia)* Van Soest, 2017

Species *Haliclona (Flagellia)* cf. *flagellifera* (Ridley & Dendy, 1886)

Locality and material: Iselin Bank. 72° 16.1196' S, 176° 36.2814' W and 72° 15.7728' S, 176° 35.5638' W. Depth 670 m. One specimen: GRC-02-223 CC.

Other material examined: None.

Description: The sample has a small size of 0.482 cm^2, is massive, greyish yellow, and has a soft and brittle consistence.

Skeleton: Not observed.

Megascleres:

1. Oxeas: slightly curved, thick, cigar-shaped and gradually pointed (figure 16 A-B).

   Size: 650 (683 ± 18) 710 x 20 (22 ± 3) 25 µm.

Microscleres:

1. Flagellosigmas: characterized by a circular or elliptical shape, with a longer and sharper curved ending at one side and a shorter and more gradually curved ending at the opposing side (figure 16 A-B).

   Size of the longer ending: 52.5 (106 ± 26) 145 µm.

   Size of the chord: 50 (74 ± 21) 162.5 µm.

2. Sigmas: small, C-shaped (figure 16 A-C-D).

   Size: 22.5 (40 ± 10) 57.5 x 12.5 (17 ± 3) 22.5 µm.

Remarks: Although the spicule set closely matches that described in the original description by Ridley and Dendy (1886) and that described by Van Soest (2017), the size of the spicules in our sample are slightly different. In

fact, size of the oxeas in our sample is larger than that reported by Ridley and Dendy (420 x 18 µm) and Van Soest (340-389.1 x 8-15.1 µm). Regarding the size of the longest flagellosigma, the length range we obtained appears slightly higher than that reported by Van Soest (82-96.2-102 µm). Size of the C-shaped sigmas is similar. Despite the above mentioned differences in size, the sponge appears to be quite consistent with the descriptions reviewed.

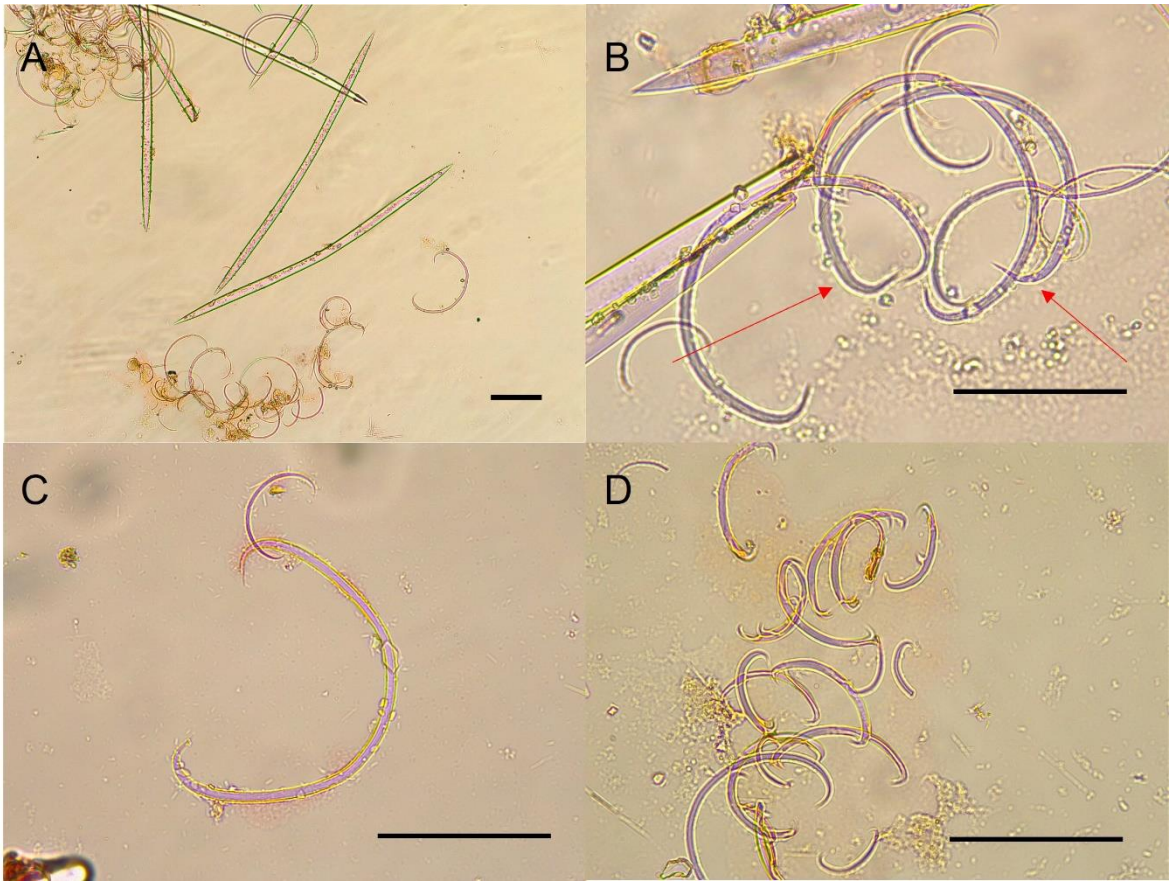

Figure 16: *Haliclona (Flagellia)* cf. *flagellifera* (Ridley & Dendy, 1886). Optical microscope images of the spicules: **A**. Oxeas and sigmas. **B**. Large flagellosigmas with a longer and sharper curved ending at one side and a shorter and more gradually curved ending at the opposing side (red arrows). **C-D** Sigmas. **Scale bars**: **A-B-C-D**: 100 µm.

Family Chalinidae Gray, 1867

Genus *Haliclona* Grant, 1841

Subgenus *Haliclona (Gellius)* Gray, 1867

Species *Haliclona (Gellius) rudis* (Topsent, 1901)

Locality and material: Iselin Bank. 72° 16.1196' S, 176° 36.2814' W and 72° 15.7728' S, 176° 35.5638' W. Depth 670 m. Cape Hallett Canyon 71° 58.8666' S, 172° 11.6298' E and 71° 59.2512' S, 172° 10.6020' E. Depth 750 m. Three specimens: GRC-08-023 DE1, GRC-08-023 DE2, GRC-02-223 AS1.

Other material examined: Slide GRC-02-223 26 sp. 3 (*Haliclona (Gellius)* cf. *rudis*), provided by Dr. Marco Bertolino, University of Genoa.

Description: The sponge samples analysed are massive and greyish with a size ranging from 0.447-1.079 cm^2.

Skeleton: Not observed.

Megascleres:

1. Oxeas: robust, gently curved, fusiform with both pointed ends (figure 17 A).

   Size: 320 (501 ± 57) 560 x 10 (17 ± 3) 20 µm.

Microscleres:

1. Sigmas: small, C-shaped (figure 17 B).

   Size: 27.5 (35 ± 3) 40 x 12.5 (15 ± 2) 20 µm.

Remarks: Comparing the measurements obtained from our samples with those in the original description by Topsent (1901), according to which the oxeas measure 480 x 20 µm, there are no significant discrepancies. As far as sigmas are concerned, Topsent's size range (40-60 x 1-2 µm) is slightly higher than ours. Despite this small difference, our samples are sufficiently in line with the characteristics given in the original description.

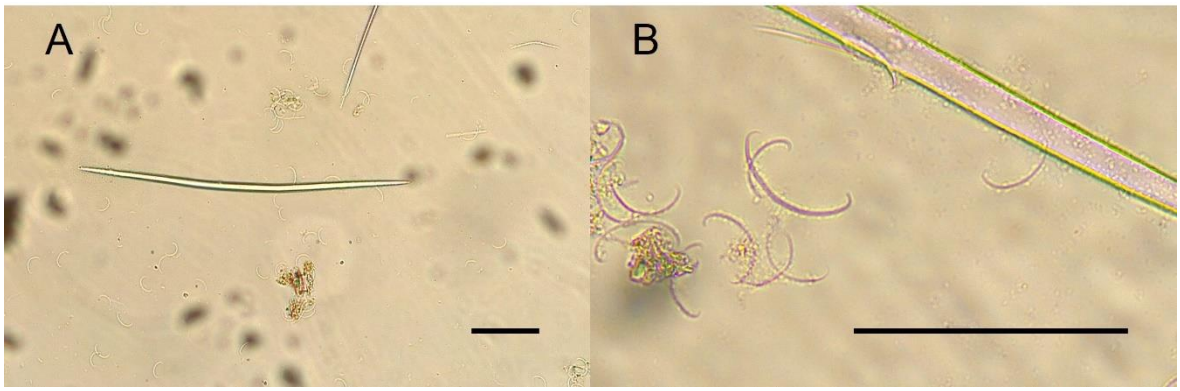

Figure 17: *Haliclona (Gellius) rudis* (Topsent, 1901). Optical microscope images of the spicules: **A**. Oxeas. **B**. Sigmas. **Scale bars**: **A**-**B**: 100 µm.

Family Chalinidae Gray, 1867

Genus *Haliclona* Grant, 1841

Species *Haliclona* cf. *virens* (Topsent, 1908)

Locality and material: Iselin Bank. 72° 16.1196' S, 176° 36.2814' W and 72° 15.7728' S, 176° 35.5638' W. Depth 670 m. Five specimens: GRC-02-223 N4, GRC-02-223 S3, GRC-02-223 AM3, GRC-02-223 BN2, GRC-02-091 CU3.

Other material examined: Slide GRC-02-222 3 sp. 2 (*Haliclona* cf. *virens*), GRC-02-223 1 sp. 6 (*Haliclona* cf. *virens*), GRC-02-223 6 sp. 1 (*Haliclona* cf. *virens*), provided by Dr. Marco Bertolino, University of Genoa.

Description: The sponge samples analysed are small in size, ranging from 0.085-0.596 cm^2, with a greyish colouration and encrusting.

Skeleton: The analysed portion of the skeleton shows an isodictyal organisation with triangular meshes.

Megascleres:

1. Oxeas: curved spicules with both pointed ends (figure 17 A-B).

   Size: 250 (287 ± 20) 320 x 10 (17 ± 3) 25 μm.

Microscleres: Absent.

Remarks: Although the measurements we obtained are in line with those reported in the original description by Topsent (1908) (280 x 11 μm), we

cannot state with certainty that it actually is *Haliclona virens* due to the scarce available material analysed.

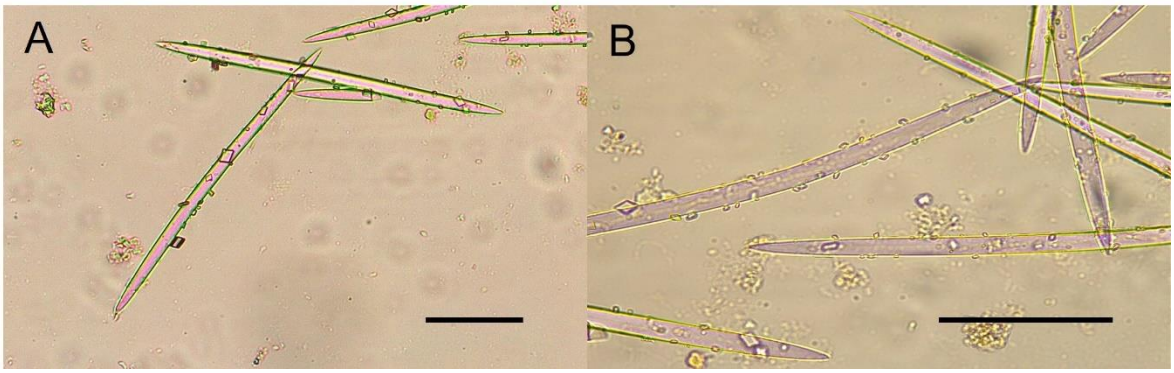

Figure 17: *Haliclona* cf. *virens* (Topsent, 1908). Optical microscope images of the spicules: **A**. Oxeas. **B**. Detail of the tips. **Scale bars**: **A-B**: 100 µm.

Family Chalinidae Gray, 1867

Genus *Haliclona* Grant, 1841

Species *Haliclona* sp. 1

Locality and material: Iselin Bank. 72° 16.1196' S, 176° 36.2814' W and 72° 15.7728' S, 176° 35.5638' W. Depth 670 m. Hallett Ridge. 72° 23.0340' S, 176° 06.1020' E and 72° 23.3868' S, 176° 06.2094' E. Depth 910 m. Three specimens: GRC-02-223 S1, GRC-07-028 CVA, GRC-07-028 CVE.

Other material examined: Slide GRC-02-222 2 sp. 1 (*Haliclona* sp. 1), provided by Dr. Marco Bertolino, University of Genoa.

Description: The sponge samples analysed are small in size, ranging from 0.350-0.665 cm^2, with a greyish colouration and encrusting.

Skeleton: The analysed portion of the skeleton shows an isodictyal organisation with triangular meshes.

Megascleres:

1. Oxeas: curved spicules with both pointed ends (figure 18 A-B).

   Size: 380 (420 ± 32) 480 x 10 (12 ± 2) 15 µm.

Microscleres: Absent.

Remarks: It was not possible to classify the samples, at species levels, due to the small amount of available material.

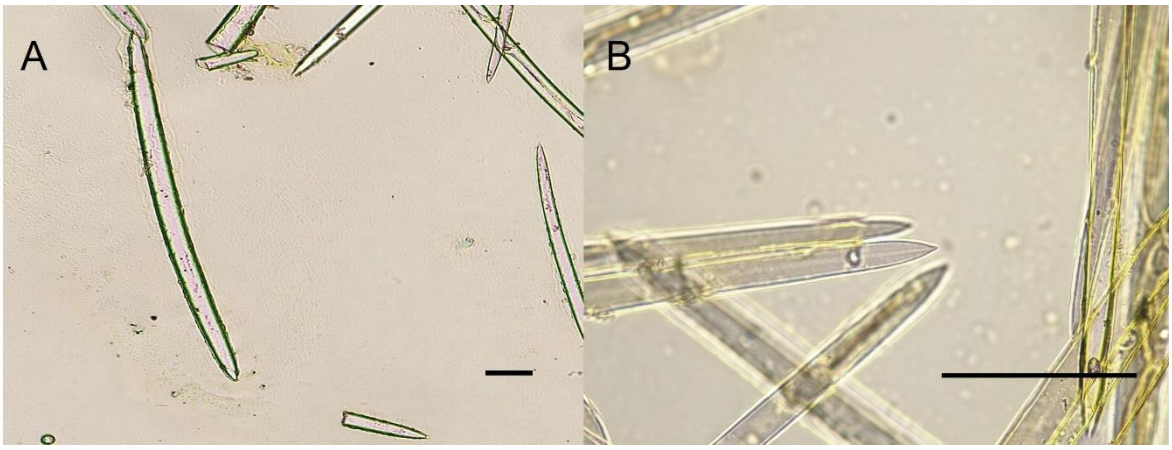

Figure 18: *Haliclona* sp. 1. Optical microscope images of the spicules: **A**. Oxeas. **B**. Detail of the tips. **Scale bars**: **A-B**: 100 µm.

Family Chalinidae Gray, 1867

Genus *Haliclona* Grant, 1841

Species *Haliclona* sp. 2

Locality and material: Iselin Bank. 72° 16.1196' S, 176° 36.2814' W and 72° 15.7728' S, 176° 35.5638' W. Depth 670 m. One specimen: GRC-02-223 AP2.

Other material examined: Slide GRC-02-223 7 sp. 3 (*Haliclona* sp. 2), provided by Dr. Marco Bertolino, University of Genoa.

Description: The sponge sample has a size of 0.115 cm^2 with a colour tending to grey. The sponge is encrusting.

Skeleton: The analysed portion of the skeleton shows an isodictyal organisation with triangular meshes.

Megascleres:

1. Oxeas: curved spicules with both pointed ends (figure 19 A-B)

   Size: 300 (333 ± 19) 350 x 5 (7 ± 3) 10 µm.

Microscleres: Absent.

Remarks: It was not possible to classify the sample, at species level, due to the small amount of available material.

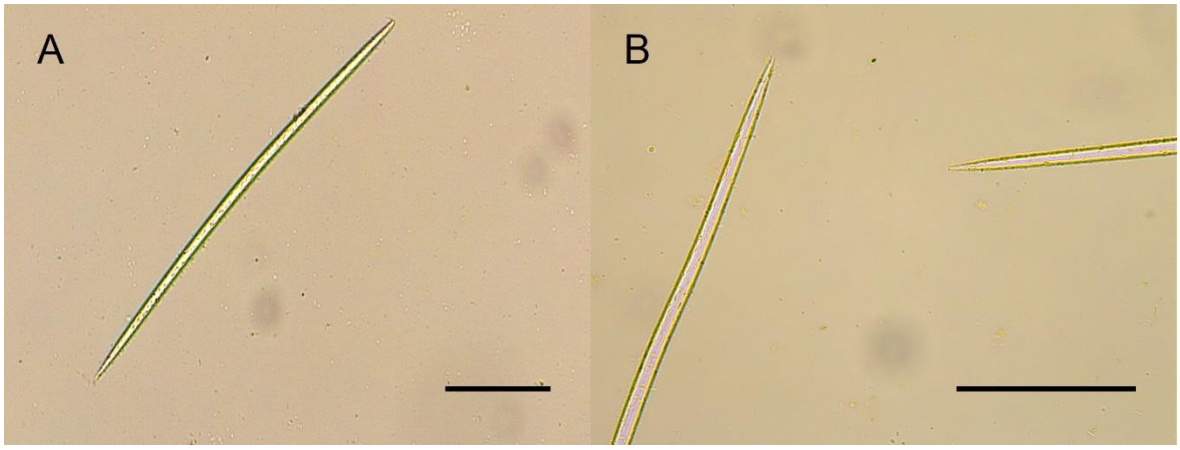

Figure 19: *Haliclona* sp. 2. Optical microscope images of the spicules: **A**. Oxea. **B**. Detail of the tips. **Scale bars**: **A-B**: 100 µm.

Order Biemnida Morrow, 2013

Family Biemnidae Hentschel, 1923

Genus *Biemna* Gray, 1867

Species *Biemna chilensis* Thiele, 1905

Locality and material: Iselin Bank. 72° 16.1196' S, 176° 36.2814' W and 72° 15.7728' S, 176° 35.5638' W. Depth 670 m. Two specimens: GRC-02-223 A2, GRC-02-093 CS7.

Other material examined: Slide GRC-02-223 sp.1 10 (*Biemna chilensis*) provided by Dr. Marco Bertolino, University of Genoa.

Description: The samples analysed are cushion-shaped with hispid surface and light beige colour. The samples are massive and show sizes ranging from 0.027 to 1.407 cm^2.

Skeleton: Not observed.

Megascleres:

1. Styles: variable in size. They are generally smooth and straight while some of them are curved (figure 20 A)

   Size: 1160 (1478 ± 159) 1820 x 10 (26 ± 8) 30 µm.

Microscleres:

1. Raphids: very thin, hair-like (figure 20 B-C-D).

   Size: 225 (366 ± 108) 600 x 2.5 µm.

2. Sigmas I: larger C-shaped (figure 20 E).

   Size: 50 (78 ± 17) 107.5 µm.

3. Sigmas II: smaller C-shaped (figure 20 F).

   Size: 25 (31 ± 5) 42.5 µm.

Remarks: In this sample, styles are longer than those of the original description by Thiele (1905) (950 x 25 µm); in the case of raphids and sigmas, the size of our samples also appears longer than those of Thiele (1905): 220 - 240 µm for the raphids, 46-55 µm for the larger sigmas and 18

µm for the smaller sigmas. Measurements of spicules similar to ours were also reported by Costa et al., in press.

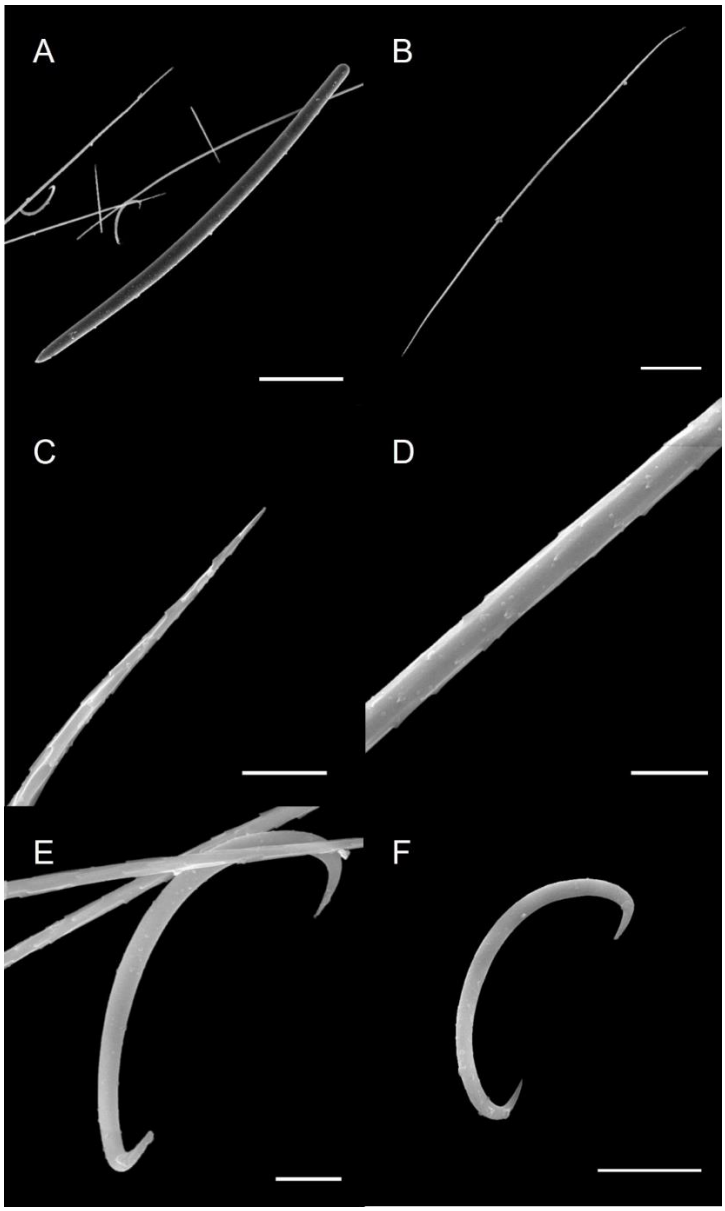

Figure 20: *Biemna chilensis* Thiele, 1905. SEM images of the spicules: **A**. Smooth style. **B**. Raphid. **C**. Magnification of the tip of a raphid. **D**. Magnification of the central portion of the raphid. **E**. Smaller C-shaped sigma. **F**. Larger C-shaped sigma. **Scale bars**: **A**-**B**: 100 µm, **C**-**D**-**F**: 10 µm, **E**: 20 µm.

Order Poecilosclerida Topsent, 1928

Family Acarnidae Dendy, 1922

Genus *Iophon* Gray, 1867

Species *Iophon abnormalis* Ridley & Dendy, 1886

Locality and material: Iselin Bank. 72° 16.1196' S, 176° 36.2814' W and 72° 15.7728' S, 176° 35.5638' W. Depth 670 m. Two specimens: GRC-02-223 AR1, GRC-02-093 AR2.

Other material examined: None.

Description: The sponge samples analysed are cylindrical, brittle, and friable, greyish in colour and range in size from 0.061 to 0.234 cm^2.

Skeleton: Not observed.

Megascleres:

1. Tylotes: with spined, strongly swollen heads (figure 21 A-B).

   Size: 240 (296 ± 30) 350 x 10 (13 ± 2) 15 μm.

2. Styles: curved, generally spined at the base and slightly at the apex (figure 21 C-D).

   Size: 410 (437 ± 17) 470 x 25 (29 ± 4) 35 μm.

Microscleres:

1. Anisochelae I: large, palmate, with a short spur, mainly organised in rosettes (figure 21 E).

   Size: 25 (36 ± 5) 45 x 12.5 (14 ± 2) 17.5 µm.

2. Anisochelae II: small, palmate, with a short spur, not organised in rosettes (figure 21 F).

   Size: 12.5 (19 ± 3) 22.5 x 7.5 (9 ± 1) 10 µm.

3. Bipocillas: very small and rounded (figure 21 F).

   Size: 7.5 (10 ± 2) 12.5 µm.

Remarks: The specimens analysed are in total conformity with the description of Ridley and Dendy (1886), with the only exception that the size of the styles is slightly larger than that reported in the original description (350 x 12 µm). In agreement with the description of *Iophon abnormalis* by Rìos (2006), our specimens also have few bipocilla, although the original description did not include the presence of these microscleres.

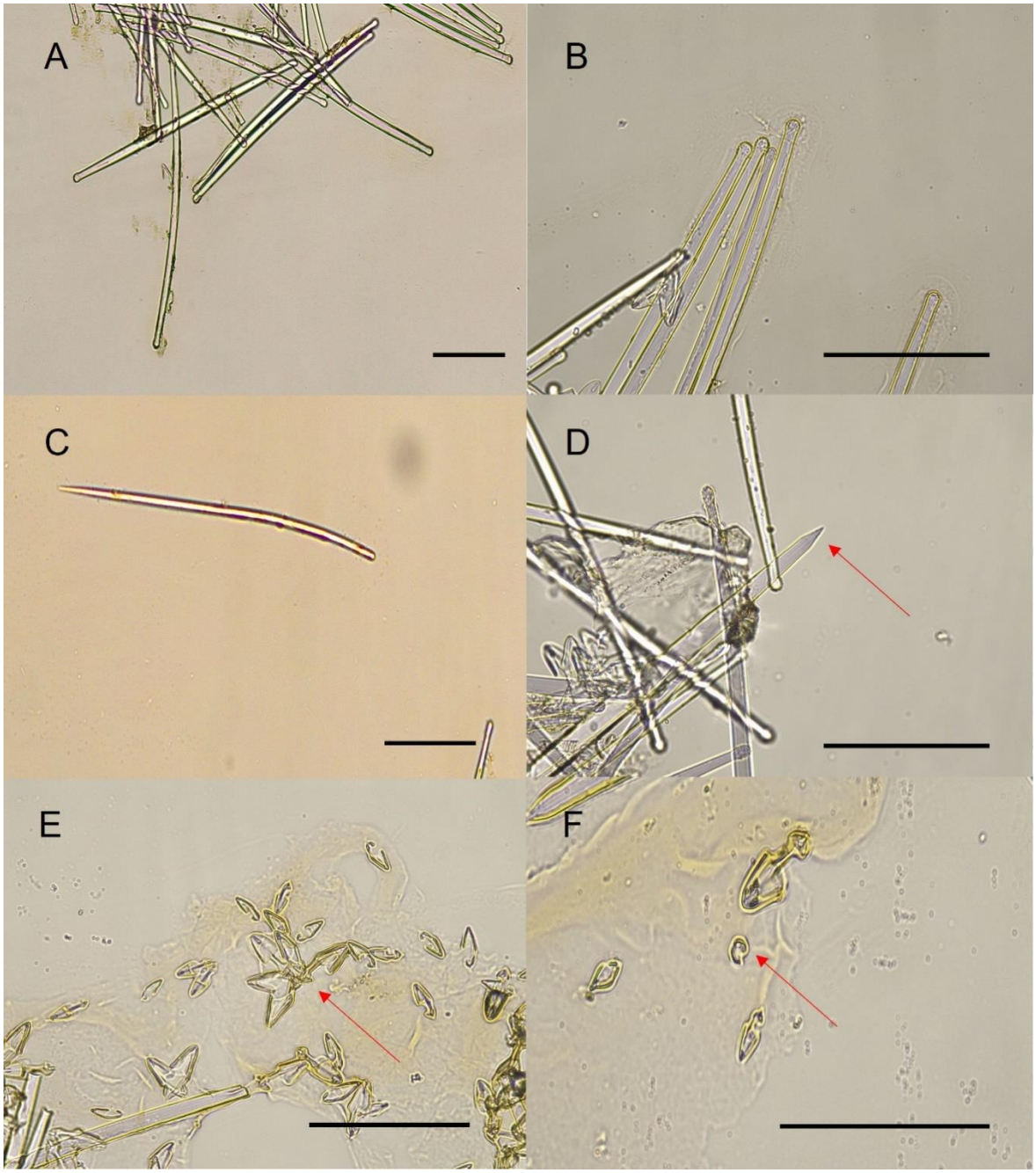

Figure 21: *Iophon abnormalis* Ridley & Dendy, 1886. Optical microscope images of the spicules: **A**. Tylotes. **B**. Detail of the spined, strongly swollen heads of tylotes. **C**. Smooth style. **D**. Detail of the slightly spined apex (red arrow) of the style. **E**. Anisochelae I organised in rosettes (red arrow). **F**. Anisochelae II not organised in rosettes and a bipocillum (red arrow). **Scale bars**: **A-B- C-D-F**: 100 µm.

Family Acarnidae Dendy, 1922

Genus *Iophon* Gray, 1867

Species *Iophon radiatum* Topsent, 1901

Locality and material: Iselin Bank. 72° 16.1196' S, 176° 36.2814' W and 72° 15.7728' S, 176° 35.5638' W. Depth 670 m. Cape Hallett Canyon. 71° 58.8666' S, 172° 11.6298' E and 71° 59.2512' S, 172° 10.6020' E. Depth 750 m. Hallett Ridge. 72° 23.0340' S, 176° 06.1020' E and 72° 23.3868' S, 176° 06.2094' E. Depth 910 m. Forty-seven specimens: GRC-02-223 F1, GRC-02-223 F2, GRC-02-223 F3, GRC-02-223 G2, GRC-02-223 I1, GRC-02-223 L1, GRC-02-223 L2, GRC-02-223 AG1, GRC-02-223 AM4, GRC-02-223 AH3, GRC-02-223 AM2, GRC-02-223 BB2, GRC-02-223 BB3, GRC-02-223 AT1, GRC-02-223 AT2, GRC-02-223 AV2, GRC-02-223 AV3, GRC-02-223 AQ4, GRC-02-223 BI1, GRC-08-023 DB1, GRC-07-028 CV2, GRC-07-028 CVK, GRC-07-028 CVI, GRC-07-028 CVH, GRC-07-028 CVC, GRC-07-028 CVF, GRC-08-023 CW1, GRC-08-023 CW2, GRC-08-023 CZ2, GRC-08-023 DD1, GRC-07-028 CVP, GRC-02-093 CS10, GRC-08-048 CL1, GRC-02-113 CQ3, GRC-02-113 CQ5, GRC-02-092 CR2, GRC-02-113 CQ6, GRC-02-223 BU1, GRC-02-223 BT1, GRC-02-223 BC2, GRC-02-223 BC1,

GRC-02-223 BI1, GRC-02-223 AH1, GRC-02-223 AP2, GRC-02-027 CN2, GRC-02-027 CN4, GRC-08-077 CO1.

Other material examined: Slide GRC-02-222 sp. 1 5 (*Iophon radiatum*), provided by Dr. Marco Bertolino, University of Genoa.

Description: The sponge samples analysed are encrusting and have a glossy surface with visible spicules, pale yellow colour, and a minimum size of 0.006 cm^2 and a maximum size of 0.234 cm^2.

Skeleton: Not observed.

Megascleres:

1. Tylotes: generally straight, with smooth, fusiform stems, swollen and oval tips usually covered with fine spines (figure 22 A-B).

   Size: 240 (337 ± 34) 420 x 5 (11 ± 3) 20 μm.

2. Acanthostyles: uncommon with spines only on the head.

   Size: 430 (517 ± 36) 580 x 10 (18 ± 4) 20 μm.

3. Styles: completely smooth and very abundant (figure 22 C).

   Size: 360 (507 ± 56) 730 x 5 (16 ± 4) 30 μm.

Microscleres:

1. Palmate anisochelae: with the shaft ending in a sharp spur and arranged in rosettes or solitary (figure 22 D-E).

   Size: 10 (22 ± 6) 52.5 x 2.5 (6 ± 3) 12.5 μm.

2. Bipocillas: very abundant and variable in size (figure 22 F).

   Size: 5 (10 ± 2) 15 µm.

Remarks:

In our specimens, acanthostyles were not as abundant as described by Topsent (1901) in the original description of the species. Styles, not mentioned in the original description, were very common.

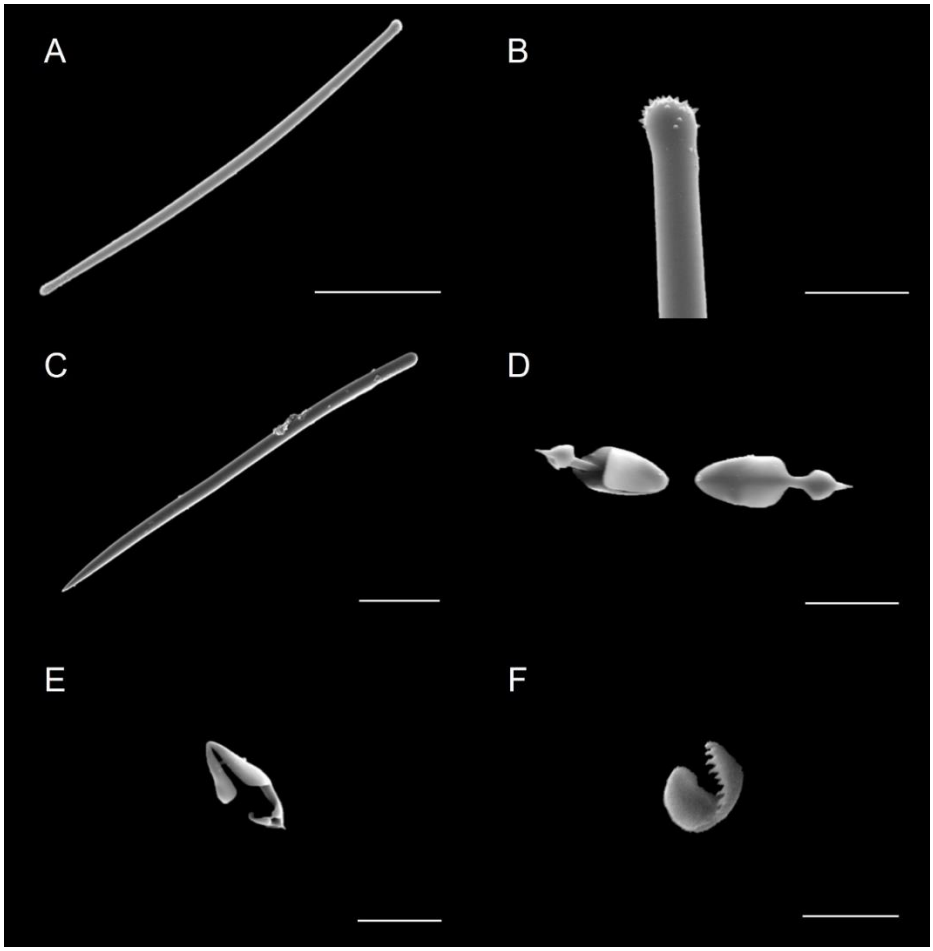

Figure 22: *Iophon radiatum* Topsent, 1901. SEM images of the spicules: **A**. Tylote. **B**. Detail of one spined head of a tylote. **C**. Smooth style. **D**. Palmate anisochelae with the shaft ending in a sharp spur. **E**. Palmate anisochela in side view. **F**. Bipocillum. **Scale bars**: **A-C**: 100 µm, **B-D-E**: 20 µm, **F**: 10 µm.

Family Acarnidae Dendy, 1922

Genus *Iophon* Gray, 1867

Species *Iophon unicorne* Topsent, 1907

Locality and material: Iselin Bank. 72° 16.1196' S, 176° 36.2814' W and 72° 15.7728' S, 176° 35.5638' W. Depth 670 m. Cape Hallett Canyon. 71° 58.8666' S, 172° 11.6298' E and 71° 59.2512' S, 172° 10.6020' E. Depth 750 m. Two specimens: GRC-02-223 BS1, GRC-08-023 DC1.

Other material examined: Slide GRC-08-022 sp. 1 4 (*Iophon unicorne*), provided by Dr. Marco Bertolino, University of Genoa.

Description: The sponge samples analysed are encrusting, with an irregular surface, brown colour, and a minimum size of 0.006 cm^2 and a maximum size of 0.234 cm^2.

Skeleton: Not observed.

Megascleres:

1. Mucronated styles: smooth, with one end mucronate and the other pointed (figure 23 A-B).

   Size: 420 (493 ± 41) 550 x 10 (15 ± 4) 20 μm.

2. Tylotes: generally straight, with smooth, fusiform stems, swollen and oval endings usually covered with fine spines (figure 23 C-D).

   Size: 170 (299 ± 77) 410 x 5 (9 ± 3) 15 µm.

Microscleres:

1. Palmate anisochelae: with the shaft ending in a sharp spur (figure 23 E-F).

   Size: 17.5 (23 ± 4) 30 x 5 (8 ± 2) 12.5 µm.

2. Bipocillas: very small and rounded.

   Size: 5 (11 ± 2) 12.5 µm.

Remarks: The samples analysed are in full compliance with the original description of the species by Topsent (1907).

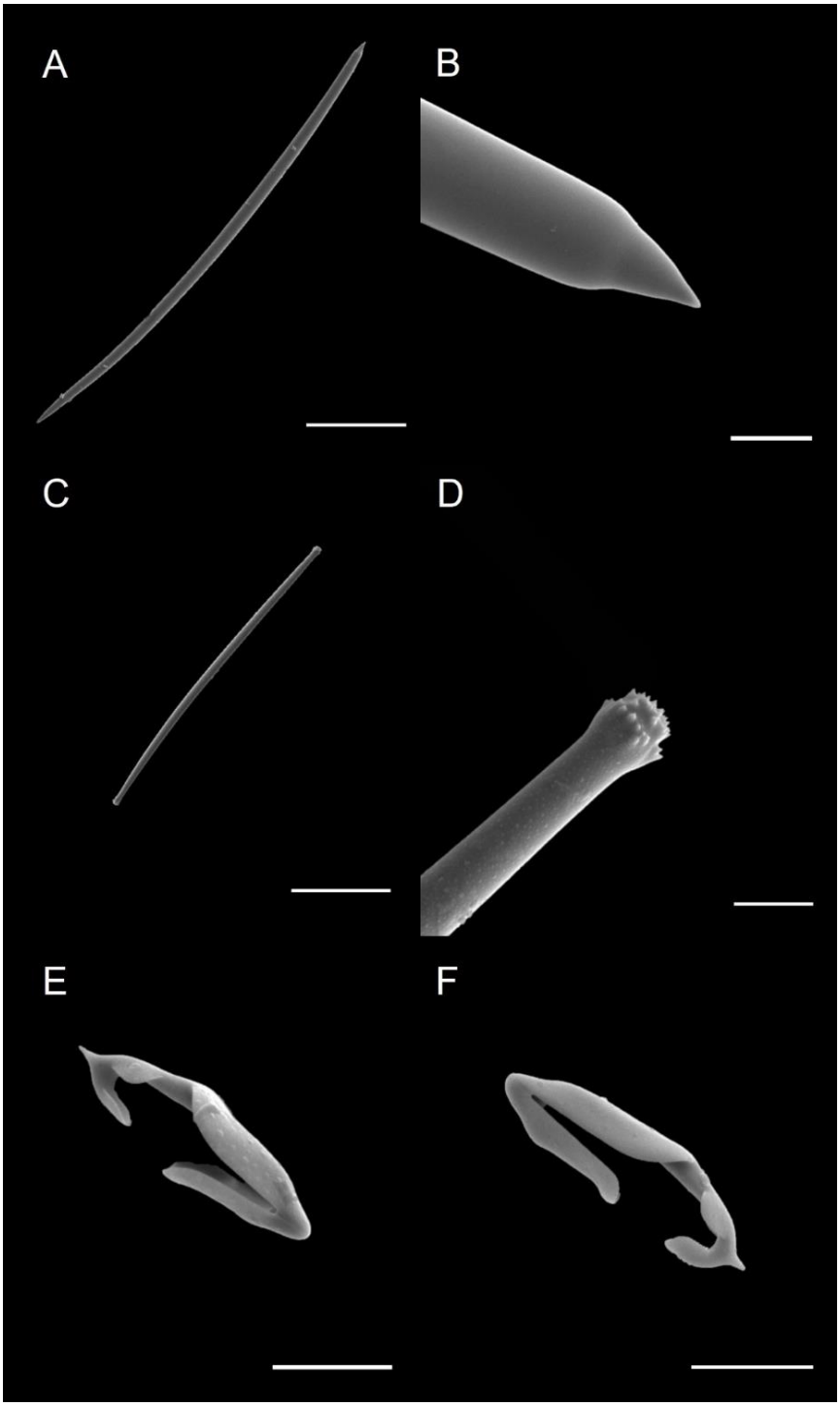

Figure 23: *Iophon unicorne* Topsent, 1907. SEM images of the spicules: **A**. Style. **B**. Detail of a mucronated head of a style. **C**. Tylote. **D**. Detail of one spined head of a tylote. **E-F**. Palmate anisochelae in side views. **Scale bars**: **A-C**: 100 µm, **B-D-E-F**: 10 µm.

Family Cladorhizidae Dendy, 1922

Genus *Asbestopluma* Topsent, 1901

Species *Abestopluma (Asbestopluma)* sp.

Locality and material: Iselin Bank. 72° 16.1196' S, 176° 36.2814' W and 72° 15.7728' S, 176° 35.5638' W. Depth 670 m. One specimen: GRC-02-223 E1.

Other material examined: Slide GRC-08-024 sp.1 11 (*Abestopluma (Asbestopluma)* sp.), provided by Dr. Marco Bertolino, University of Genoa.

Description: The sponge sample analysed has a size of 0.01 cm^2, with a massive, round shape. Tufts of strongyloxeas are visible, emerging from the sponge. The colour of the sponge is whitish.

Skeleton: Not observed.

Megascleres:

1. Strongyloxeas: very long and smooth.

   Size: 670 (930 ± 217) 1540 x 20 (22 ± 4) 30 μm.

2. Styles: smooth, variable in size and some slightly curved.

   Size: 250 (414 ± 90) 500 x 10 (17 ± 5) 20 μm.

Microscleres:

1. Anisochelae: small with unequal ends.

   Size: 12.5 (13 - 1) 15 x 2.5 μm.

2. Smooth sigmas: small and C-shaped.

Size: 42.5 (49 ± 5) 55 x 5 μm.

Remarks: Recognition of the typical spicules of this species was relatively difficult as the sample had foreign spicules, possibly due to contamination. Despite this, both macro- and miscroscleres, characteristic of the genus, have been successfully recognised.

Family Coelosphaeridae Dendy, 1922

Genus *Lissodendoryx* Topsent, 1892

Subgenus *Lissodendoryx (Lissodendoryx)* Topsent, 1892

Species *Lissodendoryx (Lissodendoryx) complicata* (Hansen, 1885) *sensu* Boury-Esnault & Van Beveren (1982)

Locality and material: Iselin Bank. 72° 16.1196' S, 176° 36.2814' W and 72° 15.7728' S, 176° 35.5638' W. Depth 670 m. Three specimens: GRC-02-223 O1, GRC-02-223 CA2, GRC-02-223 CB1.

Other material examined: None.

Description: The sponge samples analysed are encrusting with a smooth surface and an ochre colour. Their size varies from 0.027-0.132 cm^2.

Skeleton: Not observed.

Megascleres:

1. Styles: curved and slightly fusiform (figure 24 A).

   Size: 580 (735 ± 88) 880 x 20 (25 ± 5) 30 µm.

2. Tylotornotes: with one end bulging and the other pointed (figure 24 B).

   Size: 290 (369 ± 41) 425 x 10 (11 ± 2) 15 µm.

Microscleres:

1. Isochelae: small arcuate, with both tridentate ends (figure 24 C-D).

   Size: 25 (35 ± 4) 42.5 x 12.5 (17 ± 2) 22.5 µm.

2. Sigmas: C-shaped (figure 24 E-F).

   Size: 25 (32 ± 4) 40 x 2.5 (4 ± 1) 5 µm.

Remarks: Our specimens fit well, in the size and shape of the spicules, with the species described by Boury-Esnault & Van Beveren (1982). Actually, *Lissodendoryx (L.) complicata* (Hansen, 1885) is known from Arctic and Norwegian and as consequence, the conspecificity between our specimen and the species described by Hansen (1885) is unlikely considering the huge geographical separation, contrary to Boury-Esnault & Van Beveren (1982)'s claim, according to which the species has a bipolar distribution. It should be considered as a probable new species.

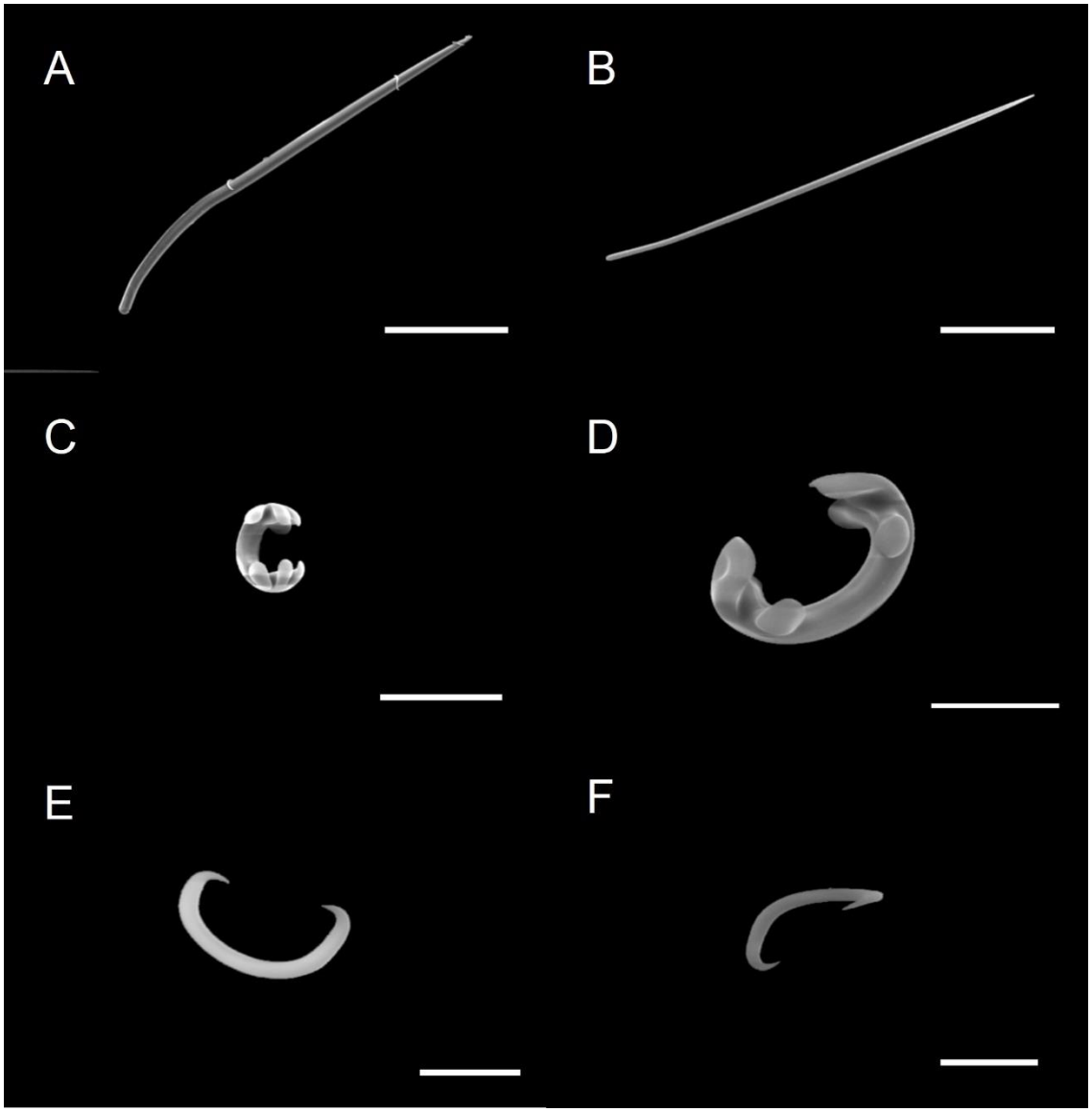

Figure 24: *Lissodendoryx (Lissodendoryx) complicata* (Hansen, 1885) *sensu* Boury-Esnault & Van Beveren (1982). SEM images of the spicules: **A**. Curved and slightly fusiform style. **B**. Tylotornote. **C-D.** Tridentate isochelae. **E-F**. Sigmas. **Scale bars**: **A**: 200 µm, **B**: 100 µm, **C**: 50 µm, **D-E-F**: 20 µm.

Family Coelosphaeridae Dendy, 1922

Genus *Lissodendoryx* Topsent, 1892

Subgenus *Lissodendoryx (Lissodendoryx)* Topsent, 1892

Species *Lissodendoryx (Lissodendoryx) styloderma* Hentschel, 1914

Locality and material: Iselin Bank. 72° 16.1196' S, 176° 36.2814' W and 72° 15.7728' S, 176° 35.5638' W. Depth 670 m. Cape Hallett Canyon. 71° 58.8666' S, 172° 11.6298' E and 71° 59.2512' S, 172° 10.6020' E. Depth 750 m. Two specimens: GRC-02-223 BV1, GRC-02-223 CX1.

Other material examined: None.

Description: The sponges analysed are encrusting with a smooth surface and a typical red-orange colour and sizes between 0.045 and 0.564 cm^2.

Skeleton: Only the ectosomal skeleton has been observed; it consists in loose bundles of dermal styles and scattered chelae.

Megascleres:

1. Styles: fusiform, slightly sinuous and with spined head and pointed tip (figure 25 A-B).

   Size: 550 (673 ± 83) 810 x 15 (16 ± 2) 20 µm.
2. Dermal styles: Thin, fusiform, markedly sinuous, with mucronate head and pointed end (figure 25 C-D).

Size: 300 (356 ± 39) 425 x 7.5 (9.5 ± 1) 10 µm.

Microscleres:

1. Isochelae: small and arcuate with characteristic folded wings (figure 25 E-F-G-H).

   Size: 22.5 (31 ± 4) 40 x 10 (11 ± 1) 12.5 µm.

Remarks: The sizes and shapes of the spicules in our specimens match the original description of the species by Hentschel (1914).

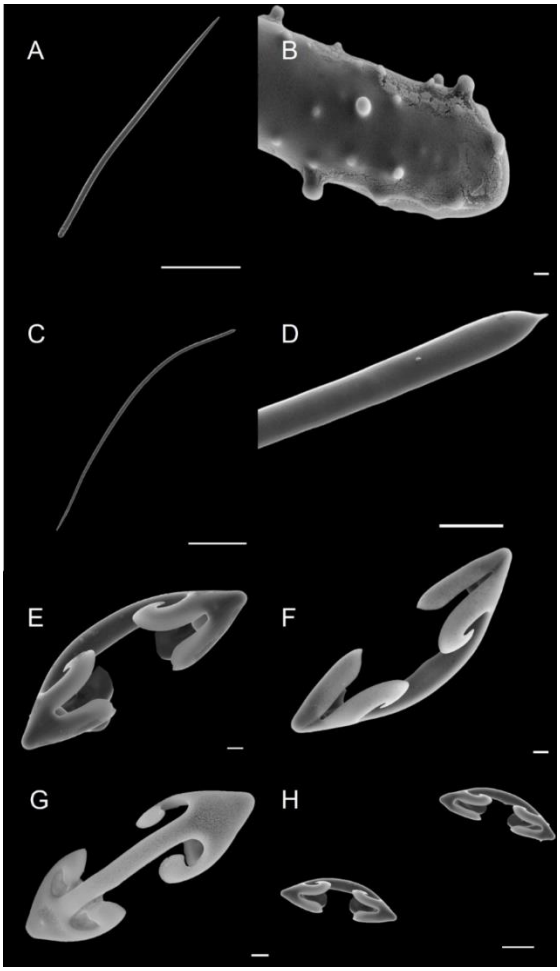

Figure 25: *Lissodendoryx (Lissodendoryx) styloderma* Hentschel, 1914. SEM images of the spicules: **A**. Sinuous, fusiform style. **B**. Magnification of the spined head of a style. **C**.

Fusiform dermal style. **D**. Detail of the mucronated head of a dermal style. **E-H**. Different side views of isochelae. **Scale bars**: **A**: 200 μm, **B**: 2 μm, **C**: 100 μm, **D**: 10 μm, **E-F-G**: 2 μm, **H**: 10 μm.

Family Coelosphaeridae Dendy, 1922

Genus *Lissodendoryx* Topsent, 1892

Subgenus *Lissodendoryx (Ectyodoryx)* Lundbeck, 1909

Species *Lissodendoryx (Ectyodoryx) nobilis* (Ridley & Dendy, 1886)

Locality and material: Iselin Bank. 72° 16.1196' S, 176° 36.2814' W and 72° 15.7728' S, 176° 35.5638' W. Depth 670 m. One specimen: GRC-02-223 AL3.

Other material examined: Slide GRC-08-023 sp. 2 5 (*Lissodendoryx (Ectyodoryx) nobilis*), provided by Dr. Marco Bertolino, University of Genoa.

Description: The sponge is encrusting and has a whitish to light yellow colouration and a size of 0.105 cm^2.

Skeleton: Not observed.

Megascleres:

1. Styles: slightly curved; entirely smooth or with a very slightly spined head, and gradually sharp-pointed (figure 26 A).

Size: 420 (467 ± 66) 600 x 10 (13 ± 3) 15 µm.

2. Smaller styles: entirely spined, and straight (figure 26 B).

   Size: 200 (215 ± 8) 225 x 10 (11 ± 2) 15 µm.

3. Tornotes: with spined heads; in some cases, tornotes have one truncated end (figure 26 C).

   Size: 200 (241 ± 15) 260 x 10 µm.

Microscleres:

1. Isochelae: small, arcuate, and tridentate (figure 26 D).

   Size: 27.5 (35 ± 3) 40 x 12.5 (13 ± 1) 15 µm.

Remarks: Shapes and sizes of spicules are entirely in line with those of the species described by Ridley and Dendy (1886).

Figure 26: *Lissodendoryx (Ectyodoryx) nobilis* (Ridley & Dendy, 1886). Optical microscope images of the spicules: **A**. slightly curved style. **B**. entirely spined, and straight smaller style. **C**. Tornote with one truncated end. **D**. Arcuate isochela. **Scale bars**: **A-B-C-D**: 100 µm.

Family Coelosphaeridae Dendy, 1922

Genus *Lissodendoryx* Topsent, 1892

Subgenus *Lissodendoryx (Ectyodoryx)* Lundbeck, 1909

Species *Lissodendoryx (Ectyodoryx)* sp.

Locality and material: Iselin Bank. 72° 16.1196' S, 176° 36.2814' W and 72° 15.7728' S, 176° 35.5638' W. Depth 670 m. One specimen: GRC-02-223 D2.

Other material examined: Slide GRC-08-024 sp. 2 9 (*Lissodendoryx (Ectyodoryx)* cf. *nobilis*), provided by Dr. Marco Bertolino, University of Genoa.

Description: The sponge sample analysed is encrusting and has a whitish to light yellow colouration and a size of 1.483 cm^2.

Skeleton: Not observed.

Megascleres:

1. Styles: with a rounded and spined head. Many styles are smooth but with a single thorn, lateral to the rounded head (figure 27 A).

   Size: 260 (476 ± 92) 620 x 10 (26 ± 7) 40 µm.

2. Acanthostyles: small, entirely spined (figure 27 B).

   Size: 125 (190 ± 22) 215 x 10 (13 ± 3) 15 µm.

3. Tornotes: with round and spined heads (figure 27 C).

   Size: 255 (265 ± 7) 275 x 10 µm.

Microscleres:

1. Sigmas: C-shaped (figure 27 D-E).

   Size: 40 (46 ± 5) 55 x 2.5 (3 ± 1) 5 µm.

2. Isochelae: small, arcuate and tridentate (figure 27 F).

   Size: 45 (50 ± 2) 55 x 5 µm.

Remarks: Although it has similar spicules set to the species *Lissodendoryx (Ectyodoryx) nobilis* (Ridley & Dendy, 1886), the differences in shape and size of the spicules do not allow it to be classified as such, so it should be considered as a new species.

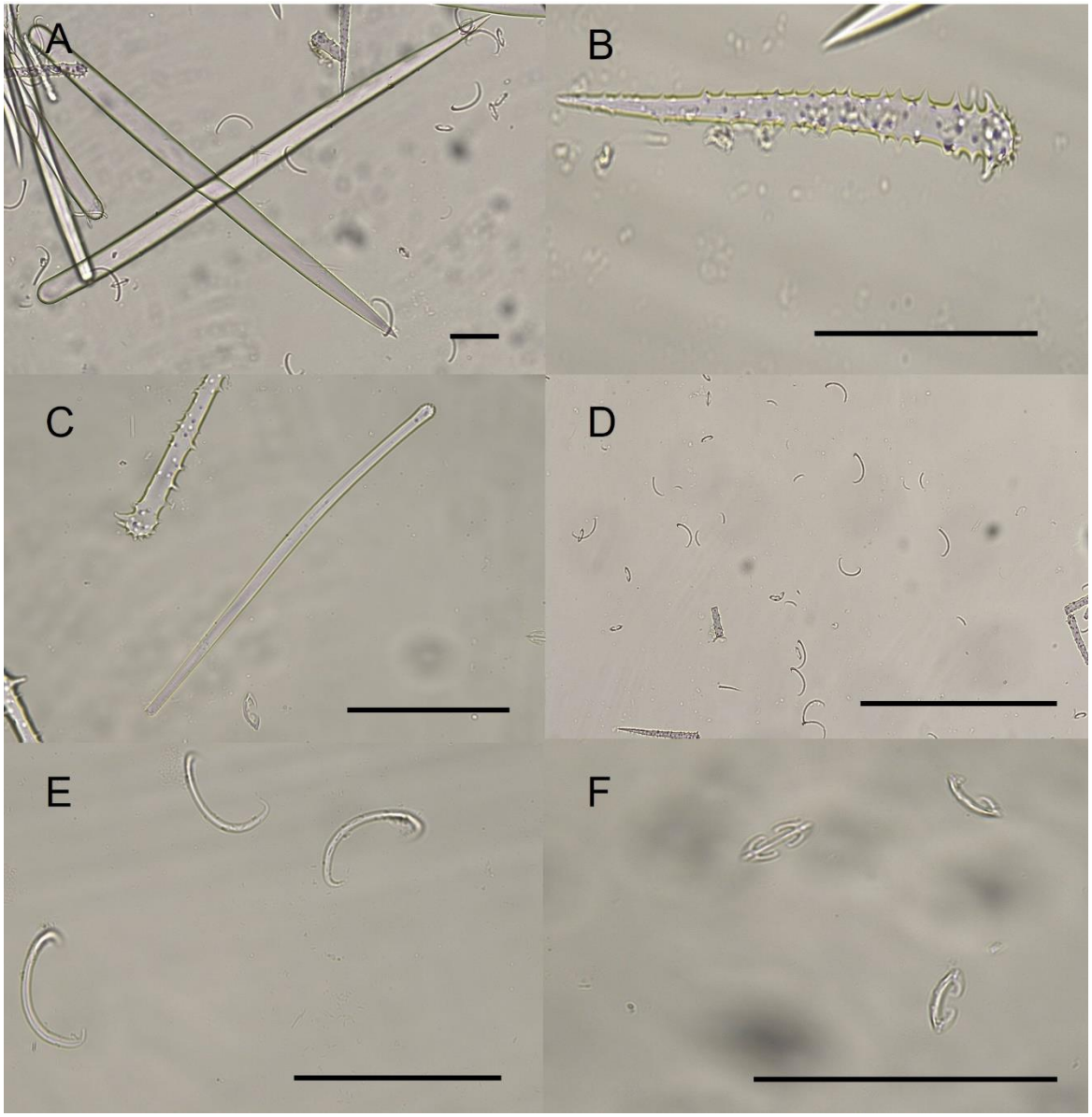

Figure 27: *Lissodendoryx (Ectyodoryx)* sp. Optical microscope images of the spicules: **A**. Smooth style. **B**. Acanthostyle. **C**. Tornote with both rounded and spined ends. **D-E**. Sigmas. **F**. Arcuate isochelae. **Scale bars**: **A-B-C-D-E-F**: 100 µm.

Family Esperiopsidae Hentschel, 1923

Genus *Amphilectus* Vosmaer, 1880

Species *Amphilectus rugosus* (Thiele, 1905)

Locality and material: Iselin Bank. 72° 16.1196' S, 176° 36.2814' W and 72° 15.7728' S, 176° 35.5638' W. Depth 670 m. Three specimens: GRC-02-223 AM5, GRC-02-223 BV2, GRC-02-223 CE1.

Other material examined: Slide GRC-02-223 sp. 4 1 (*Amphilectus rugosus*), provided by Dr. Marco Bertolino, University of Genoa.

Description: The sponge samples analysed are encrusting, ochre-coloured, with an irregular surface and a size ranging from 0.037 to 0.178 cm^2.

Skeleton: Not observed.

Megascleres:

1. Styles: smooth and slightly curved with one strongly pointed end (figure 28 A).

   Size: 400 (465 ± 54) 580 x 10 (14 ± 3) 20 μm.

Microscleres:

1. Isochelae: small and arcuate (figure 28 B).

   Size: 25 (33 ± 5) 50 x 7.5 (10 ± 2) 12.5 µm.

Remarks: Shapes and sizes of spicules are entirely in line with those of the species described by Thiele (1905).

Figure 28: *Amphilectus rugosus* (Thiele, 1905). Optical microscope images of the spicules: **A**. Smooth and slightly curved style. **B**. Isochelae. **Scale bars**: **A-B**: 100 µm.

Family Esperiopsidae Hentschel, 1923

Genus *Esperiopsis* Carter, 1882

Species *Esperiopsis villosa* (Carter, 1874) *sensu* Koltun (1964)

Locality and material: Iselin Bank. 72° 16.1196' S, 176° 36.2814' W and 72° 15.7728' S, 176° 35.5638' W. Depth 670 m. Three specimens: GRC-02-223 AO1, GRC-02-223 AV1, GRC-02-223 AV4.

Other material examined: Slide GRC-02-223 sp. 6 8 (*Esperiopsis villosa*), provided by Dr. Marco Bertolino, University of Genoa.

Description: The sponge samples analysed are encrusting, greyish in colour with a size ranging from 0.037 to 0.464 cm^2.

Skeleton: Not observed.

Megascleres:

1. Styles: smooth, characterised by one rounded and one gradually pointed end (figure 29 A).

   Size: 490 (599 ± 49) 670 x 10 (16 ± 5) 20 µm

Microscleres:

1. Sigmas: C-shaped or sigmoid; the central canal is often visible (figure 29 B).

   Size: 85 (100 ± 13) 127.5 x 17.5 (25 ± 6) 45 µm.
2. Isochelae: small and arcuate (figure 29 C-D).

   Size: 25 (43 ± 10) 62.5 x 7.5 (9 ± 1) 10 µm.

Remarks: The sponge samples analysed are in accordance with the original description of the species by Carter (1874). Actually, *Esperiopsis villosa* (Carter, 1874) is known from North Atlantic Ocean and as consequence, the conspecificity between our specimen and the species described by Carter

(1874) is unlikely considering the huge geographical separation. In addition, Koltun (1964) stated that there's an Antarctic form of these species, characterized by 2 instead of 3 types of spicules. For these reasons it should be considered as a probable new species.

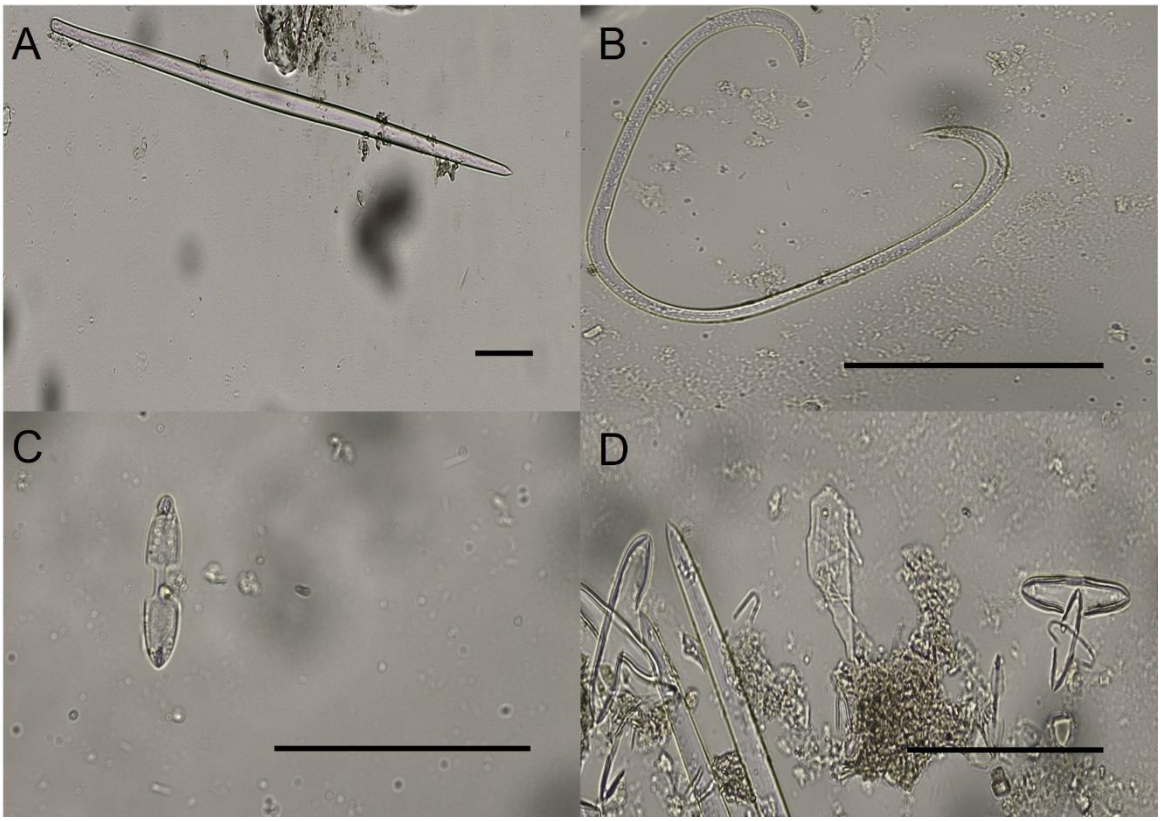

Figure 29: *Esperiopsis villosa* (Carter, 1874) *sensu* Koltun (1964). Optical microscope images of the spicules: **A**. Slightly curved style. **B**. Sigmoid sigma **C-D**. Isochelae. **Scale bars**: **A-B-C-D**: 100 µm.

Family Isodictyidae Dendy, 1924

Genus *Isodictya* Bowerbank, 1864

Species *Isodictya setifera* Topsent, 1901

Locality and material: Iselin Bank. 72° 16.1196' S, 176° 36.2814' W and 72° 15.7728' S, 176° 35.5638' W. Depth 670 m. One specimen: GRC-02-223 G1.

Other material examined: Slide GRC-02-223 27 sp.1 (*Isodictya setifera*), provided by Dr. Marco Bertolino, University of Genoa.

Description: The sponge sample analysed is encrusting, has a size of 0.003 cm^2, a yellowish colour and a soft consistency.

Skeleton: Not observed.

Megascleres:

1. Oxeas: fusiform, smooth with both strongly pointed ends (figure 30 A).

   Size: 450 (753 ± 129) 1010 x 10 (18 ± 4) 20 μm.

Microscleres:

1. Isochelae: small, very numerous (figure 30 B).

   Size: 25 (36 ± 7) 55 x 2.5 (3 ± 1) 5 μm.

Remarks: The sponge sample analysed matches perfectly with the original description of the species by Topsent (1901) in the size and shape of the spicules.

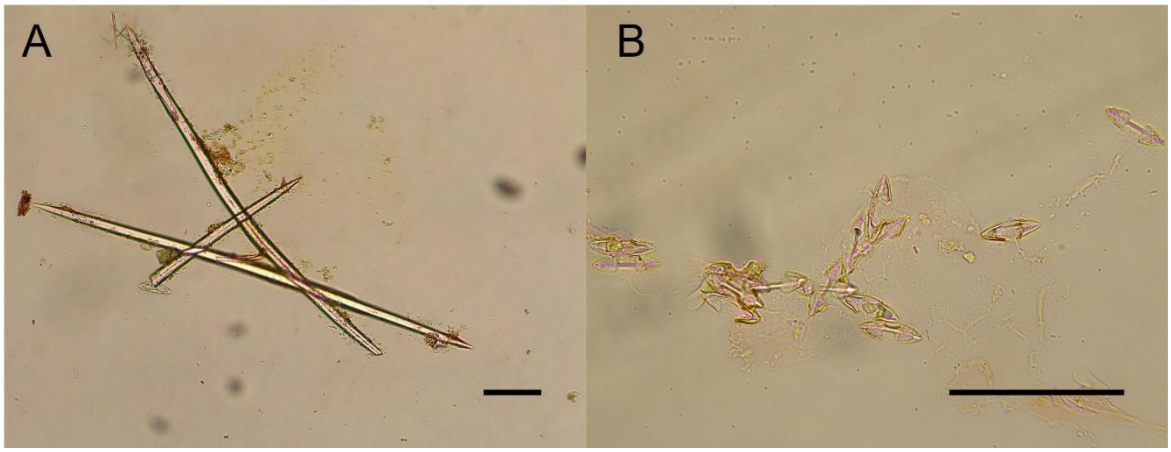

Figure 30: *Isodictya setifera* Topsent, 1901. Optical microscope images of the spicules: **A**. Fusiform oxeas. **B**. Small isochelae. **Scale bars**: **A-B**: 100 µm.

Family Crellidae Dendy, 1922

Genus *Crella* Gray, 1867

Subgenus *Crella (Crella)* Gray, 1867

Species *Crella (Crella) tubifex* (Hentschel, 1914)

Locality and material: Iselin Bank. 72° 16.1196' S, 176° 36.2814' W and 72° 15.7728' S, 176° 35.5638' W. Depth 670 m. Two specimens: GRC-02-223 BO1, GRC-02-223 BO2.

Other material examined: None.

Description: The sponge samples analysed show an irregular surface with visible spicules. They have a minimum size of 0.084 cm^2 and a maximum size of 0.103 cm^2. The colour of the samples is off-white to grey.

Skeleton: Not observed.

Megascleres:

1. Acanthostyles: rather thin, slightly curved, conical, and sharply pointed. Spines are along their whole length (figure 31 A).

   Size: 170 (221 ± 50) 310 x 15 (17 ± 2) 20 µm.
2. Anisostrongyles: straight, cylindrical, but with one well-developed heads, and the other slightly swollen (figure 31 B).

   Size: 390 (538 ± 78) 660 x 10 (15 ± 5) 20 µm.
3. Acanthostrongyles: fusiform, slightly and irregularly curved, with one swollen end. They present spines along their entire shaft (figure 31 C-D).

   Size: 340 (385 ± 33) 450 x 20 (22 ± 4) 30 µm.

Microscleres: None.

Remarks: The sizes and shapes of the spicules in our specimens match the original description of the species by Hentschel (1914).

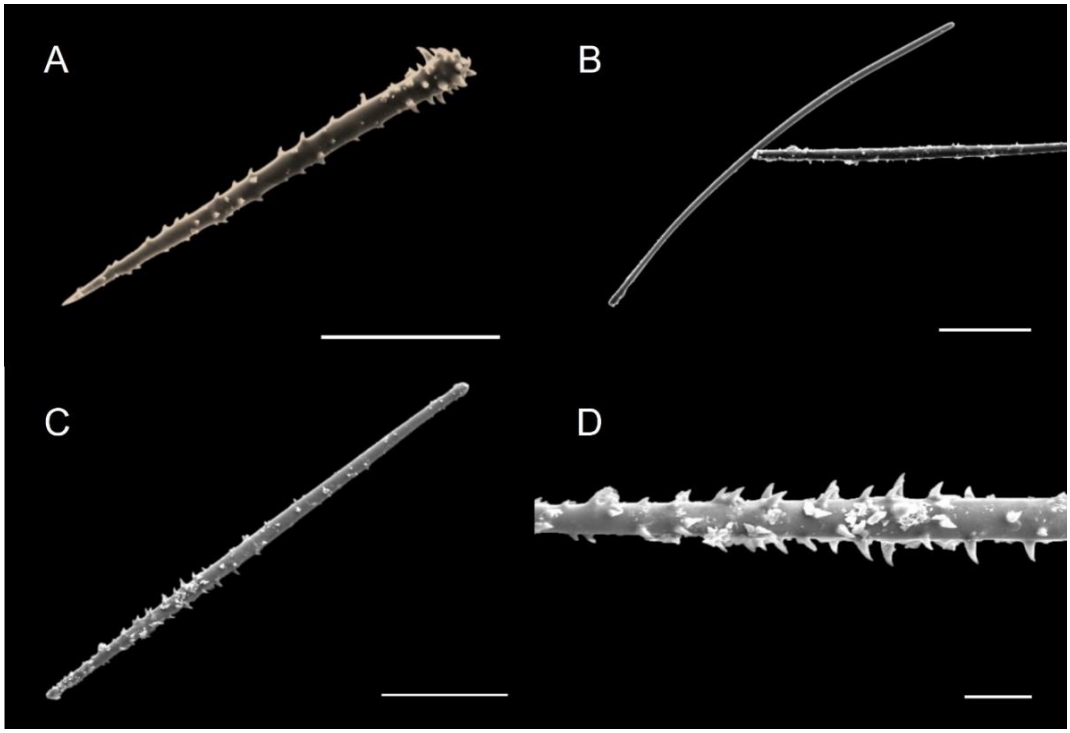

Fig 31: *Crella (Crella) tubifex* (Hentschel, 1914). SEM images of the spicules: **A**. Acanthostyle. **B**. Anisostrongyle. **C**. Acanthostrongyle. **D**. Detail of the spined central portion of acanthostrongyles. **Scale bars**: **A**: 50 µm, **B-C**: 100 µm, **D**: 20 µm.

Family Coelosphaeridae Dendy, 1922

Genus *Inflatella* Schmidt, 1875

Species *Inflatella belli* (Kirkpatrick, 1907)

Locality and material: Iselin Bank. 72° 16.1196' S, 176° 36.2814' W and 72° 15.7728' S, 176° 35.5638' W. Depth 670 m. One specimen: GRC-02-223 AL3.

Other material examined: None.

Description: The sponge is massive, spherical with a small erect, fistular appendage; it is light brown coloured and a size of 0.034 cm^2.

Skeleton: Not observed.

Megascleres:

1. Strongyles: fusiform with both blunt ends, and characterised by a central, slight swelling (figure 32 A-B).

   Size: 450 (469 ± 19) 510 x 10 (11 ± 2) 15 µm.

Microscleres: None.

Remarks: Sponge identification was hampered by the presence of foreign spicules, and the small amount of available material. Spicule size range of the sample is slightly lower than that of the original description of the species by Hentschel (1914): 560 - 720 µm in length and 11 - 13 µm in width; despite this size discrepancy, the shape of the spicules is quite consistent with the description given by Hentschel.

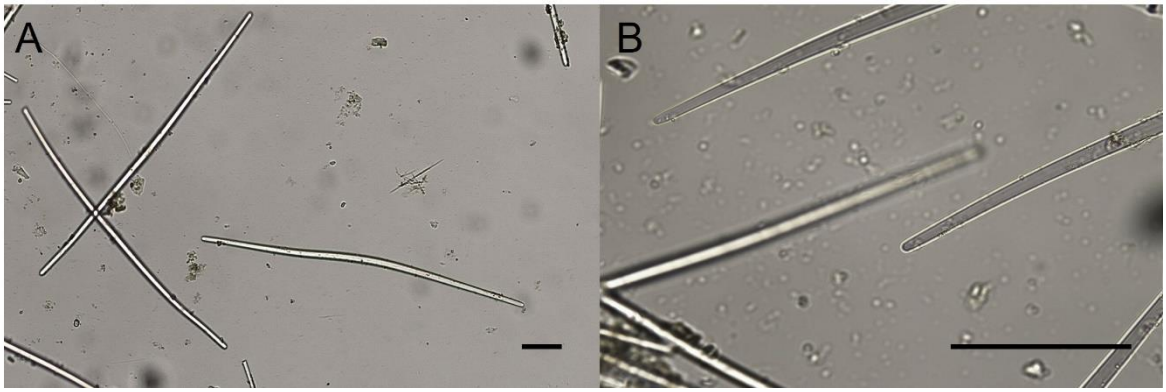

Figure 32: *Inflatella belli* (Kirkpatrick, 1907). Optical microscope images of the spicules: **A**. Fusiform strongyles. **B**. Detail of blunt ends of strongyles. **Scale bars**: **A-B**: 100 µm.

Family Microcionidae Carter, 1875

Subfamily Ophlitaspongiinae Laubenfels, 1936

Genus *Artemisina* Vosmaer, 1885

Species *Artemisina plumosa* Hentschel, 1914

Locality and material: Iselin Bank. 72° 16.1196' S, 176° 36.2814' W and 72° 15.7728' S, 176° 35.5638' W. Depth 670 m. Hallett Ridge. 72° 23.0340' S, 176° 06.1020' E and 72° 23.3868' S, 176° 06.2094' E. Depth 910 m. Five specimens: GRC-02-223 AN2, GRC-02-223 Q1, GRC-02-223 BC3, GRC-02-223 BC4, GRC-02-223 CV1.

Other material examined: None.

Description: The sponge is massive, slightly bushy light grey coloured and is characterized by a bristly surface. The sponge varied in size from 0.031 cm^2 to 0.188 cm^2

Skeleton: Not observed.

Megascleres:

1. Large styles: slightly curved, fusiform (figure 33 A).

   Size: 600 (1471 ± 501) 2600 x 20 (25 ± 4) 30 µm.

2. Small styles: fusiform, strongly curved (figure 33 B).

   Size: 380 (476 ± 50) 530 x 15 (16 ± 2) 20 µm.

3. Tylotes: with round, slightly spined heads.

   Size: 260 (372 ± 56) 480 x 5 (6 ± 2) 10 µm.

Microscleres:

1. Isochelae: small, curved (figure 33 C-D).

   Size: 7.5 (13 ± 2) 15 x 2.5 (5 ± 1) 7.5 µm

2. Toxas: characterised by a very evident, angular central curve. The size and relative angle of curves varies greatly among these spicules, which are also, but not always, characterised by spined and slightly curved ends (figure 33 E-F).

   Size: 90 (216 ± 95) 600 x 5 (5.1 ± 1) 10 µm.

Remarks: The megascleres of the present samples show a wider size range than that reported by Hentschel (1914) in his original description of the species: according to Hentschel, in fact, the large styles are up to 1232 µm long, while the small ones are up to 456 µm long. The size of the isochelae is similar, while our toxas are longer than those measured by Hentschel (96 - 144 µm).

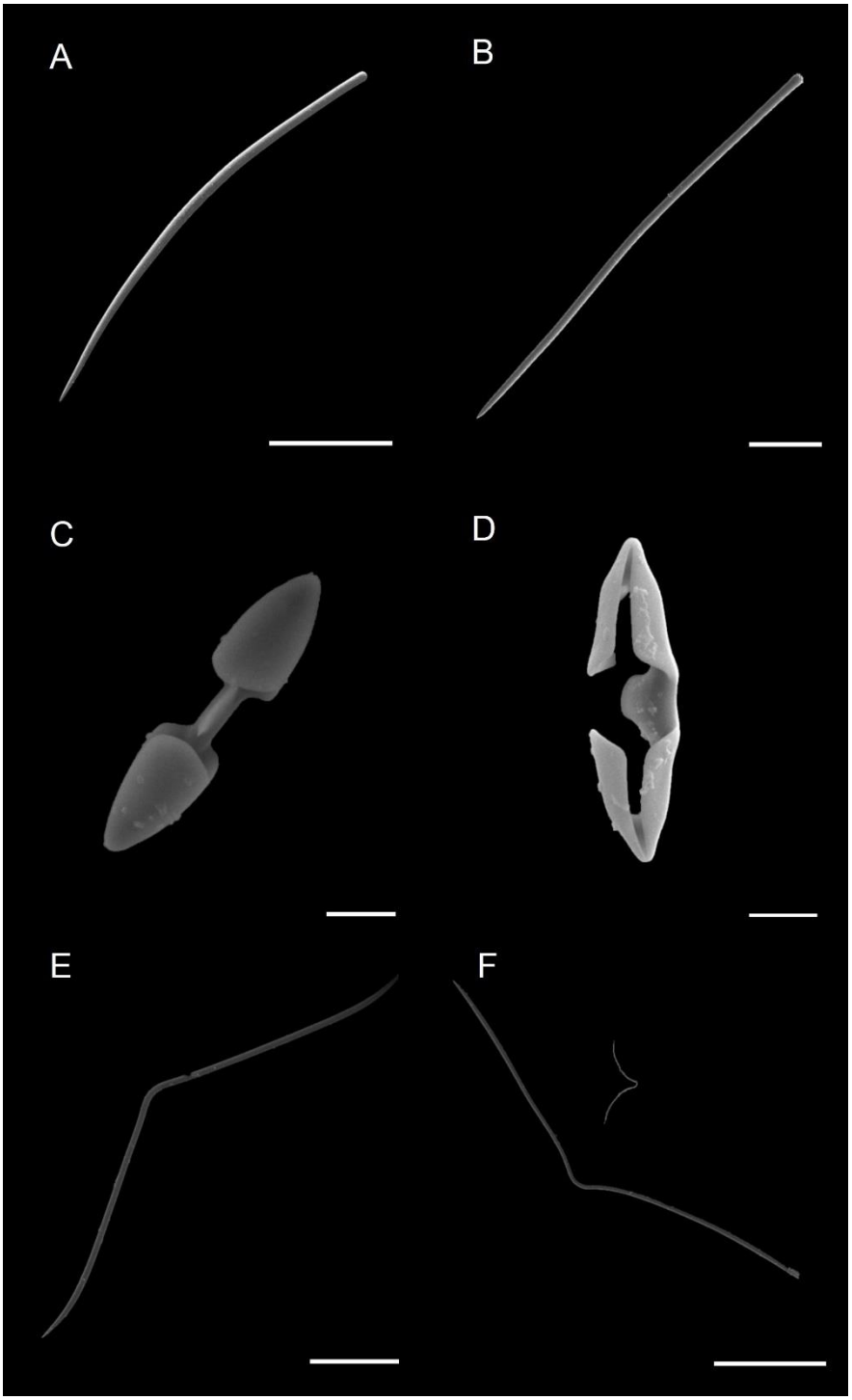

Figure 33: *Artemisina plumosa* Hentschel, 1914. SEM images of the spicules: **A**. Large styles. **B**. Small styles. **C-D**. Isochelae from different lateral views. **E-F**. Toxas. **Scale bars**: **A**: 200 µm, **B-E**: 50 µm, **F**: 100 µm, **C-D**: 5 µm.

Family Microcionidae Carter, 1875

Subfamily *Microcioninae Carter, 1875*

Genus *Clathria* Schmidt, 1862

Species *Clathria (Clathria) paucispicula* (Burton, 1932)

Locality and material: Iselin Bank. 72° 16.1196' S, 176° 36.2814' W and 72° 15.7728' S, 176° 35.5638' W. Depth 670 m. Seventeen specimens: GRC-02-223 A4, GRC-02-223 A5, GRC-02-223 C1, GRC-02-223 C2, GRC-02-223 C3, GRC-02-223 E3, GRC-02-223 O2, GRC-02-223 S2, GRC-02-223 AL, GRC-08-065 CM3, GRC-02-091 CU8, GRC-02-133 CT3, GRC-02-223 BB5, GRC-02-223 BB1, GRC-02-223 BF1, GRC-02-093 CS1, GRC-02-093 CS5.

Other material examined: GRC-02-223 sp.1 17 (*Clathria (Clathria) paucispicula*), GRC-02-223 sp.1 15 (*Clathria (Clathria) paucispicula*) provided by Dr. Marco Bertolino, University of Genoa.

Description: The sponge samples analysed were massive, round and light beige in colour. Their size ranges from 0.010 cm^2 to 1.794 cm^2.

Skeleton: Composed of irregular bundles of styles running perpendicularly to the surface.

Megascleres:

1. Styles: mainly straight, smooth, and sinuous (figure 34 A).

   Size: 540 (686 ± 76) 950 x 10 (22 ± 4) 35 µm.

2. Auxiliary styles: characterised by lesser width and a distinct sinuosity (figure 34 B).

   Size: 220 (324 ± 67) 500 x 5 (7 ± 3) 15 µm.

Microscleres: Absent.

Remarks: The spicules set and the skeletal organisation correspond to the species described by Burton (1932), although the size of the spicules is slightly larger than in the original description, according to which the main styles measure 540 to 710 µm and the auxiliary styles 240 to 310 µm.

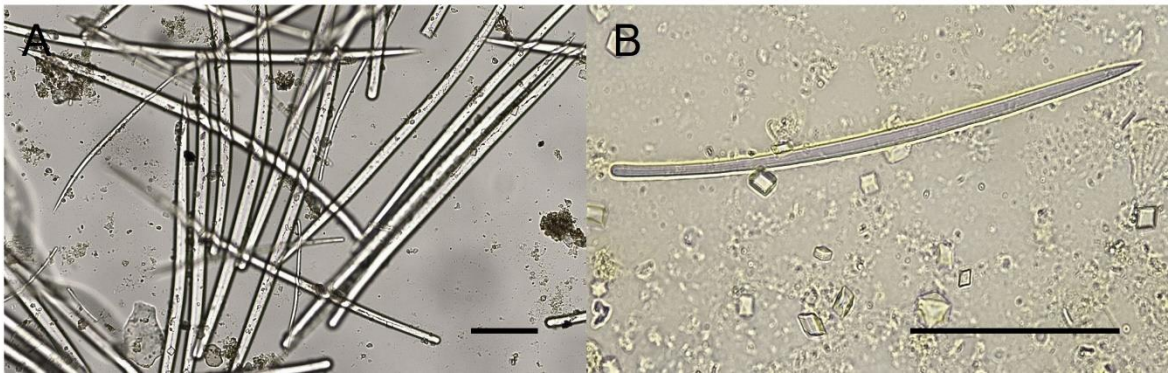

Figure 34: *Clathria (Clathria) paucispicula* (Burton, 1932). Optical microscope images of the spicules: **A**. Styles. **B**. Auxiliary styles. **Scale bars**: **A-B**: 100 µm.

Family Microcionidae Carter, 1875

Subfamily *Microcioninae Carter, 1875*

Genus *Clathria* Schmidt, 1862

Species *Clathria* sp.

Locality and material: Iselin Bank. 72° 16.1196' S, 176° 36.2814' W and 72° 15.7728' S, 176° 35.5638' W. Depth 670 m. One specimen: GRC-02-223 A3.

Other material examined: None.

Description: The sponge sample analysed is encrusting, with small spicules visible from the outside, making the surface shaggy. It shows a red to brown colouration and has a size of 0.078 cm^2.

Skeleton: Not observed.

Megascleres:

1. Styles: with a rounded and spined head. The styles are variable in length and thickness and show a very marked morphological difference, as some are completely straight, while others are sinuous.

   Size: 520 (1355 ± 828) 3000 x 20 (24 ± 8) 40 µm.
2. Acanthostyles: small, entirely spined.

   Size: 170 (231 ± 35) 300 x 5 (10 ± 3) 15 µm.
3. Tylotes: spicules with both rounded ends.

   Size: 510 (571 ± 39) 650 x 20 (21 ± 4) 30 µm.

Microscleres:

1. Oxhorns toxas: slightly curved in the middle.

   Size: 50 (68 ± 7) 70 x 10 (11 ± 4) 20 μm.

Remarks: The sample belongs to the Microconidae family, which is characterized by smooth styles, with some diactinal and acanthose modifications and palmate isochelae and toxas (Hooper, 2002). The small dimension of the sample prevented us to study the skeletal organization, but the spicule set is typical of species of the genus *Clathria*. The species is characterized by the presence of oxhorns toxas that are not present in species of the family Microcionidae known from Antarctica.

Family Microcionidae Carter, 1875

Subfamily *Microcioninae Carter, 1875*

Genus *Clathria* Schmidt, 1862

Species *Clathria (Microciona)* sp. 1

Locality and material: Hallett Ridge. 72° 23.0340' S, 176° 06.1020' E and 72° 23.3868' S, 176° 06.2094' E. Depth 910 m. One specimen: GRC-07-028 CVN.

Other material examined: Slide GRC-02-222 sp.1 10 (*Clathria (Microciona)* sp. 1), provided by Dr. Marco Bertolino, University of Genoa.

Description: The sponge sample analysed has a size of 0.193 cm^2. It has protruding spicules on its surface and is whitish to light grey in colour.

Skeleton: Hymedesmioid, with echinating styles perpendicular to the sponge surface and forming ascending tracts, typical of *Microciona*.

Megascleres:

1. Large styles: smooth, fusiform (figure 35 A).

   Size: 550 (647 ± 65) 740 x 20 (27 ± 4) 30 µm.

2. Small styles: smooth, spicules but slightly smaller in size (figure 35 B).

   Size: 250 (321 ± 38) 400 x 5 (7 ± 2) 10 µm.

3. Acanthostyles: small, entirely spined (figure 35 C).

   Size: 125 (173 ± 32) 205 x 10 (12 ± 3) 15 µm.

Microscleres:

1. Toxas: spicules characterised by angular central curve (figure 35 C-E).

   Size: 135 (343 ± 113) 600 x 10 (12 ± 4) 20 µm.

2. Isochelae: small, curved (figure 35 F).

   Size: 17.5 (23 ± 3) 27.5 x 5 (8 ± 2) 10 µm.

Remarks: Our species does not fit with any species of this subgenus described in Antarctica.

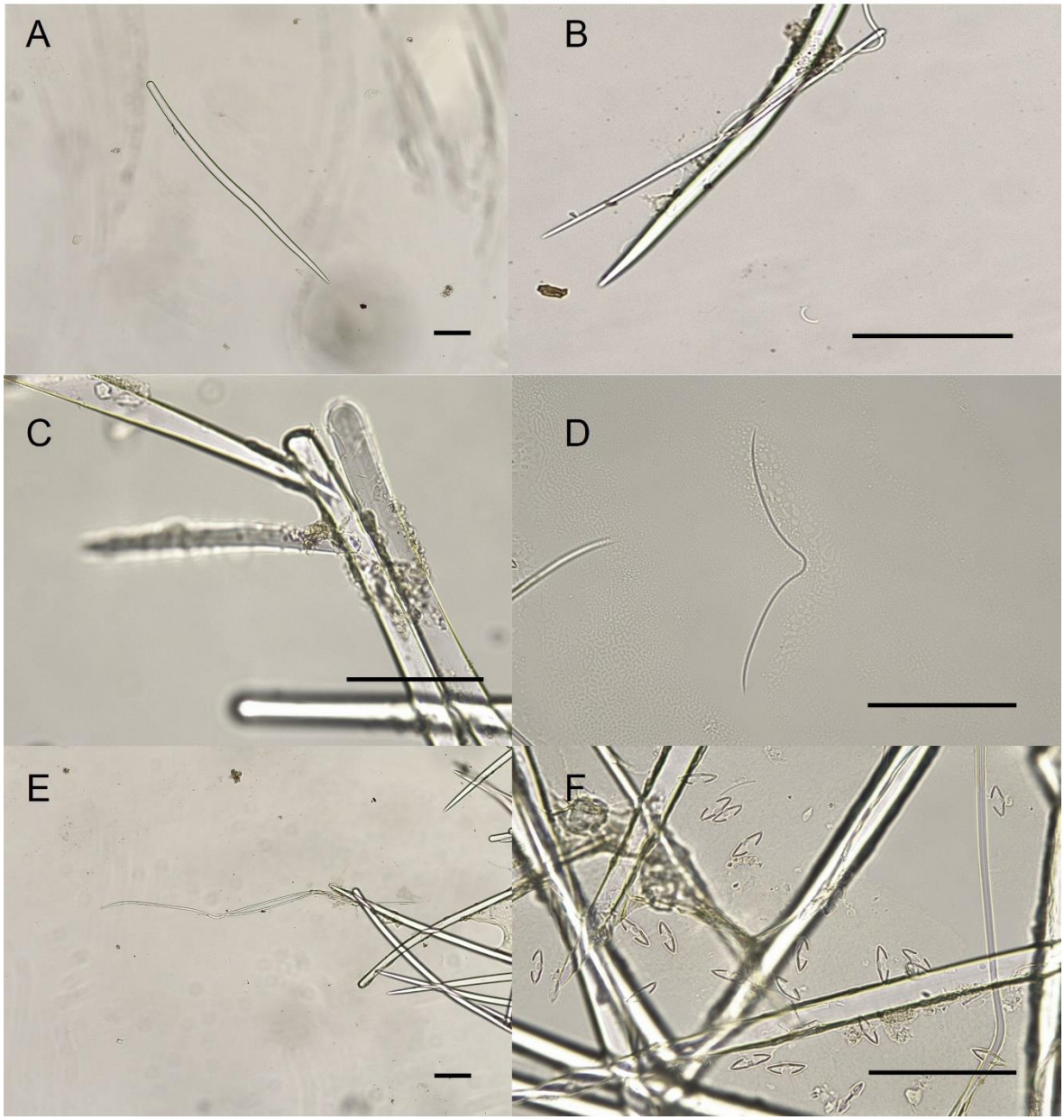

Figure 35: *Clathria (Microciona)* sp. 1. Optical microscope images of the spicules: **A**. Large style. **B**. Small style. **C**. Acanthostyle. **D-E**. Toxas of different sizes. **F**. Isochelae. **Scale bars**: **A-B-C-D-E-F**: 100 µm.

Family Microcionidae Carter, 1875

Subfamily *Microcioninae Carter, 1875*

Genus *Clathria* Schmidt, 1862

Species *Clathria (Microciona)* sp. 2

Locality and material: Iselin Bank. 72° 16.1196' S, 176° 36.2814' W and 72° 15.7728' S, 176° 35.5638' W. Depth 670 m. Hallett Ridge. 72° 23.0340' S, 176° 06.1020' E and 72° 23.3868' S, 176° 06.2094' E. Depth 910 m. Two specimens: GRC-02-223 A6, GRC-07-028 CVL.

Other material examined: Slide GRC-TR17-001 sp. 1 7L (*Clathria (Microciona)* sp. 2), provided by Dr. Marco Bertolino, University of Genoa.

Description: The sponge samples analysed are encrusting, with small spicules protruding and making a hispid appearance. Their size ranges from 0.086 mm^2 to 0.125 mm^2.

Skeleton: Hymedesmioid, with echinating styles perpendicular to the sponge surface and forming ascending tracts, typical of *Microciona*.

Megascleres:

1. Styles: slightly sinuous, with round ends that may be smooth or spined. Size: 400 (656 ± 79) 740 x 10 (22 ± 6) 30 μm.
2. Acanthostyles: small, entirely spined.

Size: 150 (183 ± 22) 250 x 5 (10 ± 4) 15 µm.

Microscleres:

1. Isochelae:

   Size: 17.5 (37 ± 13) 50 x 5 (6 ± 2) 10 µm.

2. Toxas: Characterized by a centrally curved shape, with both ends pointed and spined.

   Size: 185 (467 ± 126) 700 x 5 (10 ± 6) 20 µm.

Remarks: Our species does not fit with any species of this genus or subgenus described in Antarctica.

Family Mycalidae Lundbeck, 1905

Genus *Mycale* Gray, 1867

Subgenus *Mycale (Anomomycale)* Topsent, 1924

Species *Mycale (Anomomycale) titubans* (Schmidt, 1870) *sensu* Boury-Esnault & Van Beveren (1982)

Locality and material: Iselin Bank. 72° 16.1196' S, 176° 36.2814' W and 72° 15.7728' S, 176° 35.5638' W. Depth 670 m. One specimen: GRC-02-223 AH1, GRC-02-223 AU4, GRC-08-065 CM1.

Other material examined: Slide GRC-02-223 sp. 1 2 (*Mycale (Anomomycale) titubans*), provided by Dr. Marco Bertolino, University of Genoa.

Description: The sponge samples analysed are encrusting and have a size comprised from 0.070 to 1.615 cm^2. They are beige to greyish in colour.

Skeleton: Not observed.

Megascleres:

1. . Large styles: slightly curved fusiform with one rounded end and the other pointed (figure 36 A).

   Size: 600 (852 ± 62) 940 x 20 (25 ± 5) 30 µm.
2. Ectosomic styles: fusiform, thin and straight (figure 36 B).

   Size: 380 (441 ± 21) 480 x 10 µm.

Microscleres:

1. Anisochelae: small, curved characterised by a short spur, very distinctive (figure 36 C-D-E-F).

   Size: 27.5 (44 ± 7) 50 x 12.5 (14 ± 1) 15 µm.
2. Sigmas: highly curved C-shaped (figure 36 G-H).

   Size: 70 (80 ± 5) 87.5 x 2.5 µm.

Remarks: The sponges analysed, and the measurements of their spicules, match perfectly with the original description by Schmidt (1870) who described it for the North Atlantic Ocean. In 1982 Boury-Esnault & Van Beveren reported the presence of this species in the Kerguelen Archipelagos. The conspecificity between our specimen and the species described by Schmidt (1870) is unlikely considering the huge geographical separation, thus, it should be considered probably a new species.

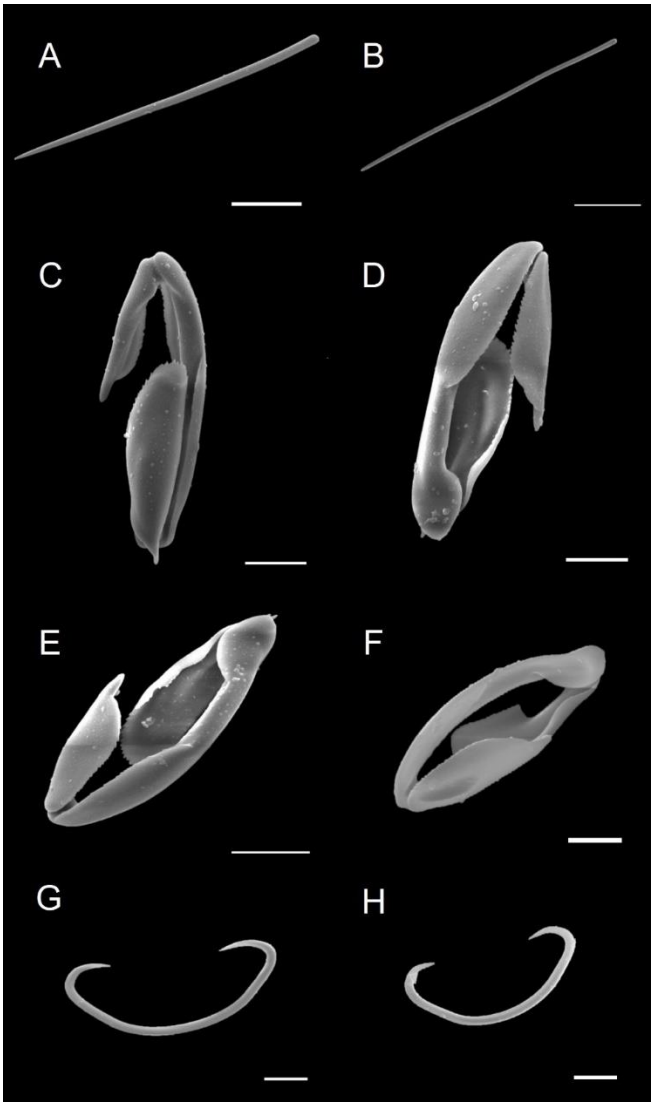

Figure 36: *Mycale (Anomomycale) titubans* (Schmidt, 1870) *sensu* Boury-Esnault & Van Beveren (1982). SEM images of the spicules: **A**. Large style. **B**. Ectosomic style. **C-F**. Anisochelae from different lateral views. **G-H**. Sigmas. **Scale bars**: **A**: 200 µm, **B**: 100 µm, **C-D-E-F-G**: 10 µm, **H**: 20 µm.

Family Myxillidae Dendy, 1922

Genus *Myxilla* Schmidt, 1862

Subgenus *Myxilla (Myxilla)* Schmidt, 1862

Species *Myxilla (Myxilla) elongata* Topsent, 1916

Locality and material: Iselin Bank. 72° 16.1196' S, 176° 36.2814' W and 72° 15.7728' S, 176° 35.5638' W. Depth 670 m. Cape Hallett Canyon. 71° 58.8666' S, 172° 11.6298' E and 71° 59.2512' S, 172° 10.6020' E. Depth 750 m. One specimen: GRC-02-223 B1, GRC-02-223 AM6, GRC-08-023 CY1.

Other material examined: Slide GRC-08-023 sp1. 5 (*Myxilla (Myxilla) elongata*), provided by Dr. Marco Bertolino, University of Genoa.

Description: The samples analysed are encrusting; their size ranges from 0.005 - 0.440 cm^2; they have a greyish colour and an irregular surface.

Skeleton: Not observed.

Megascleres:

1. Tornotes: with a characteristic fusiform shape, slightly curved and with pointed ends (figure 37 A).

   Size: 255 (295 ± 19) 330 x 5 (7 ± 3) 15 μm.

2. Acanthostyles: smooth, with small, scattered spines (figure 37 B).

   Size: 390 (485 ± 78) 680 x 10 (12 ± 3) 20 μm.

Microscleres:

1. Anchorate chelae: present in abundance (figure 37 C).

Size: 27.5 (34 ± 4) 45 x 2.5 (4 ± 1) 5 µm.

2. Sigmas: C-shaped spicules (figure 37 D).

   Size: 35 (56 ± 9) 75 x 2.5 (4 ± 1) 7.5 µm.

Remarks: The spicule size of our specimens matches that reported by Topsent (1916), in the original description of the species.

Figure 37: *Myxilla (Myxilla) elongata* Topsent, 1916. Optical microscope images of the spicules: **A**. Fusiform tornote. **B**. Acanthostyles with small spines **C**. Isochela. **D**. Sigmas. **Scale bars**: **A-B-C-D**: 100 µm.

Family Myxillidae Dendy, 1922

Genus *Myxilla* Schmidt, 1862

Subgenus *Myxilla (Myxilla)* Schmidt, 1862

Species *Myxilla (Myxilla) mollis* Ridley & Dendy, 1886

Locality and material: Iselin Bank. 72° 16.1196' S, 176° 36.2814' W and 72° 15.7728' S, 176° 35.5638' W. Depth 670 m. Cape Hallett Canyon. 71° 58.8666' S, 172° 11.6298' E and 71° 59.2512' S, 172° 10.6020' E. Depth 750 m. Hallett Ridge. 72° 23.0340' S, 176° 06.1020' E and 72° 23.3868' S, 176° 06.2094' E. Depth 910 m. Seven specimens: GRC-02-223 BF2, GRC-08-065 CM2, GRC-07-028 CVC, GRC-07-028 CVB, GRC-07-028 CV3, GRC-08-023 CZ1, GRC-08-023 DA3.

Other material examined: Slide GRC-08-023 sp. 2 1 (*Myxilla (Myxilla) mollis*), provided by Dr. Marco Bertolino, University of Genoa.

Description: The sponge samples analysed are encrusting with a size ranging from 0.179 - 0.757 cm^2, have an ochre colour and an irregular surface.

Skeleton: Not observed.

Megascleres:

1. T Tornotes: with a characteristic fusiform shape, slightly curved with pointed ends (figure 38 A).

Size: 265 (309 ± 26) 370 x 10 (12 ± 3) 15 µm.

2. Styles: smooth with small, scattered spines (figure 38 B).

   Size: 490 (580 ± 63) 660 x 20 (27 ± 3) 30 µm.

Microscleres:

1. Isochelae: small, anchorate (figure 38 C).

   Size: 25 (41 ± 8) 55 x 10 (14 ± 1) 15 µm

2. Sigmas: C-shaped (figure 38 D).

   Size: 37.5 (59 ± 10) 77.5 x 7.5 (8 ± 1) 10 µm.

Remarks: The sponge samples analysed match perfectly with the original description of the species by Topsent (1916).

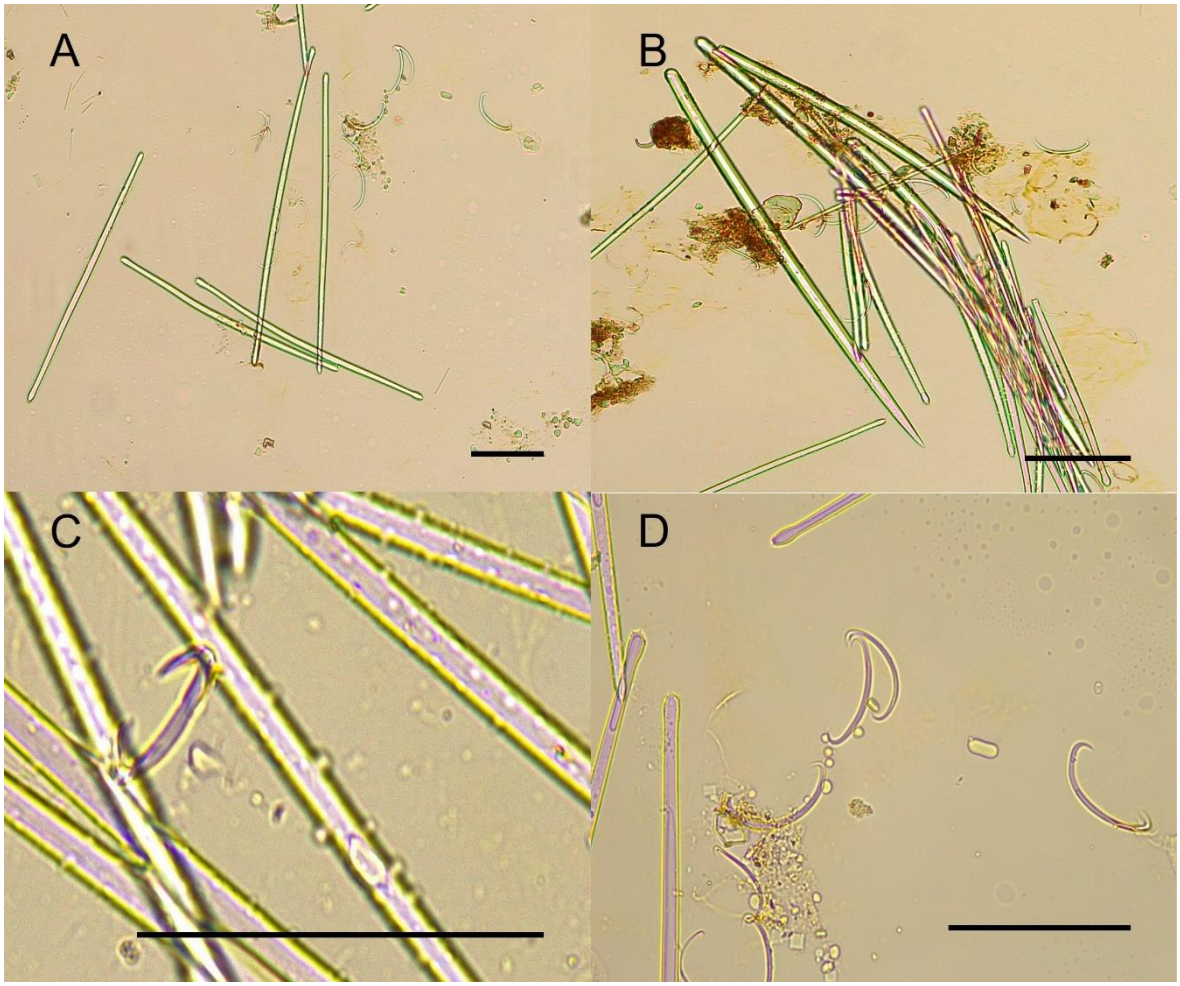

Figure 38: *Myxilla (Myxilla) mollis* Ridley & Dendy, 1886. Optical microscope images of the spicules: **A**. Fusiform tornote. **B**. Smooth styles. **C**. Isochela. **D**. Sigmas. **Scale bars**: **A-B-C-D**: 100 µm.

Family Tedaniidae Ridley & Dendy, 1886

Genus *Tedania* Gray, 1867

Subgenus *Tedania (Tedaniopsis)* Dendy, 1924

Species *Tedania (Tedaniopsis) oxeata* Topsent, 1916

Locality and material: Iselin Bank. 72° 16.1196' S, 176° 36.2814' W and 72° 15.7728' S, 176° 35.5638' W. Depth 670 m. One specimen: GRC-02-113 CQ4.

Other material examined: None.

Description: The sample analysed is whitish and encrusting sponge of 1.463 cm^2.

Skeleton: Not observed.

Megascleres:

1. Dermal tornotes: with a characteristic fusiform shape, slightly curved with both strongly pointed ends (figure 39 A-B).

   Size: 315 (346 ± 19) 375 x 10 (11 ± 2) 15 µm.

2. Oxeas: smooth with pointed ends (figure 39 C).

   Size: 600 (617 ± 19) 650 x 20 (28 ± 4) 30 µm.

Microscleres:

1. Onychaetes: thin and finely spined (figure 39 D).

   Size: 150 (244 ± 58) 350 x 2.5 µm.

Remarks: The species analysed matches perfectly with the original description of the species by Topsent (1916).

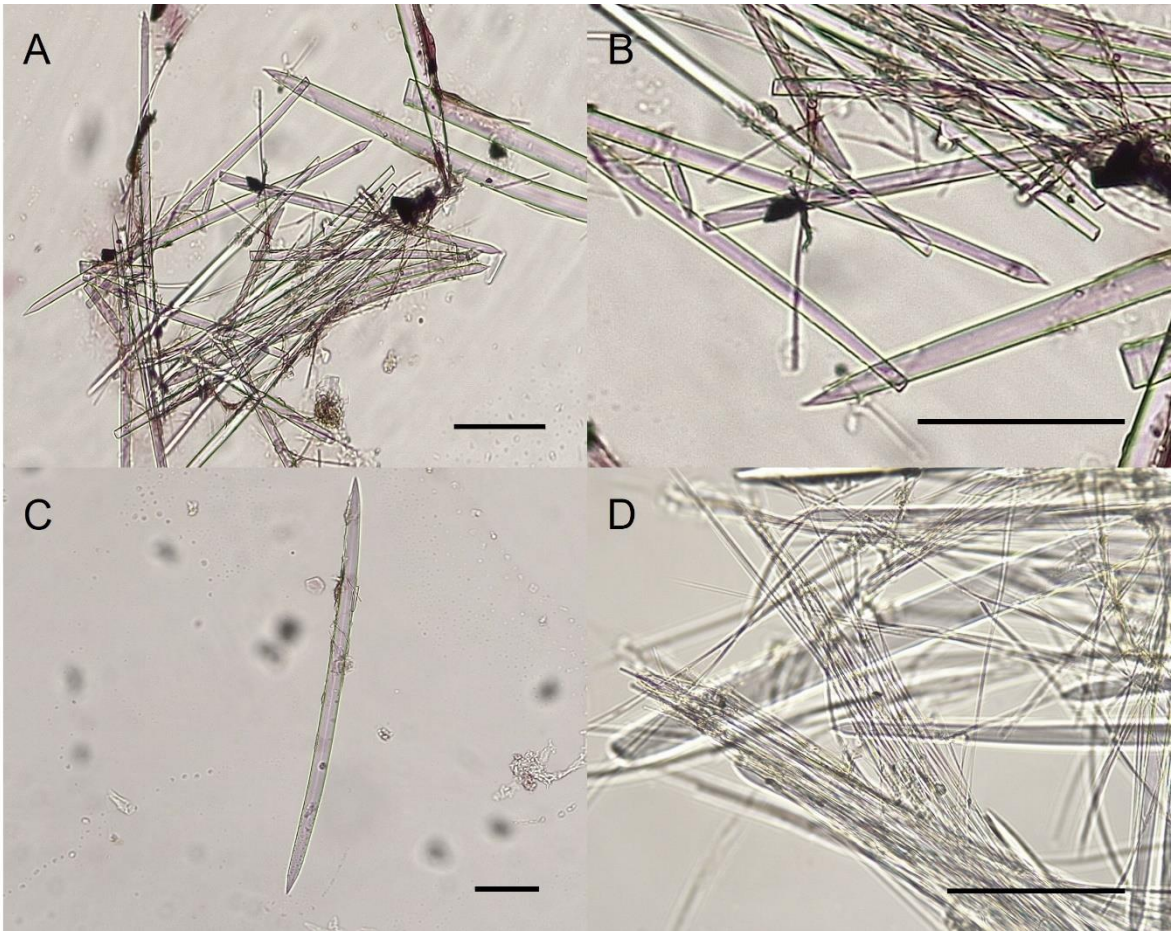

Figure 39: *Tedania (Tedaniopsis) oxeata* Topsent, 1916. Optical microscope images of the spicules: **A**. Dermal tornotes. **B**. Detail of one strongly pointed head of a tornote. **C**. Oxea. **D**. Thin onychaetes. **Scale bars**: **A-B-C-D**: 100 µm.

Family Tedaniidae Ridley & Dendy, 1886

Genus *Tedania* Gray, 1867

Subgenus *Tedania (Tedaniopsis)* Dendy, 1924

Species *Tedania (Tedaniopsis) tantula* (Kirkpatrick, 1907)

Locality and material: Iselin Bank. 72° 16.1196' S, 176° 36.2814' W and 72° 15.7728' S, 176° 35.5638' W. Depth 670 m. Two specimens: GRC-02-223 B1, GRC-02-091 CU9.

Other material examined: None.

Description: The sponge samples analysed are encrusting, with dimensions ranging from 0.004 to 0.192 cm^2 and a whitish colour.

Skeleton: Not observed.

Megascleres:

1. Tornotes: fusiform spicules with a mucronate end (figure 40 A).

   Size: 375 (432 ± 38) 500 x 20 (12 ± 3) 25 µm.

2. Styles: smooth spicules with one end gradually pointed (figure 40 B-C).

   Size: 530 (605 ± 39) 670 x 15 (22 ± 4) 25 µm.

Microscleres:

1. Onychaetes: thin spicules with an irregular surface (figure 40 D-F).

   Size: 250 (360 ± 56) 465 x 5 (9 ± 2) 10 µm.

Remarks: Comparing our measurements with those given in Kirkpatrick's original description of the species (1907), the size of styles and onychaetes are smaller than Kirkpatrick's, according to which styles measure 395 x 7.25 µm and onychaetes 600 µm in length. For onychaetes, our measurements are

closer to those that Kirkpatrick gives to the small onychaetes, according to which the length is 162 x 2.5 µm. Kirkpatrick in fact divides onychaetes into two categories: large and small. In our case, it was not possible to make such a distinction since most of the spicules appeared broken.

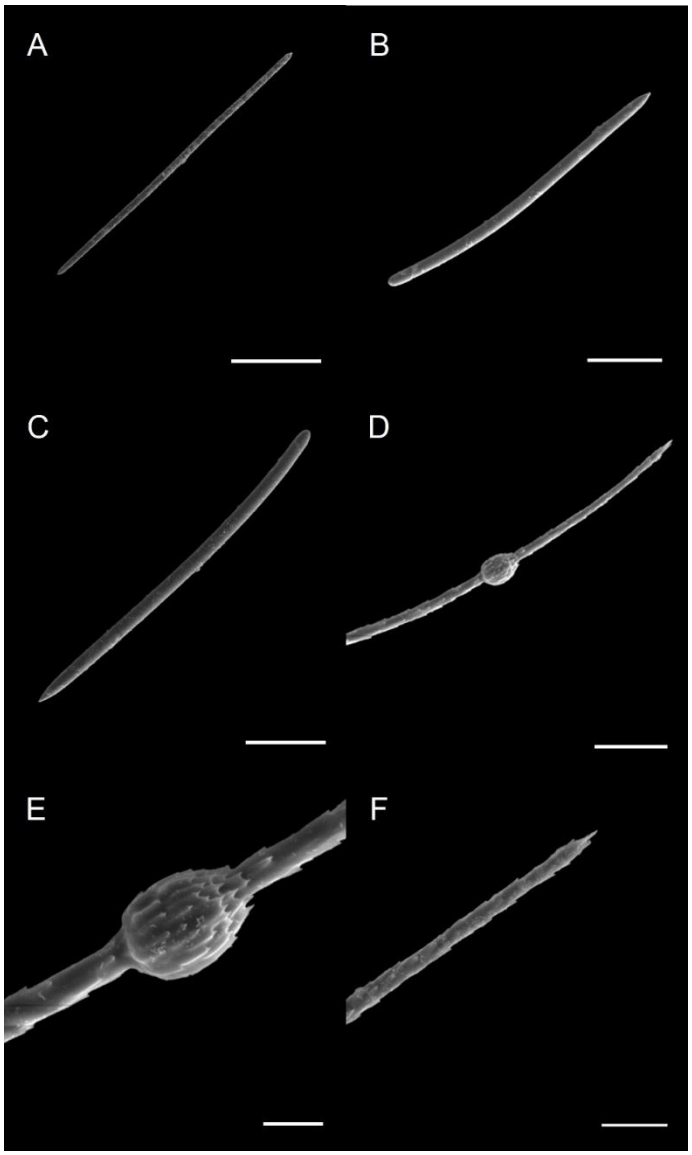

Figure 40: *Tedania (Tedaniopsis) tantula* (Kirkpatrick, 1907). SEM images of the spicules: **A**. Fusiform tornote. **B-C**. Styles. **D**. Onychaete. **E**. Detail of the tyle in the apical part of the onychaetes. **F**. Detail of the apex of the onychaete. **Scale bars**: **A**: 100 µm, **B-C**: 50 µm, **D**: 20 µm, **E**: 5 µm, **F**: 10 µm.

Order Polymastiida Morrow & Cárdenas, 2015

Family Polymastiidae Gray, 1867

Genus *Polymastia* Bowerbank, 1862

Species *Polymastia invaginata* Kirkpatrick, 1907

Locality and material: Iselin Bank. 72° 16.1196' S, 176° 36.2814' W and 72° 15.7728' S, 176° 35.5638' W. Depth 670 m. Six specimens: GRC-02-223 A1, GRC-02-223 BO1, GRC-02-223 AU1, GRC-02-223 R2, GRC-02-091 CU10, GRC-02-133 CT2.

Other material examined: None.

Description: The sponge samples analysed are encrusting with a size ranging from 0.039 to 0.279 cm^2 and a colour tending to yellow.

Skeleton: Formed by vertical bundles of tylostyles.

Megascleres:

1. Large tylostyles: fusiform with a small, spherical head (figure 41 A-B). Size: 460 (742 ± 181) 1300 x 10 (15 ± 3) 20 μm.

2. Cortical tylostyles: fusiform, slightly enlarged in the central part, with a strongly globular head (figure 41 C-D).

   Size: 240 (341 ± 38) 300 x 10 (17 ± 3) 20 µm.

3. Small tylostyles: shorter, characterised by a globular head and a less defined neck (figure 41 E-F).

   Size: 130 (205 ± 43) 310 x 5 (9 ± 3) 15 µm.

Microscleres: None.

Remarks: The present sample fits in spicule size and shape with the species described by Kirkpatrick (1907).

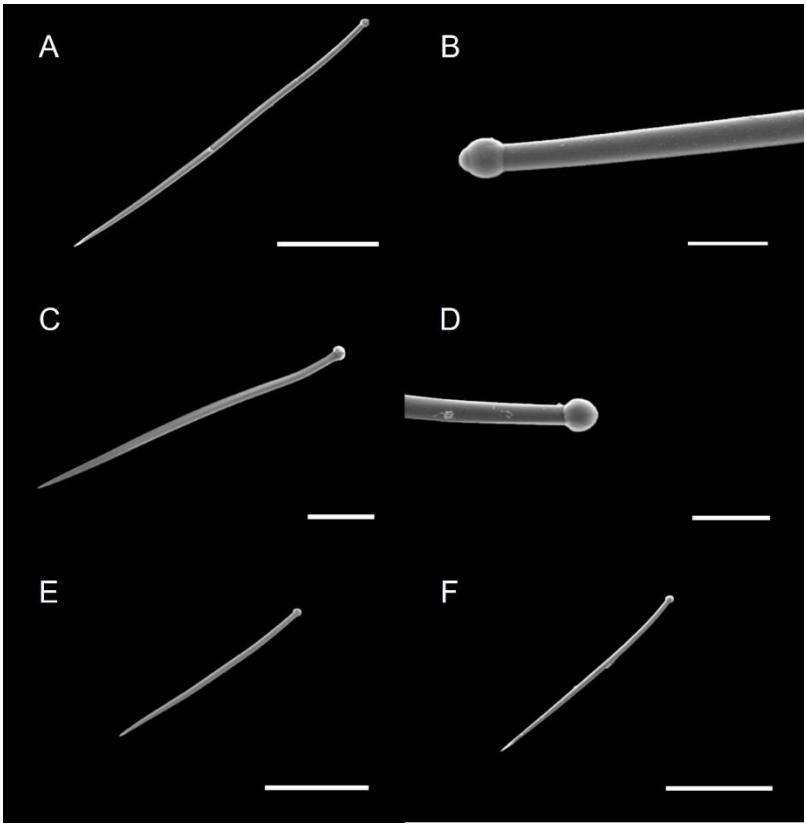

Figure 41: *Polymastia invaginata* Kirkpatrick, 1907. SEM images of the spicules: **A**. Large tylostyle. **B**. Detail of the head of a large tylostyle. **C**. Cortical tylostyle. **D**. Detail of

the head of a cortical tylostyle. **E-F**. Small tylostyles. **Scale bars**: **A-E-F**: 100 µm, **B-D**: 20 µm, **C**: 50 µm.

Order Suberitida Chombard & Boury-Esnault, 1999

Family Suberitidae Schmidt, 1870

Genus *Plicatellopsis* Burton, 1932

Species *Plicatellopsis fragilis* Koltun, 1964

Locality and material: Iselin Bank. 72° 16.1196' S, 176° 36.2814' W and 72° 15.7728' S, 176° 35.5638' W. Depth 670 m. One specimen: GRC-02-223 BZ2.

Other material examined: Slide GRC-02-223 37 A (*Plicatellopsis* cf. *fragilis*), provided by Dr. Marco Bertolino, University of Genoa.

Description: The sponge sample analysed is massive with a size of 0.051 cm^2 and ochre in colour.

Skeleton: Not observed.

Megascleres:

1. Large styles: thick, fusiform and slightly curved (figure 42 A).

Size: 640 (677 ± 34) 730 x 40 (45 ± 5) 50 µm.

2. Small styles: fusiform, slightly curved and thinner (figure 42 B).

   Size: 250 (303 ± 14) 320 x 10 µm.

Microscleres: None.

Remarks: Comparing the spicule measurements of our sponge sample with those of Koltun's description (1964), the only difference in the lower thickness of the largest styles (i.e., 20 – 30 µm).

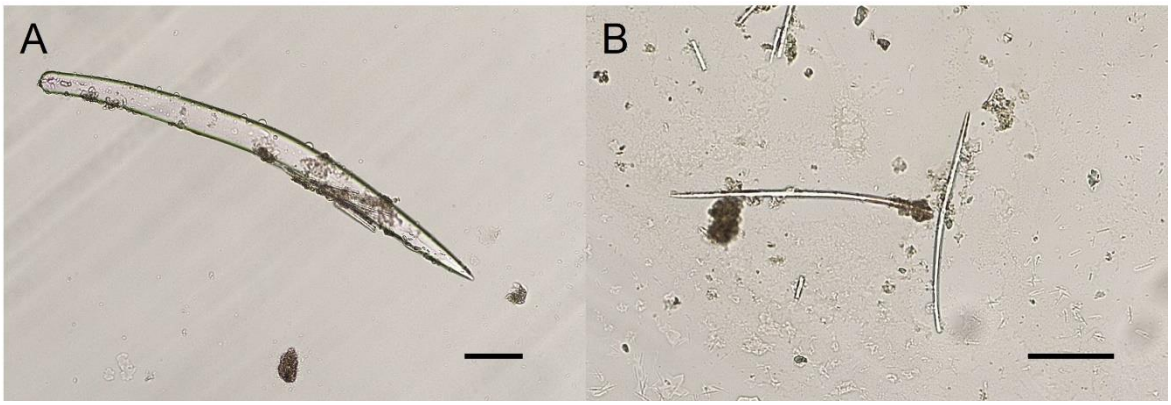

Figure 42: *Plicatellopsis fragilis* Koltun, 1964. Optical microscope images of the spicules: **A**. Large styles. **B**. Small styles. **Scale bars**: **A-B**: 100 µm.

Family Suberitidae Schmidt, 1870

Genus *Pseudosuberites* Topsent, 1896

Species *Pseudosuberites sulcatus* (Thiele, 1905)

Locality and material: Iselin Bank. 72° 16.1196' S, 176° 36.2814' W and 72° 15.7728' S, 176° 35.5638' W. Depth 670 m. One specimen: GRC-02-223 N2.

Other material examined: None.

Description: This greyish coloured sponge is encrusting and 0.072 cm^2 in size.

Skeleton: Not observed.

Megascleres:

1. Tylostyles: fusiform characterised by a well-defined globular head (figure 43 A-B).

   Size: 290 (348 ± 39) 390 x 10 µm.

Microscleres: None.

Remarks: The sponge samples analysed match perfectly with the original description of the species by Thiele (1905).

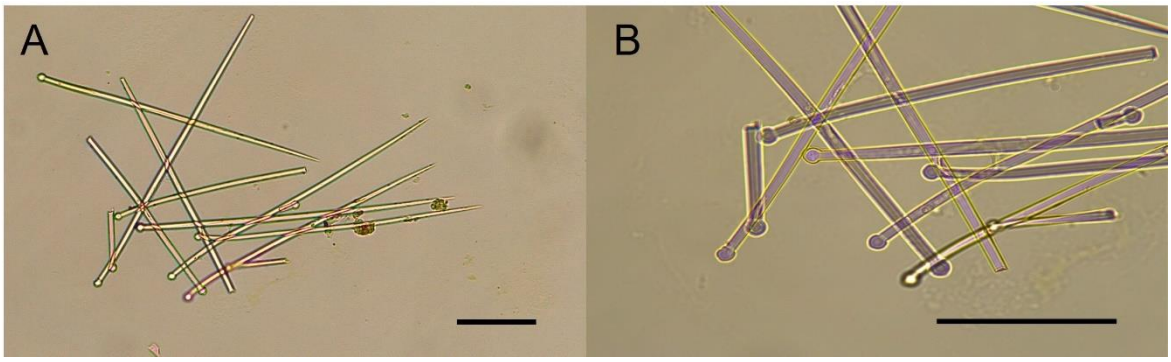

Figure 43: *Pseudosuberites sulcatus* (Thiele, 1905). Optical microscope images of the spicules: **A**. Tylostyles. **B**. Detail of the heads of tylostyles. **Scale bars**: **A-B**: 100 µm.

Family Halichondriidae Gray, 1867

Genus *Halichondria* Fleming, 1828

Subgenus *Halichondria (Halichondria)* Fleming, 1828

Species *Halichondria (Halichondria) cristata* Sarà, 1978

Locality and material: Hallett Ridge. 72° 23.0340' S, 176° 06.1020' E and 72° 23.3868' S, 176° 06.2094' E. Depth 910 m. One specimen: GRC-07-028 CVD.

Other material examined: None.

Description: The sponge sample analysed is encrusting with a size of 0.212 cm^2 and a greyish colour.

Skeleton: The ectosomal skeleton is composed by bundles of oxeas tangentially arranged, while the choanosomal skeleton is quite confused.

Megascleres:

1. Oxeas: arcuate with strongly pointed ends (figure 44 A-B).

   Size: 400 (441 ± 28) 490 x 10 (11 ± 1) 12.5 µm.

Microscleres: None.

Remarks: The shape and size of the spicules in the sponge sample analysed match the original description of the species by Sarà (1978).

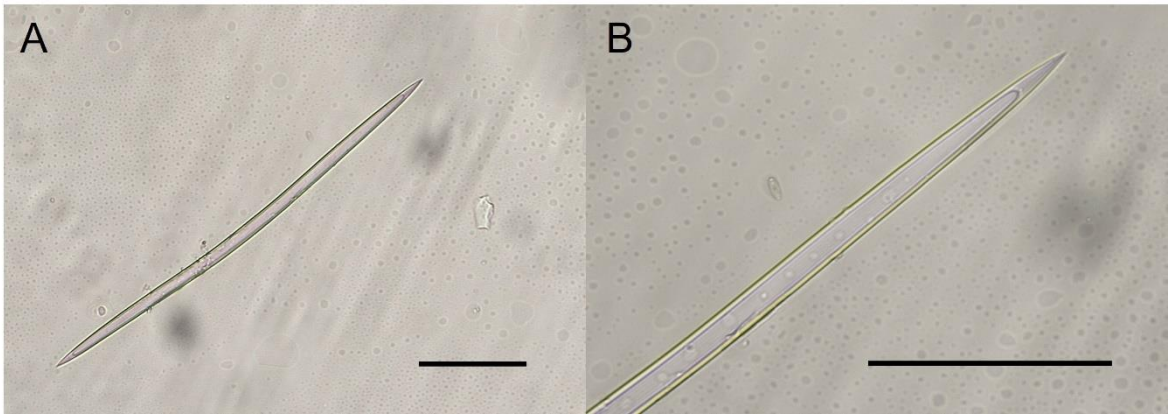

Figure 44: *Halichondria (Halichondria) cristata* Sarà, 1978. Optical microscope images of the spicules: **A**. Arcuate and strongly pointed oxea. **B**. Detail of one end of an oxea. **Scale bars**: **A-B**: 100 µm.

Family Halichondriidae Gray, 1867

Genus *Halichondria* Fleming, 1828

Subgenus *Halichondria (Halichondria)* Fleming, 1828

Species *Halichondria (Halichondria) prostrata* Thiele, 1905

Locality and material: Cape Hallett Canyon. 71° 58.8666' S, 172° 11.6298' E and 71° 59.2512' S, 172° 10.6020' E. Depth 750 m. One specimen: GRC-08-023 DA1.

Other material examined: None.

Description: The sponge sample analysed is massive with a size of 0.400 cm^2. It has a yellowish colour and spicules can be seen on the surface.

Skeleton: Not observed.

Megascleres:

1. Oxeas: arcuate with strongly pointed ends (figure 45 A-B).

   Size: 400 (921 ± 249) 1200 x 10 (11 ± 2) 15 µm

Microscleres: Absent.

Remarks: The size of the oxeas in our sample does not match those of the original description of the species by Thiele (1905) (300-320 µm long). Our specimen fits better with *Halichondria hentscheli* Koltun (1964) characterized by longer oxeas (550-1680 µm) that is actually considered a junior synonymous of *Halichondria (Halichondria) prostrata* (De Vodge et al., 2022).

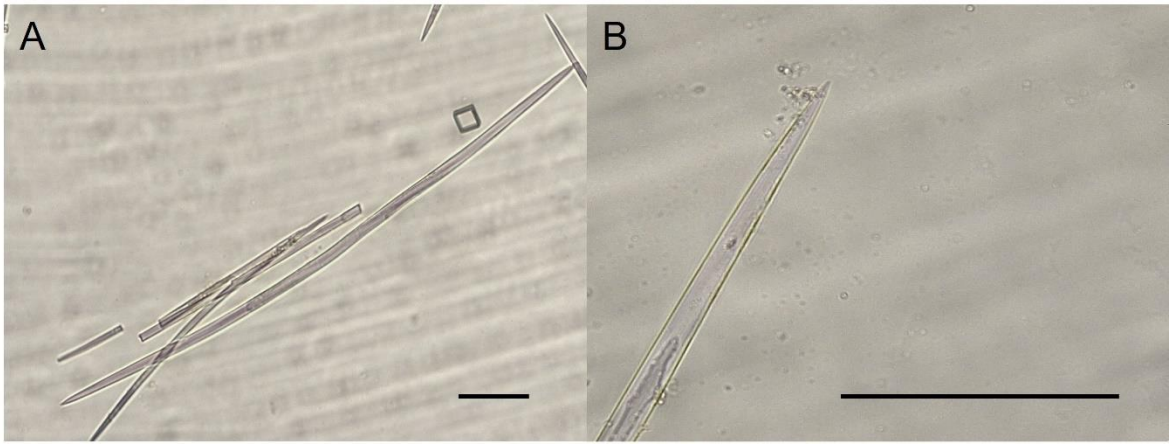

Figure 45: *Halichondria (Halichondria) prostrata* Thiele, 1905. Optical microscope images of the spicules: **A**. Oxea. **B**. Detail of one end of an oxea. **Scale bars**: **A-B**: 100 µm.

Order Tetractinellida Marshall, 1876

Family Vulcanellidae Cárdenas, Xavier, Reveillaud, Schander & Rapp, 2011

Genus *Poecillastra* Sollas, 1888

Species *Poecillastra compressa* Bowerbank, 1866

Subspecies *Poecillastra compressa antarctica* Koltun, 1964

Locality and material: Iselin Bank. 72° 16.1196' S, 176° 36.2814' W and 72° 15.7728' S, 176° 35.5638' W. Depth 670 m. Two specimens: GRC-02-223 N3, GRC-02-223 L3, GRC-02-223 AQ2.

Other material examined: Slide GRC-02-223 26 sp.1 (*Poecillastra compressa antarctica*), provided by Dr. Marco Bertolino, University of Genoa.

Description: The sponges analysed are massive with a size ranging from 0.015 to 0.315 cm^2. The sample is brown in colour with a stiff consistency.

Megascleres:

1. Oxeas: fusiform, most of them with both ends pointed, sometimes with one blunt ending (figure 46 A).

Size: 730 (1260 ± 436) 1910 x 10 (22 ± 8) 35 μm.

2. Orthotrianes: large with a short rhabdome (figure 46 B).

   Size of clads: 560 (737 ± 97) 920 x 25 (35 ± 7) 45 μm.

3. Calthrops: with three long rays (figure 46 C).

   Size of the actines: 780 (909 ± 79) 1100 x 30 (39 ± 3) 40 μm.

Microscleres:

1. Metasters: with two to five rays (figure 46 D).

   Size of the rays: 35 (56 ± 15) 90 x 5 (8 ± 3) 15 μm.

2. Amphiasters: with three to four rays (figure 46 D).

   Size: 10 (16 ± 3) 25 x 3 (4 ± 1) 5 μm.

Remarks: The shape and size of the spicules in the sponge samples analysed match the original description of the species by Koltun (1964) except for oxeas, that are longer in Koltun's species (3.2 - 3.7 mm in length).

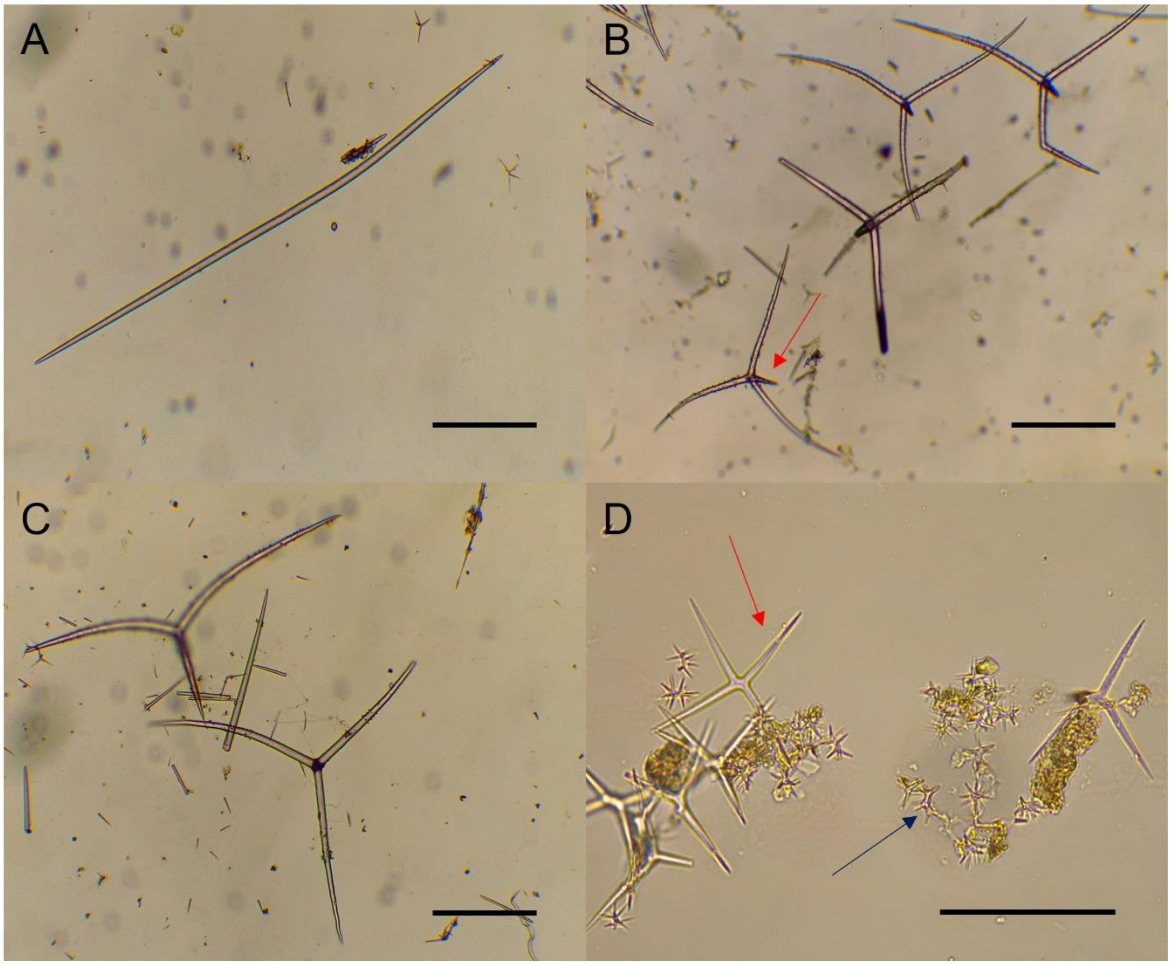

Figure 46: *Poecillastra compressa antarctica* Koltun, 1964. Optical microscope images of the spicules: **A**. Oxea. **B**. Orthotrianes with a short rhabdome (red arrow). **C**. Calthrops. **D**. Metaster (red arrow) and amphiaster (blue arrow). **Scale bars**: **A-B-C-D**: 100 µm.

Suborder Spirophorina Bergquist & Hogg, 1969

Family Tetillidae Sollas, 1886

Genus *Tetilla* Schmidt, 1868

Species *Tetilla coronida* Sollas, 1888

Locality and material: Unknown station. 71° 38.4132' S and 172° 09.3048' E. Depth 1022 m. One specimen: GRC-TR17-007 CP1.

Other material examined: None.

Description: The sponge is massive, 0.300 cm^2. The sample is white in colour, surface is hispid due to the protruding long spicules.

Megascleres:

1. Oxeas: isoactinate, fusiform and very sharply pointed (figure 47 A-B).

   Size: 610 (716 ± 46) 790 x 20 (24 ± 5) 30 μm.
2. Protriaenes: very long spicules, with a thin rhabdome (figure 47 C).

   Size of the rabdome: 1600 (2082 ± 383) 2800 x 10 μm.
3. Anatriaenes: similar to protriaenes but with the clads facing the central axis of the spicule.

   Size of the clads: 3000 (3830 ± 279) 4300 x 15 (20 ± 4) 27.5 μm.
4. Anamonaene: modified protriaene where two of the clads being suppressed, and the remaining one recurved at about the middle of its length (figure 47 D).

   Size: 210 (280 ± 38) 330 x 20 (23 ± 3) 25 μm.

Microscleres:

1. Sigmaspires: small C- or S-shaped with an irregular, rough surface (figure 47 E-F).

   Size: 15 (20 ± 4) 27.5 μm.

Remarks: The spicule size reported by Sollas (1888) in the original description of the species, is larger considering the length of protiaenes (3.37 mm) and anatriaenes (7.14 mm). In our specimens, however, most of the spicules were broken due to their size and fragility, so it is possible that our spicules were much longer than the reported size. Nevertheless, the spicule set of our sample matches perfectly with the spicules reported by Sollas (1888).

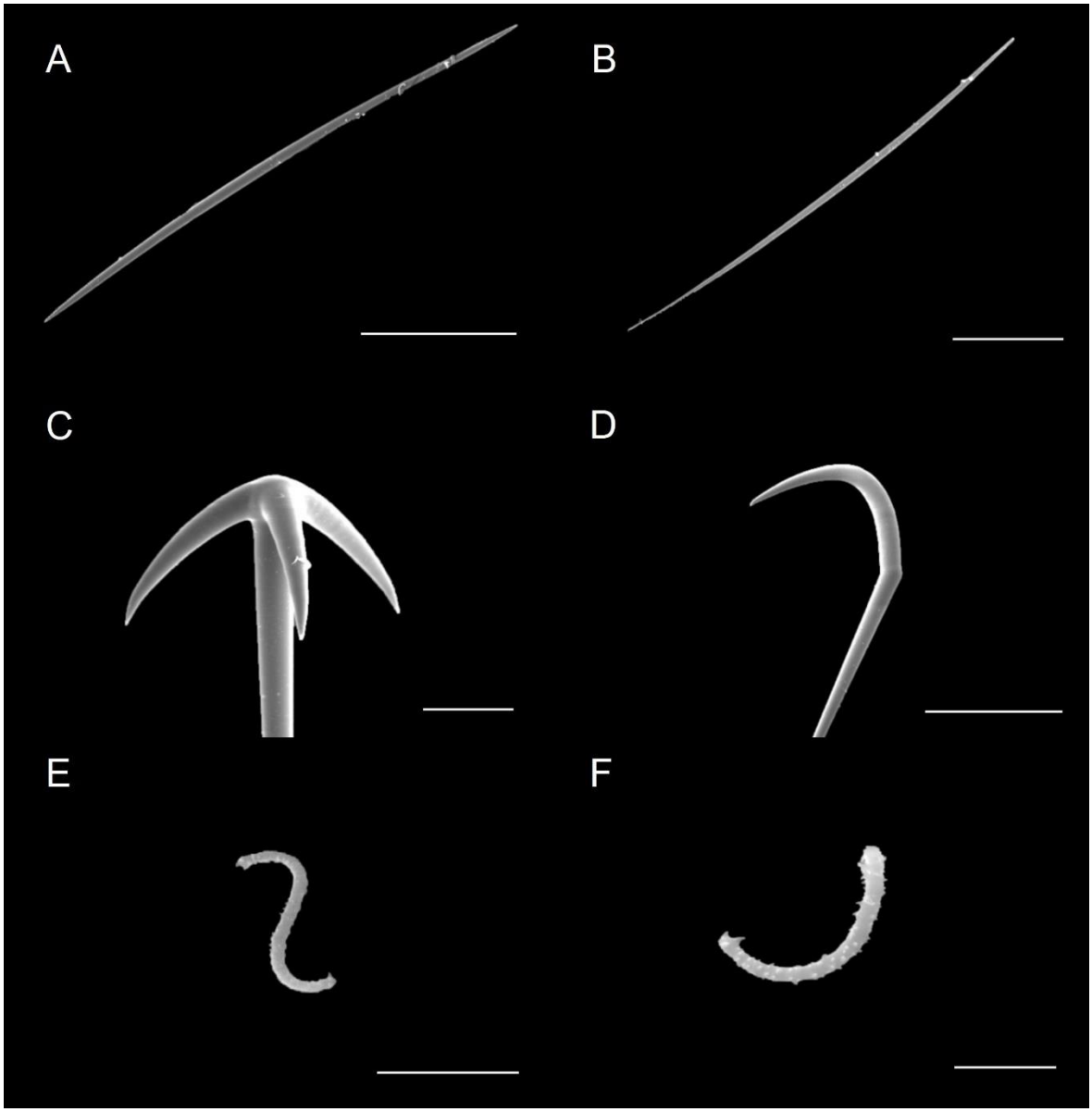

Figure 47: *Tetilla coronida* Sollas, 1888. SEM images of the spicules: **A**-**B**. Oxeas. **C**. Head of an anatriaene. **D**. Head of a anamonaene. **E-F**. Sigmaspires. **Scale bars**: **A-D**: 200 µm, **B**: 500 µm, **C**: 50 µm, **E**: 20 µm, **F**: 10 µm.

Class Hexactinellida Schmidt, 1870

Order Lyssacinosida Zittel, 1877

Family Lyssacinosida *incertae sedis* Tabachnick, 2002

Genus *Clathrochone* Tabachnick, 2002

Species *Clathrochone* cf. *clathroclada* (Lévi & Lévi, 1982)

Locality and material: Iselin Bank. 72° 16.1196' S, 176° 36.2814' W and 72° 15.7728' S, 176° 35.5638' W. Depth 670 m. Hallett Ridge. 72° 23.0340' S, 176° 06.1020' E and 72° 23.3868' S, 176° 06.2094' E. Depth 910 m. Twenty-four specimens: GRC-02-223 T1, GRC-02-223 AM1, GRC-02-223 AQ1, GRC-02-223 AU3, GRC-02-223 BF4, GRC-02-223 BL1, GRC-02-027 CN3, GRC-02-113 CQ1, GRC-02-113 CQ2, GRC-02-092 CR3, GRC-02-092 CR4, GRC-02-092 CR6, GRC-02-093 CS3, GRC-02-093 CS4, GRC-02-093 CS7, GRC-02-093 CS10, GRC-02-091 CU 1, GRC-02-091 CU 2, GRC-02-091 CU 3, GRC-02-091 CU 4, GRC-02-091 CU 7, GRC-07-028 CVM, GRC-07-028 CVQ, GRC-07-028 CVR.

Other material examined: Slide GRC-08-024 sp. 1 5 (*Clathrochone clathroclada*), provided by Dr. Marco Bertolino, University of Genoa.

Description: Sponges are massive, whitish in colour with long spicules visible on the surface. Their size varies from 0.008 to 3.563 cm^2.

Skeleton: Not observed.

Megascleres:

1. Choanosomal diactine: long with both ends finely spined (figure 48 A).

   Size: more than 3000 µm x 30 (25 ± 4) µm.

2. Dermal pentactine: entirely spined (figure 48 B-C).

   Size of the actine: 380 (842 ± 98) 1128 µm x 20 (18 ± 6) 30 µm.

Microscleres:

1. Hexactines: finely pointed.

   Size of the actine: 92 (146 ± 12) 135 µm x 15 (17 ± 3) 20 µm

2. Spherical microdiscohexaster: consisting of 6 rays ending in stellate ends (figure 48 D).

   Size of the diameter: 80 (94 ± 12) 135 µm.

Remarks: The identification of this species is uncertain. It was not possible to collect the entire set of measurements from all samples, as several were missing multiple spicule types. A common element found within all the samples was represented by the spherical microdiscohexaster which allowed us to identify our samples, with high confidence, as the species *Clathrochone clathroclada* (Lévi & Lévi, 1982).

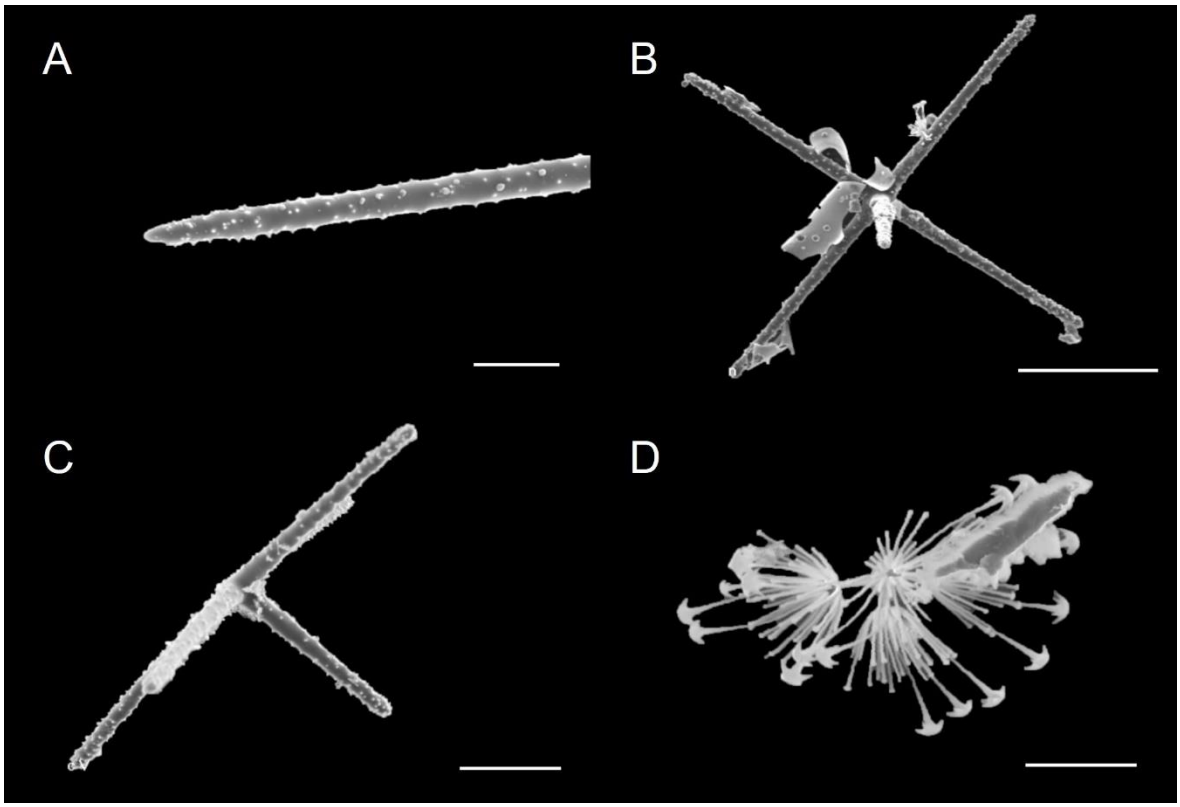

Figure 48: *Clathrochone* cf. *clathroclada* (Lévi & Lévi, 1982). SEM images of the spicules: **A**. Detail of the end of a diactine. **B-C**. Dermal pentactine. **D**. Spherical microdiscohexaster. **Scale bars**: **A-D**: 20 µm, **B**: 100 µm, **C-D-E-F-G**: 10 µm, **H**: 20 µm.

Family Rossellidae Schulze, 1885

Subfamily Acanthascinae Schulze, 1897

Genus *Rhabdocalyptus* Schulze, 1886

Species *Rhabdocalyptus australis* Topsent, 1901

Locality and material: Iselin Bank. 72° 16.1196' S, 176° 36.2814' W and 72° 15.7728' S, 176° 35.5638' W. Depth 670 m. Two specimens: GRC-02-223 D1, GRC-02-223 BF3.

Other material examined: Slide GRC-02-222 sp. 8 (*Rhabdocalyptus australis*), Genoa; GRC-02-223 sp. 4 (*Rhabdocalyptus australis*), provided by Dr. Marco Bertolino, University of Genoa.

Description: Sponges are massive, whitish in colour with long spicules visible on the surface. Their size varies from 0.008 to 3.563 cm^2.

Skeleton: Not observed.

Megascleres:

1. Diactine: long with both ends finely spined (figure 49 A-B-C).

   Size: 1800 (2381 ± 476) 3420 x 10 (19 ± 5) 30 µm.

2. Pentactine: entirely spined.

   Size of the actine: 600 (1809 ± 1279) 3800 x 20 (24 ± 8) 40 µm

Microscleres:

1. Tetractine: entirely spined.

   Size of the actine: 45 (64 ± 13) 100 µm x 2.5 (3 ± 1) 5 µm.

2. Hexactine: with 6 rays, finely spined (figure 49 D-E).

   Size of the diameter: 90 (134 ± 8) 160 µm.

3. Discoctaster: with a toothed disc and the surface of secondary rays is slightly rough or spiny (figure 49 F).

   Size of the diameter: 89 (96 ± 6) 185 µm.

Remarks: Classifying the analysed specimens was not easy due to the lack of some spicules within our individuals. What led us to identify it as *Rhabdocalyptus australis* was the presence of discoctasters (figure 49 F), as a spicule of great taxonomic value for the species. However, the size obtained from the present spicules match those reported in the original description by Topsent (1901).

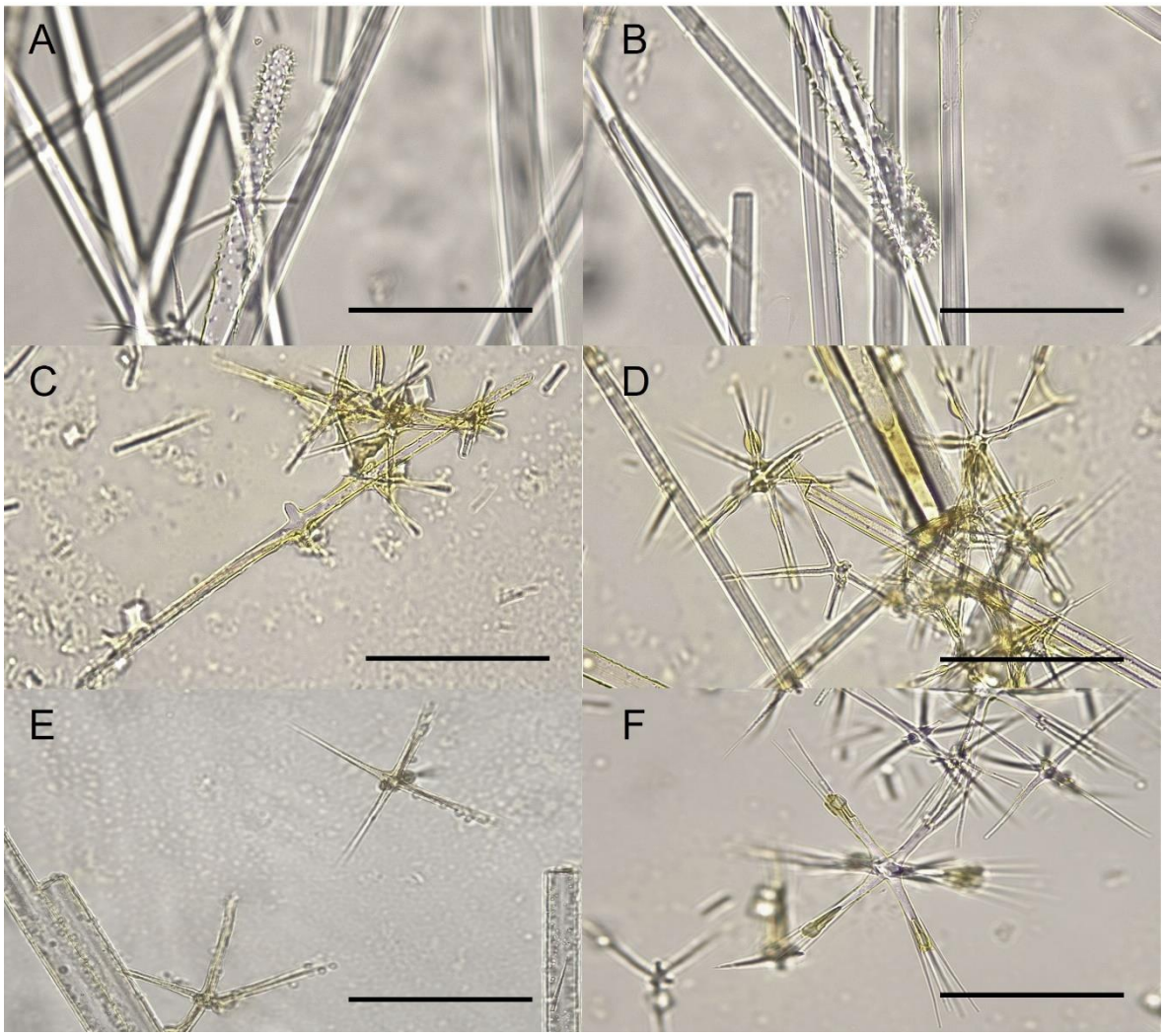

Figure 49: *Rhabdocalyptus australis* Topsent, 1901. Optical microscope images of the spicules: **A-B**. Detail of the ends of diactines. **C-E**. Hexactines. **F**. Discoctaster. **Scale bars**: **A-B-C-D-E-F**: 100 µm.

3.2.2. Sponge covering on stylasterids

In terms of size, the largest sponge analysed belongs to the species *Iophon unicorne* Topsent, 1907 and measures 3.611 cm^2 (figure 50), while the smallest sponge found measures 0.003 cm^2 and belongs to the species *Isodictya setifera* Topsent, 1901.

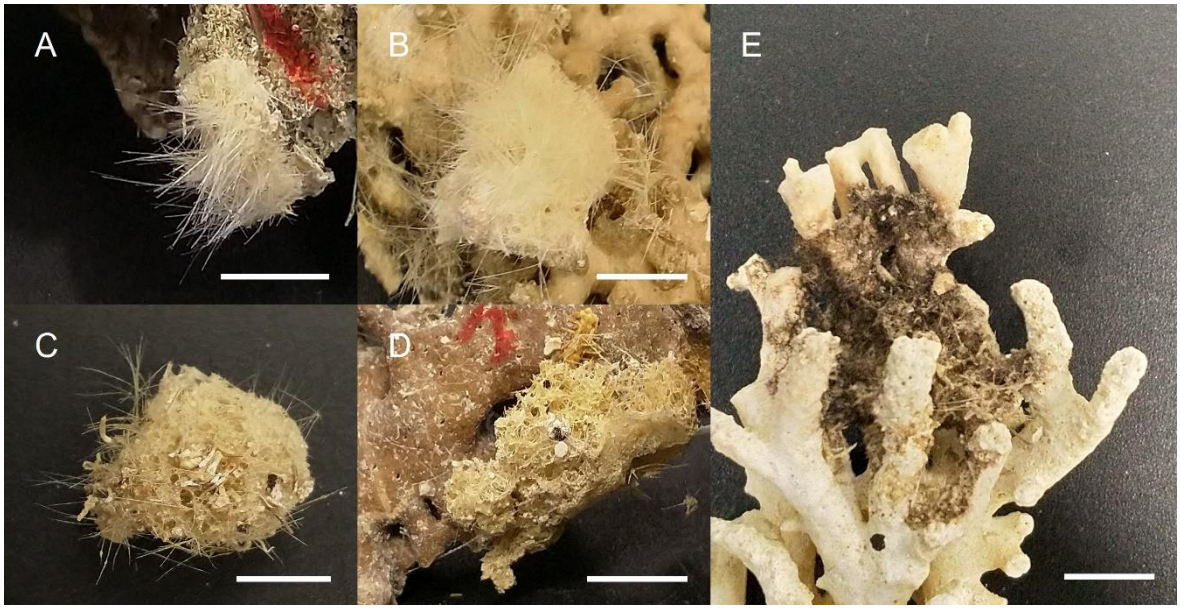

Figure 50: Some samples of sponge with larger dimensions. **A-B-C**: *Clathrochone* cf. *cladoclada*. **D**: *Clathria paucispicula*. E: *Iophon unicorne*. **Scale bars**: **A-B-C-D-E**: 1 cm.

Our sponge samples show an average density of 0.11 individuals per cm^2, with a minimum density of 0.01 individuals per cm^2 and a maximum of 0.52 individuals per cm^2. In addition, it was possible to assess the frequency with which certain size classes were recurring; in the graph (figure 51), it is possible to note that the most frequent sizes are found within the range 0.003 - 0.5 cm^2, for a total of 185 samples (81% of the total number of samples analysed). Within the range 0.5 - 1 cm^2, there are 17 samples, in the following range between 1 and 3 cm^2 there are 23 samples, while only 3 samples show a size over 3 cm^2.

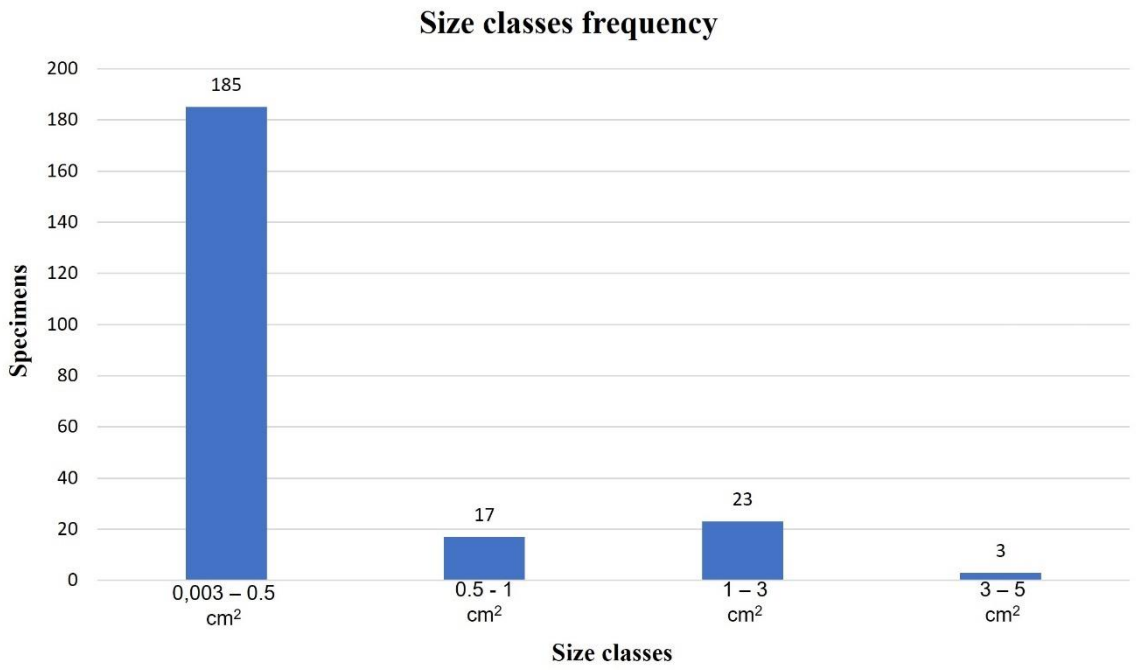

Figure 51: Number of sponge samples belonging to the following size classes: 0.003 – 0.5 cm^2, 0.5 – 1 cm^2, 1 – 3 cm^2 and 3 – 5 cm^2.

In the following graph (figure 52), the 10 species with the highest cover values are shown. The species with the highest average percentage cover is *Haliclona* sp.1 with 2.29%, followed by *Haliclona (Gellius) rudis* with 2.06%, *Mycale (Anomycale) titubans* with 1.53%, *Myxilla (Myxilla) mollis* with 1.21%, *Myxilla (Myxilla) elongata* with 1.06%, *Clathrochone* cf. *clathroclada* with 0.87%, *Clathria (Clathria) paucispicula* with 0.79%, *Esperiopsis villosa* with 0.65%, , *Iophon radiatum* with 0.59% and finally *Amphilectus rugosus* with 0.56%.

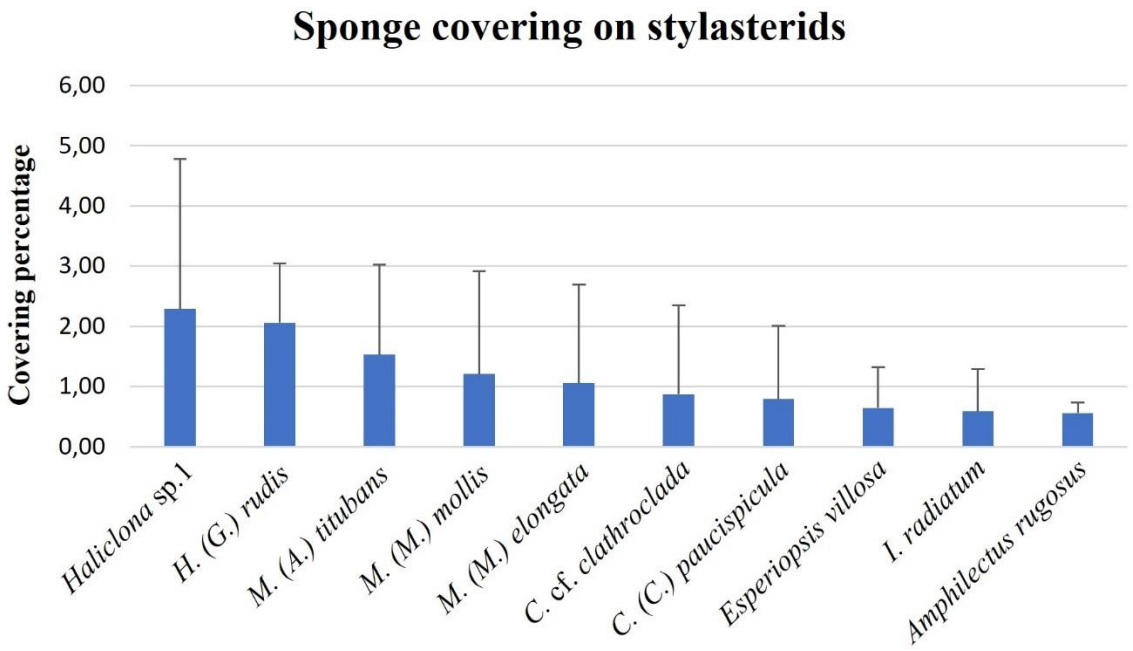

Figure 52: Percentages of sponge covering on samples of *Inferiolabiata labiata*.

Chapter 4

4. DISCUSSIONS

Stylasterids are known to be distributed worldwide with the exception of the Arctic area (Cairns, 1992; 2011). Their diversity in the Southern Ocean results higher than other oceans and around the Antarctic continent have been collected 14 of the 30 known genera of this family (Bax and Cairns, 2014).

All the stylasterid samples analysed within the present study were collected from the Ross Sea, and we reported 4 (*Errina fissurata*, *E. gracilis*, *E. laterorifa* and *Inferiolabiata labiata*) of the 32 species known from Antarctic area (Bax and Cairns, 2014) corresponding to the 12.5%. As highlited by Bax and Cairns (2014) the first report of stylasterid from Southern Ocean dates back to 1800 and despite they are recorded from many recent collections, this taxonomic group is still understudied in this geographic area. These four species, perfectly match with the species listed by Bax and Cairns (2014) as the "Circum-Antarctic field-forming corals". Cairns (1983) reported *E. fissurata* as the most frequently collected species of the assemblage followed by *E. laterorifa* and occasionally they were collected together with *E. gracilis* and *I. labiata* specimens. However, considering the species composition of our specimens, the dominant component resulted *E. laterorifa* followed by *E.*

fissurata and in accord with previous data only a few colonies of the other two species were identified. Anyway, this information should be cautionally considered since most of specimens were fragments of colonies therefore it is difficult to assess the actual number of colonies.

Literature data on the geographical distributions of the four identified species showed a wider distribution along the Antarctic coast (figure 53). According to Bax and Cairns (2014), the distribution of *E. fissurata*, *E. laterorifa*, *E. gracilis* and *I. labiata*, is not restricted to the Ross Sea only, as this assortment of stylasterids is representative of coral-fields in other Antarctic areas (Bax and Cairns, 2014).

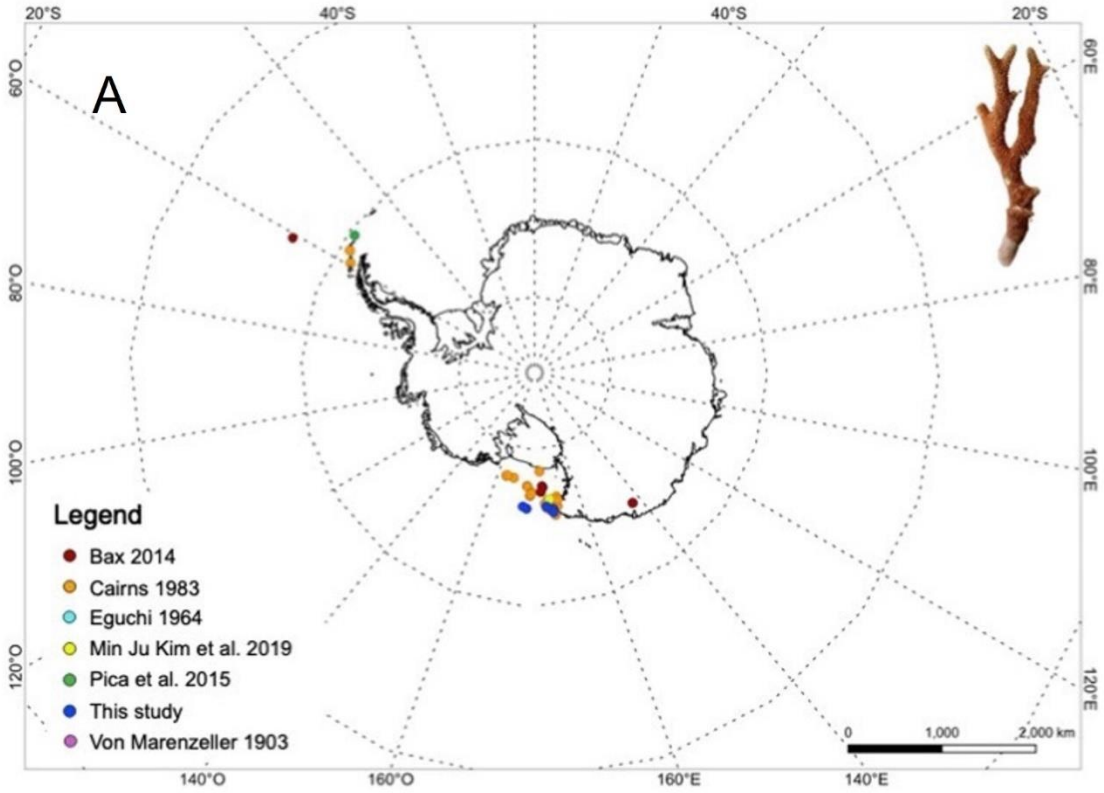
A
20°S
40°S
40°S
20°S
60°O
80°O
100°O
120°O
60°E
80°E
100°E
120°E
140°O
160°O
160°E
140°E
Legend
Bax 2014
Cairns 1983
Eguchi 1964
Min Ju Kim et al. 2019
Pica et al. 2015
This study
Von Marenzeller 1903
0
1,000
2,000 km

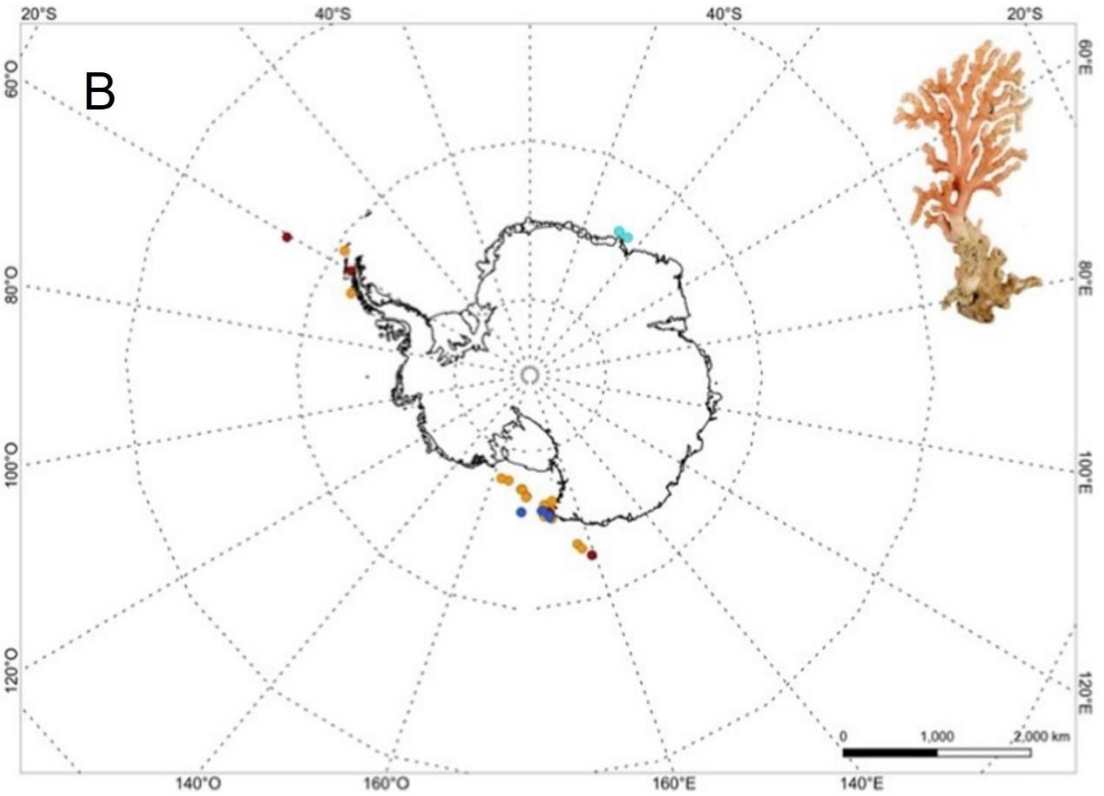
B
20°S
40°S
40°S
20°S
60°O
80°O
100°O
120°O
60°E
80°E
100°E
120°E
140°O
160°O
160°E
140°E
0
1,000
2,000 km

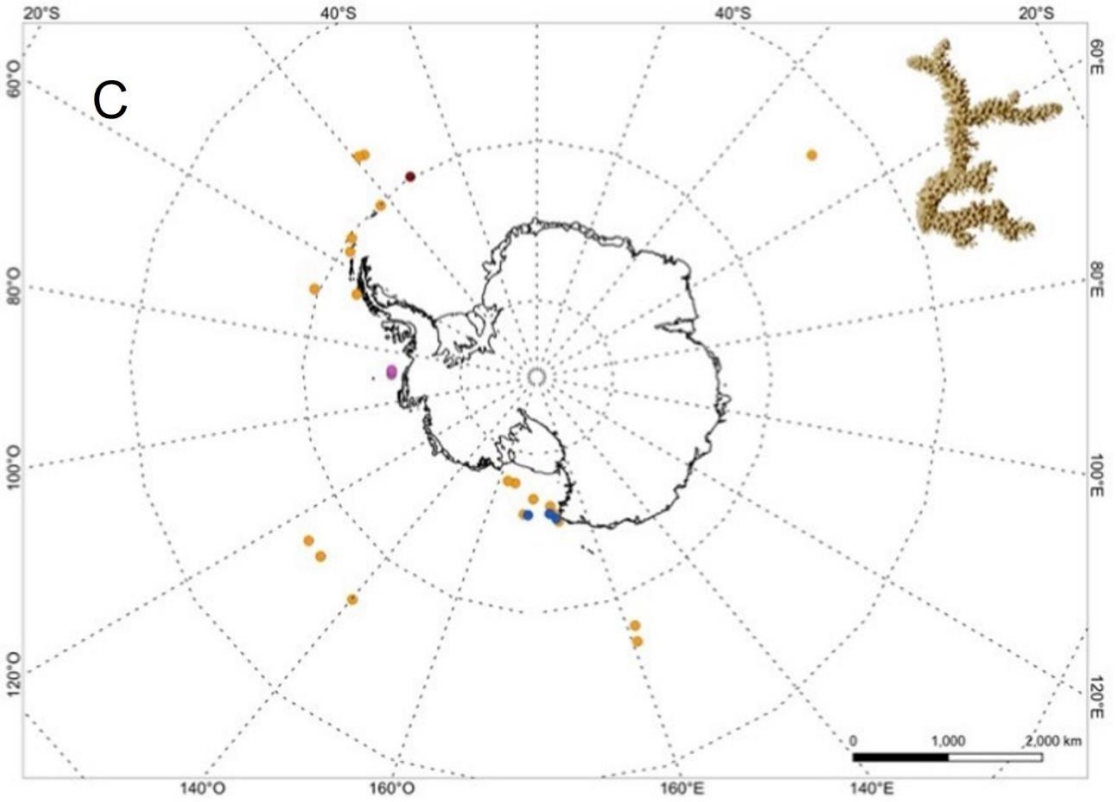
C
20°S
40°S
40°S
20°S
60°O
80°O
100°O
120°O
60°E
80°E
100°E
120°E
140°O
160°O
160°E
140°E
0
1,000
2,000 km

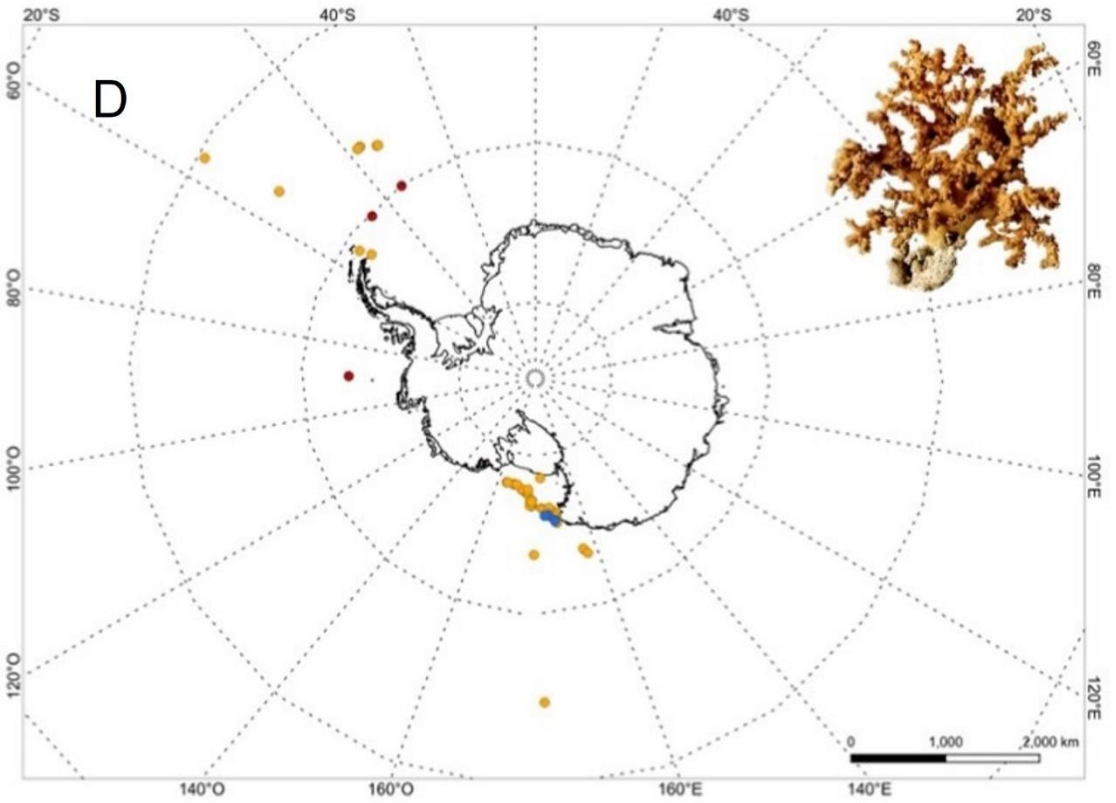
D
20°S
40°S
40°S
20°S
60°O
80°O
100°O
120°O
60°E
80°E
100°E
120°E
140°O
160°O
160°E
140°E
0
1,000
2,000 km

Figure 53: Maps showing the Antarctic distribution of **A**. *Errina fissurata*, **B**. *E. gracilis*, **C**. *E. laterorifa* and **D**. *Inferiolabiata labiata*.

In fact, a similar distribution of *E. fissurata* was reported by Cairns (1983), Pica et al. (2015) and Min Ju Kim et al. (2019), while Bax (2011) reported the presence of this species also along the Antarctic Peninsula and the Dumont d'Urville Sea (figure 53 A). Von Marenzeller (1903), Cairns (1983) and Bax (2014) reported *E. gracilis* as widely distributed in the Antarctic and sub-Antarctic waters, including South Georgia, South Shetland Islands, Ross Sea, Macquarie Ridge, Crozet Islands, sub-Antarctic seamounts in the South Pacific, the eastern continental coast of Antarctica, and in the waters of the Belling Shausen Sea (figure 53 B). As *E. fissurata*, *E. laterorifa* shows a less wide distribution along the Antarctic coast compared to *E. gracilis*. In fact, its observations around the Antarctic continent are mainly concentrated in the Ross Sea and Antarctic Peninsula, as noticed by Cairns (1983) and Bax (2014) (figure 53 C). Only Eguchi (1964) recorded the species near Cape Cook and Gunnerus Bank, on the eastern coast of the Antarctic continent (figure 53 C). Lastly, *Inferiolabiata labiata* seems to be largely distributed in the Antarctic and sub-Antarctic regions (figure 53 D). Cairns (1983) stated that the species is broadly distributed, including off southeastern America, Scotia Ridge, Ross Sea, Scott Island, Balleny Islands, Antipodes Islands, and probably circumantarctic (figure 53 D). In addition, Bax (2014) recorded the

presence of *I. labiata* off the Antarctic Peninsula, in the waters bathing the west coast of the Antarctic continent (figure 53 D).

The recent discovery of field-like aggregations of stylasterid corals and a high abundance of associated fauna in the east Antarctica (Post et al., 2010), clearly points out the high diversity of the Antarctic benthos (Bax, 2014). The biogeographic assessment of stylasterid coral fields in the Antarctic and sub-Antarctic regions defined two main areas with the highest stylasterid aggregations: 1) deep water aggregations (> 200 m) in the East Antarctic in the Dumont d'Urville Sea (Post et al., 2010; Bax and Cairns, 2014), with the main presence of *E. fissurata*, *E. laterorifa*, *E. gracilis* and *I. labiata,* and 2) shallow forests (10-20 m) in the Chilean fiords (Häussermann and Försterra, 2007; Salvati et al., 2010), exclusively characterized by the presence of very dense, three-dimensional reef-like aggregations of *Errina antarctica*. However, shallow water (20-30 m) aggregations of another stylaserid species, *Errina novaezelandiae*, were described for the New Zeland fjords by Miller et al. (2004). The presence of stylasterids in fjords' shallow waters, instead of colonizing grater depths, could be explained by the fact that the first few metres of fjord are characterised by a more or less distinct pycno-thermocline coupled with light absorption due to a large influx of detritus into the waters (Grange et al., 1981). This would reduce interspecific competition in fjord

communities, thus allowing the establishment of epifauna at a shallower depth than usual (Grange et al., 1981). In addition, Cairns (1992) suggested that the dark lens of freshwater reduces the number of aggressive opportunistic species that occur typically at shallow depths, allowing species that are usually deeper and less competitive (e.g., stylasterids) to colonise unusually shallow waters. For example, *Stylaster eguchii*, a species presenting a wide depth range (15-1483 m), is found in shallow waters only in the fjords of New Zealand (Cairns, 1991b). The shallowest cold water stylaterid populations in fjord regions extend from 10 m depth suggesting stylasterid corals can have a eurybathic distribution (Grange 1990, Miller et al. 2004, Häussermann & Försterra 2007).

Interestingly, with the exception of the field-like aggregations described by Bax and Cairns (2014), which involve the presence of different species, the other coral aggregations described for the the Antarctic and sub-Antarctic regions are monospecific (Miller et al., 2004; Häussermann and Försterra, 2007; Salvati et al., 2010). Monospecific aggregations of stylasterids have also been recorded in other areas of the world, such as in the Strait of Messina, where Salvati et al. (2010) recorded the presence of dense communities of *Errina aspera* at depths between 83 and 105 metres. While in the Aleutian Islands, Brooke and Stone (2007) registered the presence of

several species (*Stylaster brochi* (Fisher, 1938), *Stylaster verrillii* (Dall, 1884), *Stylaster campylecus* (Fisher, 1938), *Stylaster cancellatus* Fisher, 1938, *Stylaster* sp. 1, *Stylaster* sp. 2, *Errinopora nanneca* Fisher, 1938, *Errinopora pourtalesi* (Dall, 1884), *Distichopora borealis* Fisher, 1938, *Distichopora* sp. 1, *Cyclohelia lamellata* Cairns, 1991, *Crypthelia trophostega* Fisher, 1938) of Stylastertidae at depths greater than 100 m, involved in the formation of coral gardens. The phenomenon of multispecific aggregations is best known for scleractinias. For example, Le Danois (1948) in the Bay of Biscay, recorded the presence of dense communities of *Madrepora oculata* Linnaeus, 1758, and *Lophelia pertusa* (Linnaeus, 1758), involved in the formation of extensive coral fields with a maximum height of 2 m. Afterwards these cold-water corals were also reported at different locations in the Bay of Biscay by Altuna (1995), Alvarez-Claudio (1994), Zibrowius (1985, 1980) and Zibrowius et al. (1975).

However, field-like aggregations of stylasterids risult patchily distributed throughout the Antarctica, sub-Antarctica, Patagonia (Bax, 2014) and New Zeland (Miller et al., 2004). These areas are recommended for priority protection, in order to maintain benthic biodiversity, as these field-like aggregations support a diverse array of associated fauna (e.g., Post et al., 2010; Waller et al., 2012; Kaiser et al., 2013), and may provide important

ecosystem services, such as secondary substrate, refuge for juveniles, aggregation sites for spawning and feeding, and potentially factor in the trajectory of deep-water current systems and house economically important fish populations and biomedical compounds (Bax, 2014).

The tridimensional structure of their calcareous skeleton enhances the complexity of the habitat, by creating refuges for a variety of mobile, sessile and boring organisms (Braga-Henriques et al. 2010), such as algae, sponges, anthozoans, hydroids, gastropods, annelids, cirripeds, copepods, echinoderms (Zibrowius 1981, Braga-Henriques et al. 2010, Goud and Hoeksema 2001, Pica et al. 2012, Pica et al. 2016).

Sponges are important components of Antarctic marine benthic assemblages, being often dominant in the Southern Ocean communities (Downey et al., 2012). Recent studies (Downey et al., 2012) have found that there are 397 sponge species from Antarctica, representing 139 genera in 70 families. This high abundance in the Antarctic continent is likely related to its geographic isolation, great age, pronounced structural heterogeneity (particularly epibiotic communities), and large geographic area (Brey et al., 1994; Gray, 2001; Starmans and Gutt, 2002). Interesting is also the high frequency of endemisms. In fact, the study conducted by Downey et al. (2012) showed that of the 397 sponge species, 43% (170 species) are endemic to Antarctica.

Data from our surveys indicated a rich and diverse sponge fauna associated with stylasterid beds in deep Antarctic waters, in line with the registered levels of diversity. In the present study, in fact, a total of 38 species associated to *Inferiolabiata labiata*, were identified, representing about the 10% of the sponge biodiversity of the entire Antarctic continent. The last published biogeographic work (Janussen and Tendal, 2007) highlights how little is known about the Antarctic deep-sea fauna and in particular about the sponge diversity of the deep communities; the authors underline how, in the near future, the number of Antarctic species, genera, families, and endemism are likely to increase in relation to the more and more frequent morphological and molecular research. The present study reflects the conclusions of Janussen and Tendal (2007) considering that, out of 38 classified sponge species, 8 of them are probably new, one represents a first record in the Antarctic continent while 10 species are first record in the Ross Sea.

One of the main factors controlling distribution and abundance of sessile organisms in benthic communities is the occurrence of free substrates (Connell and Keough 1985). Secondary hard substrates represent, for benthic species, a suitable alternative (Gutt and Schickan 1998) particularly in habitat characterized by a scarcity of primary rocky substrata, as Antarctica is (Gili et al. 1993). For example, mollusc shells of the scallop *Adamussium colbeki* (E.

A. Smith, 1902) are typically fouled by many invertebrate taxa, and sponges are the most frequent group, with different levels of substratum preference (Cerrano et al., 2009). In this way, the stylasterid beds play, at greater depths, the same role of the aggregations of *A. colbecki* (E. A. Smith, 1902) in more shallow waters (Cerrano et al., 2006; 2009).

The stylasterids analyzed in the present study have been dead for quite some time, therefore in agreement with Gutt et al.'s (1998) assertion that filter-feeding epibionts prefer living and elevated substrates, the large abundance of sponges species identified on the *I. labiata* fragments appears interesting when comparing our results with those of Cerrano et al. (2009), in which a similar number of sponge species (28 in 86 individuals) on *A. colbecki* was recorded in the Ross Sea. In fact, our stylasterid samples were neither elevated nor living substrate and this may be the reason why very low levels of coral coverage by sponges were found despite of the large number of species. On average, we estimated the presence of 2 different species per fragment of *I. labiata* with a maximum of 8 different species on a single fragment. This value is close to that estimated by Cerrano et al. (2009), where a maximum of 10 different species was estimated on a single scallop. Among the most recurring species recorded in the present study, the species *Iophon radiatum,* with a total of 47 individuals, shows the highest value of abundance

with a percentage of 21%. The species of the genus *Iophon* would seem to be very common as epibiont considering the results of Cerrano et al. (2009). In fact, these authors recorded high abundance values of the species *Iophon unicorne* on the valves of *A. colbecki*, while in the same study, the presence of *Iophon radiatum* on the spines of the sea-urchin *Ctenocidaris perrieri* Koehler, 1912 was observed several times. In addition, Gutt et al. (1998) also report very high values of absolute abundance of the species *I. radiatum* encrusting on the ophiuroids *Ophiurolepis* spp. within the Weddel Sea.

Regarding sponge coverage on fragments of *I. labiata*, the highest estimated value belongs to the species *Haliclona* sp. 1 with only 2.9% and the highest value considering all the sponges present in a single specimen of *I. labiata* is 13%. The average density of sponges on our stylasterid samples (0.11 individuals per cm^2) is comparable to that reported by Cerrano et al. (2009), according to which 0.2 individuals per cm^2 of surface of *A. colbecki* was extimated. The maximum size measured among our samples is 3.611 cm^2 relative to the species *Iophon unicorne* and the most frequent size class in our samples is between 0.003 and 0.5 cm^2, including 185 sponge specimens (81%). It would seem, therefore, that Antarctic stylasterid beds are not a substrate favored by sponges and that the high number of sponges detected is probably justified by the fact that our *I. labiata* specimens, being dead,

represented only a simple mineral but not elevated substrate that sponges, as filter feeders, can exploit to their advantage. In addition, such small values in terms of size could be justified by the three-dimensional pattern typical of *I. labiata*. In fact, *Inferolabiata* produces colonies characterised by a dense anastomosed branching pattern offering a three-dimensional scaffold (Cairns, 1983) and creating an optimal shelter for the sponge fauna. Moreover, the presence of reticulate tubes of thin branches induced by commensal polynoid worms invariably associated to the colonies (Cairns 1983) increases the three-dimensional pattern, as observed in various scleractinians, such as *Madrepora oculata* and *Desmophillum pertusum* (Linnaeus, 1758) (Bertolino et al., 2019). Thus, sponges, thanks to their plasticity, are probably suitable for occupy similar structures *via* a miniaturization of their size, however more studies are needed to confirm our observations.

The only study focusing on the relationships between stylasterids and sponges is the one by Pica et al. (2012) dealing with stylasterid species collected in Indonesia, while no data are currently available about Stylasterids and sponges from Antarctica. In the paper by Pica et al. (2012), authors recorded 15 sponge species from 70 colonies of *Distichopora* spp., of which 10 were boring and and five cryptic sponges filling the excavations previously produced and subsequently left vacant by other boring organisms. The

distribution of sponges along the colonies of *Distichopora* spp. is interesting. In fact, these authors reported the presence of boring sponges only on the dead basal portion of the *Distichopora* axis (Pica et al., 2012; these authors suggested that living stylasterids are probably not a suitable substrate for sponges. In fact, their surface might be covered by a sheet of chitinous perisarc preventing sponge adesion, while the penetration of boring species is faced by a dense network of coenosarc tubes. On the contrary, as previously noted, the studied antarctic stylasterids, being dead, may be more easily colonized by sponges; nevertheless, no boring sponges were found. This is not surprising considering that no boring sponge species have been found on the Antarctic continent so far. Nevertheless, several organisms show high bioerosive activity on the Antarctic continent, attacking carbonate and playing a key role in the global carbon cycle such as cyanobacteria, chlorophytes, fungi, foraminifera, algae and barnacles (Cerrano et al., 2001; Meyer et al., 2021). According to Skinner (1983), in Antarctica, the calcareous substrata are poorly represented, mainly biogenic, and there is no evidence of dissolution, even in aragonitic and delicate skeletons (Taviani et al., 1993). Thus, to date, our data, together with data obtained from previous studies dealing with the bioerosive activity of Antarctic organisms, confirm the lack of boring sponge species in the Southern Ocean.

It should be clear that a long-term research program would be necessary to successfully collect enough deep-sea samples to further improve the knowledge on the rich sponge fauna inhabiting Antarctic waters. Finally, reports in other invertebrate groups show that Antarctic deep-sea communities can be as rich or even richer than those of shallower environments (Brandt et al., 2004). Our estimations are in agreement with this pattern, providing further support to the hypothesis that the cold Southern Ocean is a diversity hot-spot.

Chapter 5

5. CONCLUSIONS

The results of our investigations provide the description of four species of stylasterids sampled in the Ross Sea: *Errina fissurata*, *Errina laterorifa*, *Errina gracilis*, and *Inferiolabiata labiata*. As already known, these four species are often associated together to form extensive field-like coral aggregations, characterizing the seabed of the Ross Sea and other areas of the Antarctic continent, representing, to date, one of the very few multispecific associations of stylasterids in the world. Two fundamental concepts that emerged from this study are represented by the importance of observing a large number of samples for a correct taxonomic classification, together with the analysis of different portions within the same colonies or fragments in order to observe how some characters can assume different appearances according to their arrangement on the samples. From a taxonomic point of view, regarding *E. laterorifa*, it has emerged that this species is characterized by a high morphological plasticity, presenting specimens of remarkably different in term of size and morphology. In addition, the already known distributions of the four classified species are confirmed.

Associated with the *I. labiata* specimens, a total of 38 sponge species were identified, of which 10 representing a first record in the Ross Sea, one a first

record for the Antarctica, and 9 may be new. Our study also shows that sponges, as filter-feeders, do not seem to prefer stylasterid beds as secondary substrate and that the three-dimensional pattern typical of the *I. labiata* species could induce a miniaturization process to allow sponges to find shelter on it.

In conclusion, the present study shows how little the benthic communities of Antarctica are still studied and how little is still known about the existing relationships among the organisms of the Southern Ocean. In the near future, a increment of the sampling effort and more in-depth studies should be carried out synergically in order to support the hypothesis that the Southern Ocean represents a biodiversity hot-spot.

REFERENCES

Agardy, M. T. (1994). Advances in marine conservation: the role of marine protected areas. *Trends in ecology & evolution*, *9*(7), 267-270.

Allemand, D., Cuif, J. P., Watabe, N., Oishi, M., & Kawaguchi, T. (1994). The organic matrix of skeletal structures of the Mediterranean red coral, *Corallium rubrum*. *Bulletin de l'Institut océanographique*, 129-139.

Altuna, A., 1995. El orden Scleractinia (Cnidaria, Anthozoa) en la costa vasca (Golfo de Vizcaya): especies batiales de la fosa de CapBreton. *Munibe 47*, 85–96.

Alvarez-Claudio, C., 1994. Deep-water Scleractinia (Cnidaria: Anthozoa) from southern Bay of Biscay. *Les Cahiers de Biologie Marine 35*, 461–469.

Babcock, R. C. (1991). Comparative demography of three species of scleractinian corals using age-and size-dependent classifications. *Ecological Monographs*, *61*(3), 225-244.

Babcock, R. C., Kelly, S., Shears, N. T., Walker, J. W., & Willis, T. J. (1999). Changes in community structure in temperate marine reserves. *Marine ecology progress series*, *189*, 125-134.

Badalamenti, F., Ramos, A. A., Voultsiadou, E., Lizaso, J. S., D'Anna, G., Pipitone, C., Mas, J., Ruiz Fernandez, J. A., Whitmarsh, D., & Riggio, S. (2000). Cultural and socio-economic impacts of Mediterranean marine protected areas. *Environmental conservation*, *27*(2), 110-125.

Bak, R. P., & Meesters, E. H. (1998). Coral population structure: the hidden information of colony size-frequency distributions. *Marine Ecology Progress Series*, *162*, 301-306.

Bavestrello, G., Calcinai, B., Cerrano, C., & Sarà, M. (1998). *Alectona* species from north-western Pacific (Demospongiae: Clionidae). *Journal of the Marine Biological Association of the United Kingdom*, *78*(1), 59-73.

Bax N. 2014. Deep-Sea Stylasterid corals in the Antarctic, Sub-Antarctic and Patagonian Benthos: biogeography, phylogenetics, connectivity and conservation. PhD in Marine Biology, University of Tasmania (UTas) at the Institute for Marine and Antarctic Studies (IMAS).

Bax, N. N., & Cairns, S. D. (2014). Stylasteridae (Cnidaria; Hydrozoa). *Biogeographic atlas of the southern ocean*.

Bernal, P. A., Oliva, D., Aliaga, B., & Morales, C. (1999). New regulations in Chilean fisheries and aquaculture: ITQ's and territorial users rights. *Ocean & Coastal Management*, *42*(2-4), 119-142.

Bertolino, M., Ricci, S., Canese, S., Cau, A., Bavestrello, G., Pansini, M., & Bo, M. (2019). Diversity of the sponge fauna associated with white coral banks from two Sardinian canyons (Mediterranean Sea). *Journal of the Marine Biological Association of the United Kingdom*, *99*(8), 1735-1751.

Bohnsack, J. A. (1998). Application of marine reserves to reef fisheries management. *Australian Journal of Ecology*, *23*(3), 298-304.

Boury-Esnault, N., & Van Beveren, M. (1982). *Les démosponges du plateau continental de Kerguellen-Heard*. Comité national français des recherches antarctiques.

Braga-Henriques, A., Carreiro-Silva, M., Porteiro, F. M., de Matos, V., Sampaio, Í., Ocana, O., & Avila, S. P. (2011). The association between a deep-sea gastropod *Pedicularia sicula* (Caenogastropoda: Pediculariidae) and its coral host *Errina dabneyi* (Hydrozoa: Stylasteridae) in the Azores. *ICES Journal of Marine Science*, *68*(2), 399-407.

Brandt, A., De Broyer, C., Gooday, A. J., Hilbig, B., & Thomson, M. R. (2004). Introduction to ANDEEP (ANtarctic benthic DEEP-sea biodiversity: colonization history and recent community patterns)—a tribute to Howard L. Sanders. *Deep Sea Research Part II: Topical Studies in Oceanography*, *51*(14-16), 1457-1465.

Brey, T., Klages, M., Dahm, C., Gorny, M., Gutt, J., Hain, S., Stiller, M., Arntz, W. E., Wägele J. W., & Zimmermann, A. (1994). Antarctic benthic diversity. *Nature*, *368*(6469), 297-297.

Broch H (1914) Stylasteridae. Dan Tngolf-Exped 5:1–28.

Broch H. 1942. Investigations on Stylasteridae (Hydrocorals). Skr Norske Vidensk Akad I Math-Naturw Klasse, 3: 1–113.

Brooke, S., & Stone, R. (2007). Reproduction of deep-water hydrocorals (family Stylasteridae) from the Aleutian Islands, Alaska. *Bulletin of Marine Science*, *81*(3), 519-532.

Buhl-Mortensen, L. E. N. E., & Mortensen, P. B. (2004). Symbiosis in deep-water corals. *Symbiosis*.

Burton, M. (1932). Sponges. *Discovery Reports.* 6: 237-392

Cairns, S. D. (1978). *Distichopora (Haplomerismos) anceps*, a new stylasterine coral (Coelenterata: Stylasterina) from deep water off the Hawaiian Islands. *Micronesica*.

Cairns, S. D. (1983). Antarctic and Subantarctic Stylasterina (Coelenterata: Hydrozoa). *Antarctic Research Series*.

Cairns, S. D. (1986). A revision of the northwest Atlantic Stylasteridae (Coelenterata: Hydrozoa).

Cairns, S. D. (1991). New records of Stylasteridae (Hydrozoa: Hydroida) from the Galápagos and Cocos Islands. *Proceedings of the Biological Society of Washington*.

Cairns, S. D. (1992). Worldwide distribution of the Stylasteridae (Cnidaria: Hydrozoa). *Scientia Marina*.

Cairns, S. D. (1999). Species richness of recent Scleractinia.

Cairns, S. D. (2011). Global diversity of the stylasteridae (Cnidaria: Hydrozoa: Athecatae). *PloS one*, *6*(7), e21670.

Cairns, S. D. (2015). Tropical Deep-Sea Benthos 28. Stylasteridae (Cnidaria: Hydrozoa: Anthoathecata) of the New Caledonian Region.

Cairns, S. D., & Macintyre, I. G. (1992). Phylogenetic implications of calcium carbonate mineralogy in the Stylasteridae (Cnidaria: Hydrozoa). *Palaios*, 96-107.

Cairns, S. D., & Samimi-Namin, K. (2015). A new species of Stylaster (Cnidaria: Hydrozoa: Stylasteridae) from the Arabian Sea, off Oman. *Proceedings of the Biological Society of Washington*, *128*(4), 209-215.

Cairns, S. D., & Zibrowius, H. (2013). Stylasteridae (Cnidaria, Hydrozoa, Filifera) from South Africa. *Zootaxa*, *3691*(1), 1-57.

Calcinai, B., Cerrano, C., Iwasaki, N., & Bavestrello, G. (2008). Sponges boring into precious corals: an overview with description of a new species of *Alectona* (Demospongiae, Alectonidae) and a worldwide identification key for the genus. *Marine Ecology*, *29*(2), 273-279.

Carter, H.J. (1874). Descriptions and Figures of Deep-sea Sponges and their Spicules from the Atlantic Ocean, dredged up on board H.M.S.‘Porcupine', chiefly in 1869; with Figures and Descriptions of some remarkable Spicules from the Agulhas Shoal and Colon, Panama. *Annals and Magazine of Natural History*. (4) 14 (79): 207-221, 245-257.

Castilla, J. C., & Duran, L. R. (1985). Human exclusion from the rocky intertidal zone of central Chile: the effects on *Concholepas concholepas* (Gastropoda). *Oikos*, 391-399.

Cerrano, C., Bertolino, M., Valisano, L., Bavestrello, G., & Calcinai, B. (2009). Epibiotic demosponges on the Antarctic scallop *Adamussium colbecki* (Smith, 1902) and the cidaroid urchins *Ctenocidaris perrieri* Koehler, 1912 in the nearshore habitats of the Victoria Land, Ross Sea, Antarctica. *Polar Biology*, *32*(7), 1067-1076.

Cerrano, C., Calcinai, B., Bertolino, M., Valisano, L., & Bavestrello, G. (2006). Epibionts of the scallop *Adamussium colbecki* (Smith, 1902) in the Ross Sea, Antarctica. *Chemistry and Ecology*, *22*(sup1), S235-S244.

Cerrano, C., Puce, S., Chiantore, M., Bavestrello, G., Cattaneo-Vietti, R. (2001) The influence of the epizoic hydroid *Hydractinia angusta* on the recruitment of the Antarctic scallop *Adamussium colbecki*. *Polar Biol* 24:577–581

CITES. 1975. Appendices I, II, III. https://www.cites.org(last check: 21.11.2016).

Clarke, A., & Johnston, N. M. (2003). Antarctic marine benthic diversity. *Oceanography and marine biology*, *41*, 47-114.

Cole, R. G., Villouta, E., & Davidson, R. J. (2000). Direct evidence of limited dispersal of the reef fish *Parapercis colias* (Pinguipedidae) within a marine reserve and adjacent fished areas. *Aquatic Conservation: Marine and Freshwater Ecosystems*, *10*(6), 421-436.

Connell, J. H., Keough, M. J. (1985). Disturbance and patch dynamics of subtidal marine animals on hard substrata. *Natural Disturbance and Patch Dynamics*, 125-151.

Cortesogno, L., Gaggero, L., Bavestrello, G., Cerrano, C., & Cattaneo-Vietti, R. (1999). Struttura, mineralogia, minerochimica e chimismo del corallo rosso. *Biologia e tutela del corallo rosso e di altri ottocoralli del Mediterraneo. Ministero per le Politiche Agricole, Almentari e Forestali, Roma*, 83-97.

Daly, H. E. (2007). *Ecological economics and sustainable development*. Edward Elgar Publishing.

Davis, D., & Tisdell, C. (1995). Recreational scuba-diving and carrying capacity in marine protected areas. *Ocean & Coastal Management*, *26*(1), 19-40.

Di Camillo, C.G., Bavestrello, G., Cerrano, C., Gravili, C., Piraino, S., Puce, S., Boero, F. 2017. Hydroids (Cnidaria, Hydrozoa): A Neglected Component of Animal Forests.

Downey, R. V., Griffiths, H. J., Linse, K., & Janussen, D. (2012). Diversity and distribution patterns in high southern latitude sponges. *PLoS One*, *7*(7), e41672.

Edwards, H. M., & Haime, J. (1850). A Monograph of the British Fossil Corals. First Part. Introduction; Corals from the Tertiary and Cretaceous Formations. *Monographs of the Palaeontographical Society*, *3*(7), i-71.

Eguchi, M. (1964). A study of Stylasterina from the Antarctic Sea.

England, H. M. (1926, April). Development of Gonophores of the Stylasteridsæ. In *Proceedings of the Zoological Society of London* (Vol. 96, No. 1, pp. 265-283). Oxford, UK: Blackwell Publishing Ltd.

Fritchman, H. K. (1974). The planula of the stylasterine hydrocoral *Allopora petrograpta* Fisher: its structure, metamorphosis and development of the primary cyclosystem. In *Proceedings of the Second International Coral Reef Symposium* (Vol. 2, pp. 245-258).

Giacobbe, S., Laria, G., & Spanò, N. (2007). Hard bottom assemblages in the Strait of Messina: distribution of *Errina aspera* L. (Hydrozoa: Stylasteridae). *Rapports Commission International Mer Méditerranée*, *38*, 485.

Gili, J. M., & Hughes, R. G. (1995). The ecology of marine benthic hydroids. *Oceanography and marine biology: an annual review*.

Gili, J. M., Abello, P., & Villanueva, R. (1993). Epibionts and intermoult duration in the crab Bath vnectes~ i~ eritus. *Marine ecology Progress series*, *98*, 107-113.

Goedbloed AF (1962) The dactylozooids of *Allopora blattea* and *Stylaster roseus*. Proc Acad Wetens 65:438–446.

Goud, J. Hoeksema BW (2001). *Pedicularia vanderlandi* spec. nov., a symbiotic snail (Caenogastropoda: Ovulidae) on the hydrocoral *Distichopora vervoorti* Cairns and Hoeksema, 1998 (Hydrozoa: Stylasteridae), from Bali, Indonesia. *Zool Verh Leiden*, *334*, 77-97.

Grange KR, Singleton RJ, Richardson JR, Hill PJ, Main WDeL. 1981. Shallow rock wall biological associations of some southern fiords of New Zealand. *New Zealand Journal of Zoology* 8: 209–227.

Grange KR. 1990. Unique marine habitats in the New Zealand fiords: a case for preservation. *New Zealand Oceanographic Institute Report 1990/7*, 70.

Grange, K. R., & Singleton, R. J. (1988). Population structure of black coral, *Antipathes aperta*, in the southern fiords of New Zealand. *New Zealand Journal of Zoology*, *15*(4), 481-489.

Gray, J. S. (2001). Antarctic marine benthic biodiversity in a world-wide latitudinal context. *Polar Biology*, *24*(9), 633-641.

Grigg, R. W. (1977). Population dynamics of two gorgonian corals. *Ecology*, *58*(2), 278-290.

Guinotte, J. M., & Fabry, V. J. (2008). Ocean acidification and its potential effects on marine ecosystems. *Annals of the New York Academy of Sciences*, *1134*(1), 320-342.

Guinotte, J. M., Orr, J., Cairns, S., Freiwald, A., Morgan, L., & George, R. (2006). Will human-induced changes in seawater chemistry alter the distribution of deep-sea scleractinian corals?. *Frontiers in Ecology and the Environment*, *4*(3), 141-146.

Gutt, J., & Schickan, T. (1998). Epibiotic relationships in the Antarctic benthos. *Antarctic Science*, *10*(4), 398-405.

Hansen, G.A. (1885). Spongiadae. The Norwegian North-Atlantic Expedition 1876-1878. *Zoology.* 13: 1-26.

Harriott, V. J., Davis, D., & Banks, S. A. (1997). Recreational diving and its impact in marine protected areas in eastern Australia. *Ambio*, 173-179.

Häussermann, V., & Försterra, G. (2007). Extraordinary abundance of hydrocorals (Cnidaria, Hydrozoa, Stylasteridae) in shallow water of the Patagonian fjord region. *Polar Biology, 30*(4), 487-492.

Heifetz, J. (2002). Coral in Alaska: distribution, abundance, and species associations. *Hydrobiologia*, *471*(1), 19-28.

Hentschel, E. (1914). Monaxone Kieselschwämme und Hornschwämme der Deutschen Südpolar-Expedition 1901-1903. *Deutsche Südpolar-Expedition.* 15 (1): 35-141.

Hickson, S. J. (1890). Memoirs: On the Maturation of the Ovum and the Early Stages in the Development of *Allopora*. *Journal of Cell Science*, *2*(120), 579-598.

Hickson, S. J. (1891). Memoirs: The Medusæ of *Millepora murrayi* and the Gonophores of *Allopora* and *Distichopora*. *Journal of Cell Science*, *2*(127), 375-408.

Hickson, S. J. (1892). *Notes on a small collection of Hydrocorallinae*.

Hughes, T. P., & Jackson, J. B. C. (1980). Do corals lie about their age? Some demographic consequences of partial mortality, fission, and fusion. *Science*, *209*(4457), 713-715.

Janussen, D., & Tendal, O. S. (2007). Diversity and distribution of Porifera in the bathyal and abyssal Weddell Sea and adjacent areas. *Deep Sea Research Part II: Topical Studies in Oceanography*, *54*(16-17), 1864-1875.

Kaiser, S., Brandão, S.N., Brix, S., Barnes, David, K.A., Bowden, D.A., Ingels, J., Leese, F., Schiaparelli, S., Arango, C.P., Renuka, B., Bax, N., Blazewicz-Paszkowycz, M., Brandt, A., Brenke, N., Catarino, A., David, B., De Ridder, C., Dubois P., Ellingsen, K., Glover, A.G., Griffiths, H.J., Gutt, J., Halanych, K.M., Havermans, C., Held, C., Janussen, D., Lörz, A., Pearce, D.A., Pierrat, B., Riehl, T., Rose, A., Sands, C.J., Soler-Membrives, A., Schüller, M., Strugnell, J.M., Vanreusel, A., Veit-Köhler, G., Wilson, N.G., Yasuhara, M., (2013) Patterns, processes and vulnerability of the Southern Ocean benthos: a decadal leap in knowledge and understanding. *Marine biology*, 160: 2295-2317.

Kim, M. J., Park, H. J., Youn, U. J., Yim, J. H., & Han, S. J. (2019). Diversity of Culturable Bacteria Associated with Hard Coral from the Antarctic Ross Sea. *Journal of Marine Life Science*, *4*(1), 22-28.

Kirkpatrick, R. (1907). Preliminary Report on the Monaxonellida of the National Antarctic Expedition. *Annals and Magazine of Natural History.* 7(20): 271-291.

Koltun, V.M. (1964). Sponges of the Antarctic. 1 Tetraxonida and Cornacuspongida. Pp. 6-133, 443-448. *In: Pavlovskii, E.P., Andriyashev,A.P. & Ushakov, P.V. (Eds), Biological Reports of the Soviet Antarctic Expedition (1955-1958).* Akademya Nauk SSSR.

Le Danois, E. (1948). Les Profondeurs de la Mer. Trente Ans de Recherches sur la Faune Sous-marine au Large des CoÃtes de France. *Payot, Paris*.

Lévi, C.; Lévi, P. (1982). Spongiaires Hexactinellides du Pacifique Sud-Ouest (Nouvelle-Calédonie). *Bulletin du Muséum national d'Histoire naturelle.* 4(3-4): 283-317.

Lindner, A., Cairns, S. D., & Cunningham, C. W. (2008). From offshore to onshore: multiple origins of shallow-water corals from deep-sea ancestors. *PLoS One*, *3*(6), e2429.

Love, M. S., Lenarz, B., & Snook, L. (2010). A survey of the reef fishes, purple hydrocoral (*Stylaster californicus*), and marine debris of Farnsworth Bank, Santa Catalina Island. *Bulletin of Marine Science*, *86*(1), 35-52.

McClanahan, T. R., & Mangi, S. (2000). Spillover of exploitable fishes from a marine park and its effect on the adjacent fishery. *Ecological applications*, *10*(6), 1792-1805.

Meyer, N., Wisshak, M., & Freiwald, A. (2021). Bioerosion ichnodiversity in barnacles from the Ross Sea, Antarctica. *Polar Biology*, *44*(4), 667-682.

Miller, J., Mundy, K., C. N., & Lindsay Chadderton, W. (2004). Ecological and genetic evidence of the vulnerability of shallow-water populations of the stylasterid hydrocoral *Errina novaezelandiae* in New Zealand's fiords. *Aquatic Conservation: Marine and Freshwater Ecosystems*, *14*(1), 75-94.

Moseley, H. N. (1879). On the Structure of the Stylasteridæ a Family of Hydroid Stony Corals. *Nature*, *20*(510), 339-341.

Moseley, H. N. (1881). *Report on certain Hydroid, Alcyonarian and Madreporarian Corals procured during the voyage of HMS Challenger* (Vol. 2).

Mosquera, I., Côté, I. M., Jennings, S., & Reynolds, J. D. (2000, November). Conservation benefits of marine reserves for fish populations. In *Animal Conservation forum* (Vol. 3, No. 4, pp. 321-332). Cambridge University Press.

Ostarello, G. L. (1973). Natural history of the hydrocoral *Allopora californica* Verrill (1866). *The Biological Bulletin*, *145*(3), 548-564.

Peyton Jones, S. L., & Wadler, P. (1993, March). Imperative functional programming. In *Proceedings of the 20th ACM SIGPLAN-SIGACT symposium on Principles of programming languages* (pp. 71-84).

Pica, D. (2012). Morphology and ecology of Stylasteridae. PhD in Marine Biology and Ecology, Università Politecnica delle Marche.

Pica, D., Bertolino, M., Calcinai, B., Puce, S., & Bavestrello, G. (2012). Boring and cryptic sponges in stylasterids (Cnidaria: Hydrozoa). *Italian Journal of Zoology*, *79*(2), 266-272.

Pica, D., Tribollet, A., Golubic, S., Bo, M., Di Camillo, C.G., Bavestrello, G., Puce, S. (2016). Microboring organisms in living stylasterid corals (Cnidaria, Hydrozoa). *Marine Biology Research*, *12* (6): 573-582.

Plathong, S., Inglis, G. J., & Huber, M. E. (2000). Effects of self-guided snorkeling trails on corals in a tropical marine park. *Conservation biology*, *14*(6), 1821-1830.

Post, A. L., O'Brien, P. E., Beaman, R. J., Riddle, M. J., & De Santis, L. (2010). Physical controls on deep water coral communities on the George V Land slope, East Antarctica. *Antarctic Science*, *22*(4), 371-378.

Probert, P. K., Mckinght, D. G., & Grove, S. L. (1997). Benthic invertebrate bycatch from a deep-water trawl fishery, Chatham Rise, New Zealand. *Aquatic Conservation: marine and freshwater ecosystems*, *7*(1), 27-40.

Puce, S., Bo, M., Di Camillo, C. G., Paoli, L., Pica, D., & Bavestrello, G. (2010). Morphology and development of the early growth stages of an Indonesian *Stylaster* (Cnidaria: Hydrozoa). *Journal of the Marine Biological Association of the United Kingdom*, *90*(6), 1145-1151.

Puce, S., Pica, D., Mancini, L., Brun, F., Peverelli, A., & Bavestrello, G. (2011). Three-dimensional analysis of the canal network of an Indonesian *Stylaster* (Cnidaria, Hydrozoa, Stylasteridae) by means of X-ray computed microtomography. *Zoomorphology*, *130*(2), 85-95.

Puce, S., Pica, D., Schiaparelli, S., & Negrisolo, E. (2016). Integration of morphological data into molecular phylogenetic analysis: Toward the identikit of the stylasterid Ancestor. *PloS one*, *11*(8), e0161423.

Puce, S., Tazioli, S., & Bavestrello, G. (2009). First evidence of a specific association between a stylasterid coral (Cnidaria: Hydrozoa: Stylasteridae) and a boring cyanobacterium. *Coral Reefs*, *28*(1), 177-177.

Rasband, W. S. (2011). ImageJ. US National Institutes of Health; Bethesda, Maryland, USA: 1997–2011

Ridley, S. O., & Dendy, A. (1886). XXXIV.—Preliminary Report on the Monaxonida collected by HMS 'Challenger'. *Journal of Natural History*, *18*(107), 325-351.

Rìos, P. L. (2006) Esponjas del orden Poecilosclerida de las campana Española de bentos antártico. Universidade de Santiago De Compostela.

Roberts, J. M., Wheeler, A. J., & Freiwald, A. (2006). Reefs of the deep: the biology and geology of cold-water coral ecosystems. *Science*, *312*(5773), 543-547.

Rogers, A. D., Baco, A., Griffiths, H., & Hall-Spencer, J. M. (2007). Corals on seamounts. In *Seamounts: Ecology Fisheries and Conservation, Blackwell Fisheries and Aquatic resources Series*. Blackwell Scientific.

Rouphael, A. B., & Inglis, G. J. (1997). Impacts of recreational scuba diving at sites with different reef topographies. *Biological conservation*, *82*(3), 329-336.

Russ, G. R., & Alcala, A. C. (1996). Do marine reserves export adult fish biomass? Evidence from Apo Island, central Philippines. *Marine Ecology Progress Series*, *132*, 1-9.

Sala, E., & Zabala, M. (1996). Fish predation and the structure of the sea urchin *Paracentrotus lividus* populations in the NW Mediterranean. *Marine ecology progress series*, *140*, 71-81.

Salvati, E., Angiolillo, M., Bo, M., Bavestrello, G., Giusti, M., Cardinali, A., Puce, S., Spaggiari, C., Greco, S., & Canese, S. (2010). The population of *Errina aspera* (Hydrozoa: Stylasteridae) of the Messina Strait

(Mediterranean Sea). *Journal of the Marine Biological Association of the United Kingdom*, *90*(7), 1331-1336.

Sarà, M. (1978). Demospongie di acque superficiali della Terra del Fuoco (Spedizioni AMF Mares - GRSTS e SAI). *Bollettino dei Musei e degli Istituti Biologici della (R.) Università di Genova.* 46: 7-117.

Schmidt, O. (1870). Grundzüge einer Spongien-Fauna des atlantischen Gebietes. (Wilhelm Engelmann: Leipzig): iii-iv, 1-88.

Skinner, D. N. B. (1983). The geology of Terra Nova Bay. *Antarctic Earth Science. Australian Academy of Science, Canberra*, 150-155.

Sollas, W.J. (1888). Report on the Tetractinellida collected by H.M.S. Challenger, during the years 1873-1876. *Report on the Scientific Results of the Voyage of H.M.S. Challenger during the years 1873–76. Zoology.* 25 (part 63): 1-458.

Starmans, A., & Gutt, J. (2002). Mega-epibenthic diversity: a polar comparison. *Marine Ecology Progress Series*, *225*, 45-52.

Stosch, H. V. (1974). Pleurax, seine Synthese und seine Verwendung zur Einbettung und Darstellung det Zellwande von Diatomeen, Peridineen und anderen Algen, sowie fur eine neue Methode zur Electivfarbung von Dinoflagellaten-Penzern. *Archiv fur Protistenkunde*, *116*, 132-141.

Taviani, M., Reid, D. E., & Anderson, J. B. (1993). Skeletal and isotopic composition and paleoclimatic significance of late Pleistocene carbonates, Ross Sea, Antarctica. *Journal of Sedimentary Research*, *63*(1), 84-90.

Thiele, J. (1905) Die Kiesel-und Hornschwämme der Sammlung Plate. *Zoologische Jahrbücher*, *6*, 407-495.

Thresher, R. E., Tilbrook, B., Fallon, S., Wilson, N. C., & Adkins, J. (2011). Effects of chronic low carbonate saturation levels on the distribution, growth and skeletal chemistry of deep-sea corals and other seamount megabenthos. *Marine Ecology Progress Series*, *442*, 87-99.

Tilmant, J. T., & Schmahl, G. P. (1981). A comparative analysis of coral damage on recreationally used reefs within Biscayne National Park, Florida. In *4. International Coral Reef Symposium, Manila (Philippines), 18-22 May 1981*.

Topsent, E. (1901). Spongiaires. Résultats du voyage du S.Y. 'Belgica'en 1897-99 sous le commandement de A. de Gerlache de Gomery. *Expédition antarctique belge. Zoologie.* 4: 1-54.

Topsent, E. (1907). Poecilosclérides nouvelles recueillies par le Français dans l'Antarctique. *Bulletin du Muséum national d'histoire naturelle, Paris.* 13: 69-76.

Topsent, E. (1908). Spongiaires. *Expédition antarctique française (1903-1905) commandée par le Dr Jean Charcot (Paris).* 4: 1-37.

Topsent, E. (1916). Diagnoses d'éponges recueillies dans l'Antarctique par le Pourquoi-Pas?. *Bulletin du Muséum national d'histoire naturelle, Paris.* (1) 22(3): 163-172.

Van Soest, R. W. (2017). *Flagellia*, a new subgenus of Haliclona (Porifera, Haplosclerida). *European Journal of Taxonomy*, *351*, 1-48.

von Marenzeller, E. (1903). *Steinkorallen* (Vol. 3). G. Fischer.

Waller, R. G., & Robinson, L. F. (2012). Southern ocean corals: Cabo de Hornos. *Coral Reefs*, *31*(1), 205-205.

Waller, R. G., Scanlon, K. M., & Robinson, L. F. (2011). Cold-water coral distributions in the Drake Passage area from towed camera observations–initial interpretations. *PLoS One*, *6*(1), e16153.

Wisshak, M., Correa, M. L., Gofas, S., Salas, C., Taviani, M., Jakobsen, J., & Freiwald, A. (2009). Shell architecture, element composition, and stable isotope signature of the giant deep-sea oyster *Neopycnodonte*

zibrowii sp. n. from the NE Atlantic. *Deep Sea Research Part I: Oceanographic Research Papers*, *56*(3), 374-407.

WoRMS Editorial Board (2022). World Register of Marine Species. Available from https://www.marinespecies.org at VLIZ. Accessed 2022-02-04.

Zakai, D., & Chadwick-Furman, N. E. (2002). Impacts of intensive recreational diving on reef corals at Eilat, northern Red Sea. *Biological Conservation*, *105*(2), 179-187.

Zibrowius, H. (1980). Les Scléractiniaires de la Méditerranée et de l'Atlantique nord-oriental. *Mémoires de l'Institut océanographique, Monaco*.

Zibrowius, H. (1981). Associations of Hydrocorallia Stylasterina with gall-inhabiting Copepoda Siphonostomatoidea from the south-west Pacific. Part I. On the stylasterine hosts, including two new species, *Stylaster papuensis* and *Crypthelia cryptotrema*. *Bijdragen tot de Dierkunde*, *51*(2), 268-281.

Zibrowius, H. (1985). Scléractiniaires bathyaux et abyssaux de l'Atlantique nordoriental: campagnes BIOGAS (POLGAS) et INCAL. *Peuplements profonds du Golfe de Gascogne. IFREMER, Brest, France*, 311-324.

Zibrowius, H., Southward, E. C., & Day, J. H. (1975). New observations on a little-known species of *Lumbrineris* (Polychaeta) living on various Cnidarians, with notes on its recent and fossil Scleractinian hosts. *Journal of the Marine biological Association of the United Kingdom*, *55*(1), 83-108.

SUPPLEMENTARY MATERIAL

Table s. 1: list of all identified stylasterid samples with additionally information.

Sample n.	Date	Locality	Depth (m)	Stylasterid species
GRC-08-024	03/02/2017	Cape Hallett Canyon	750	*Errina fissurata* (Gray, 1872)
				Errina laterorifa Eguchi, 1964
				Inferiolabiata labiata (Moseley, 1879)
GRC-08-022	03/02/2017	Cape Hallett Canyon	750	*Errina fissurata* (Gray, 1872)
				Errina laterorifa Eguchi, 1964
GRC-02-038 MNA9250	07/01/2017	Iselin Bank	670	*Errina laterorifa* Eguchi, 1964
GRC-C2-T2-R2-007	09/02/2017	/	434	*Errina laterorifa* Eguchi, 1964
GRC-02-035 MNA9274	07/01/2017	Iselin Bank	670	*Errina laterorifa* Eguchi, 1964
GRC-02-104	07/01/2017	Iselin Bank	670	*Errina laterorifa* Eguchi, 1964
GRC-02-102	07/01/2017	Iselin Bank	670	*Errina laterorifa* Eguchi, 1964
GRC-02-101	07/01/2017	Iselin Bank	670	*Errina laterorifa* Eguchi, 1964
GRC-02-080 MNA9263	07/01/2017	Iselin Bank	670	*Errina laterorifa* Eguchi, 1964
GRC-C2-R4-011	31/01/2017	/	434	*Errina fissurata* (Gray, 1872)

				Errina laterorifa Eguchi, 1964
GRC-C2-R4-005	31/01/2017	/	434	*Errina fissurata* (Gray, 1872)
				Errina laterorifa Eguchi, 1964
GRC-08-087	03/02/2017	Cape Hallett Canyon	750	*Errina laterorifa* Eguchi, 1964
GRC-C2-T2-R1-003	09/02/2017	/	434	*Errina laterorifa* Eguchi, 1964
GRC-08-049 MNA9216	03/02/2017	Cape Hallett Canyon	670	*Errina laterorifa* Eguchi, 1964
GRC-02-081 MNA9260	07/01/2017	Iselin Bank	670	*Errina laterorifa* Eguchi, 1964
GRC-02-129	07/01/2017	Iselin Bank	670	*Errina laterorifa* Eguchi, 1964
GRC-02-106	07/01/2017	Iselin Bank	670	*Errina laterorifa* Eguchi, 1964
GRC-02-103	07/01/2017	Iselin Bank	670	*Errina laterorifa* Eguchi, 1964
GRC-02-082 MNA9261	07/01/2017	Iselin Bank	670	*Errina laterorifa* Eguchi, 1964
GRC-C1-T2-R2-002	09/02/2017	/	434	*Errina laterorifa* Eguchi, 1964
GRC-02-074 MNA9266	07/01/2017	Iselin Bank	670	*Errina laterorifa* Eguchi, 1964
GRC-C1-T2-R3-002	09/02/2017	/	432	*Errina laterorifa* Eguchi, 1964
GRC-02-077 MNA9264	07/01/2017	Iselin Bank	670	*Errina laterorifa* Eguchi, 1964

GRC-02-083 MNA9262	07/01/2017	Iselin Bank	670	*Errina laterorifa* Eguchi, 1964
GRC-02-078 MNA9268	07/01/2017	Iselin Bank	670	*Errina laterorifa* Eguchi, 1964
GRC-02-079 MNA9269	07/01/2017	Iselin Bank	670	*Errina laterorifa* Eguchi, 1964
GRC-02-057 MNA10226	07/01/2017	Iselin Bank	670	*Errina laterorifa* Eguchi, 1964
GRC-02-037 MNA9277	07/01/2017	Iselin Bank	670	*Errina laterorifa* Eguchi, 1964
GRC-02-076 MNA9265	07/01/2017	Iselin Bank	670	*Errina laterorifa* Eguchi, 1964
GRC-08-004 MNA9222	03/02/2017	Cape Hallett Canyon	750	*Errina fissurata* (Gray, 1872) *Errina laterorifa* Eguchi, 1964
GRC-08-006 MNA9226	03/02/2017	Cape Hallett Canyon	750	*Errina laterorifa* Eguchi, 1964
GRC-08-003 MNA9229	03/02/2017	Cape Hallett Canyon	750	*Errina laterorifa* Eguchi, 1964
GRC-08-001 MNA9227	03/02/2017	Cape Hallett Canyon	750	*Errina fissurata* (Gray, 1872) *Errina laterorifa* Eguchi, 1964
GRC-02-100	07/01/2017	Iselin Bank	670	*Errina laterorifa* Eguchi, 1964
GRC-02-105	07/01/2017	Iselin Bank	670	*Errina laterorifa* Eguchi, 1964
GRC-08-025	03/02/2017	Cape Hallett Canyon	750	*Errina fissurata*

				(Gray, 1872)
				Errina laterorifa Eguchi, 1964
GRC-08-088	03/02/2017	Cape Hallett Canyon	750	*Errina fissurata* (Gray, 1872)
				Errina laterorifa Eguchi, 1964
GRC-TR17-001	09/02/2017	/	1022	*Errina fissurata* (Gray, 1872)
				Errina laterorifa Eguchi, 1964
				Inferiolabiata labiata (Moseley, 1879)
GRC-02-075	07/01/2017	Iselin Bank	670	*Errina laterorifa* Eguchi, 1964
GRC-08-067	03/02/2017	Cape Hallett Canyon	750	*Errina fissurata* (Gray, 1872)
GRC-08-083	03/02/2017	Cape Hallett Canyon	750	*Errina fissurata* (Gray, 1872)
GRC-08-079	03/02/2017	Cape Hallett Canyon	750	*Errina fissurata* (Gray, 1872)
GRC-C2-T2-R2-008	09/02/2017	/	434	*Errina fissurata* (Gray, 1872)
GRC-08-092	03/02/2017	Cape Hallett Canyon	750	*Errina fissurata* (Gray, 1872)
GRC-02-109	07/01/2017	Iselin Bank	670	*Errina fissurata* (Gray, 1872)
GRC-C2-R4-003	09/02/2017	/	434	*Errina fissurata* (Gray, 1872)
GRC-02-036 MNA9276	07/01/2017	Iselin Bank	670	*Errina fissurata* (Gray, 1872)

GRC-TR17-005	09/02/2017	/	1022	*Errina fissurata* (Gray, 1872)
GRC-C2-T2-R5-002	09/02/2017	/	433	*Errina fissurata* (Gray, 1872)
GRC-02-033 MNA9273	07/01/2017	Iselin Bank	670	*Errina fissurata* (Gray, 1872)
GRC-C2-T2-R1-002	09/02/2017	/	434	*Errina fissurata* (Gray, 1872)
GRC-C2-R4-001 MNA9280	09/02/2017	/	434	*Errina fissurata* (Gray, 1872)
GRC-08-050 MNA9214	03/02/2017	Cape Hallett Canyon	750	*Errina fissurata* (Gray, 1872)
GRC-TR17-004	09/02/2017	/	434	*Errina fissurata* (Gray, 1872)
GRC-02-032 MNA9275	07/01/2017	Iselin Bank	670	*Errina fissurata* (Gray, 1872)
GRC-08-086	03/02/2017	Cape Hallett Canyon	750	*Errina fissurata* (Gray, 1872)
GRC-02-034 MNA9254	07/01/2017	Iselin Bank	670	*Errina fissurata* (Gray, 1872)
GRC-02-030 MNA9253	07/01/2017	Iselin Bank	670	*Errina fissurata* (Gray, 1872)
GRC-C2-R4-004 MNA9282	31/01/2017	/	434	*Errina fissurata* (Gray, 1872)
GRC-C2-R1-003 MNA9279	09/02/2017	/	434	*Errina fissurata* (Gray, 1872)
GRC-02-031 MNA9252	07/01/2017	Iselin Bank	670	*Errina fissurata* (Gray, 1872)
GRC-02-029 MNA9272	07/01/2017	Iselin Bank	670	*Errina fissurata* (Gray, 1872)
GRC-02-028	07/01/2017	Iselin Bank	670	*Errina fissurata*

MNA9256				(Gray, 1872)
GRC-02-128	07/01/2017	Iselin Bank	670	*Errina fissurata* (Gray, 1872)
GRC-02-184	07/01/2017	Iselin Bank	670	*Errina fissurata* (Gray, 1872)
GRC-C2-T2-R2-002	09/02/2017	/	434	*Errina fissurata* (Gray, 1872)
GRC-08-080	03/02/2017	Cape Hallett Canyon	750	*Errina fissurata* (Gray, 1872)
GRC-08-081	03/02/2017	Cape Hallett Canyon	750	*Errina fissurata* (Gray, 1872)
GRC-08-082	03/02/2017	Cape Hallett Canyon	750	*Errina fissurata* (Gray, 1872)
GRC-08-084	03/02/2017	Cape Hallett Canyon	750	*Errina fissurata* (Gray, 1872)
GRC-08-085	03/02/2017	Cape Hallett Canyon	750	*Errina fissurata* (Gray, 1872)
GRC-TR17-006	09/02/2017	/	1022	*Errina fissurata* (Gray, 1872)
GRC-02-107	07/01/2017	Iselin Bank	670	*Errina fissurata* (Gray, 1872)
GRC-02-118	07/01/2017	Iselin Bank	670	*Errina (Errina) gracilis* von Marenzeller, 1903
GRC-02-119	07/01/2017	Iselin Bank	670	*Errina (Errina) gracilis* von Marenzeller, 1903
GRC-02-123	07/01/2017	Iselin Bank	670	*Errina (Errina) gracilis* von Marenzeller, 1903
GRC-02-124	07/01/2017	Iselin Bank	670	*Errina (Errina) gracilis* von Marenzeller, 1903

GRC-C2-R4-012	31/01/2017	/	434	*Errina (Errina) gracilis* von Marenzeller, 1903
GRC-08-093	03/02/2017	Cape Hallett Canyon	750	*Errina (Errina) gracilis* von Marenzeller, 1903
GRC-C2-T2-R2-006	09/02/2017	/	434	*Errina (Errina) gracilis* von Marenzeller, 1903
GRC-C2-T2-R6-003	09/02/2017	/	434	*Errina (Errina) gracilis* von Marenzeller, 1903
GRC-02-057 MNA10226	07/01/2017	Iselin Bank	670	*Errina (Errina) gracilis* von Marenzeller, 1903
GRC-C1-R3-003 MNA9278	31/01/2017	/	432	*Errina (Errina) gracilis* von Marenzeller, 1903
GRC-C2-R4-002 MNA9281	31/01/2017	/	432	*Errina (Errina) gracilis* von Marenzeller, 1903
GRC-02-117	07/01/2017	Iselin Bank	670	*Errina (Errina) gracilis* von Marenzeller, 1903
GRC-02-122	07/01/2017	Iselin Bank	670	*Errina (Errina) gracilis* von Marenzeller, 1903
GRC-08-023	03/02/2017	Cape Hallett Canyon	750	*Inferiolabiata labiata* (Moseley, 1879)
GRC-02-127	07/01/2017	Iselin Bank	670	*Inferiolabiata labiata* (Moseley, 1879)
GRC-08-087	03/02/2017	Cape Hallett Canyon	750	*Inferiolabiata labiata* (Moseley, 1879)
GRC-02-144 MNA 10231	07/01/2017	Iselin Bank	670	*Inferiolabiata labiata* (Moseley, 1879)
	31/01/2017	Hallett Ridge	910	

GRC-07-030 MNA10230				*Inferiolabiata labiata* (Moseley, 1879)
GRC-08-005 MNA9223	03/02/2017	Cape Hallett Canyon	750	*Inferiolabiata labiata* (Moseley, 1879)
GRC-02-027 MNA9251	07/01/2017	Iselin Bank	670	*Inferiolabiata labiata* (Moseley, 1879)
GRC-02-046 MNA9259	07/01/2017	Iselin Bank	670	*Inferiolabiata labiata* (Moseley, 1879)
GRC-08-048 MNA9215	03/02/2017	Cape Hallett Canyon	750	*Inferiolabiata labiata* (Moseley, 1879)
GRC-02-049 MNA92	07/01/2017	Iselin Bank	670	*Inferiolabiata labiata* (Moseley, 1879)
GRC-02-041 MNA9258	07/01/2017	Iselin Bank	670	*Inferiolabiata labiata* (Moseley, 1879)
GRC-02-040 MNA9271	07/01/2017	Iselin Bank	670	*Inferiolabiata labiata* (Moseley, 1879)
GRC-02-223	07/01/2017	Iselin Bank	670	*Inferiolabiata labiata* (Moseley, 1879)
GRC-02-114	07/01/2017	Iselin Bank	670	*Inferiolabiata labiata* (Moseley, 1879)
GRC-08-065	03/02/2017	Cape Hallett Canyon	750	*Inferiolabiata labiata* (Moseley, 1879)
GRC-08-077	03/02/2017	Cape Hallett Canyon	750	*Inferiolabiata labiata* (Moseley, 1879)
GRC-TR17-007	09/02/2017	/	1022	*Inferiolabiata labiata* (Moseley, 1879)
GRC-02-113	07/01/2017	Iselin Bank	670	*Inferiolabiata labiata* (Moseley, 1879)
GRC-02-092	07/01/2017	Iselin Bank	670	*Inferiolabiata labiata* (Moseley, 1879)
GRC-02-093	07/01/2017	Iselin Bank	670	*Inferiolabiata labiata* (Moseley, 1879)

GRC-02-133	07/01/2017	Iselin Bank	670	*Inferiolabiata labiata* (Moseley, 1879)
GRC-02-091	07/01/2017	Iselin Bank	670	*Inferiolabiata labiata* (Moseley, 1879)
GRC-07-028	31/01/2017	Hallett Ridge	910	*Inferiolabiata labiata* (Moseley, 1879)
GRC-08-002 MNA9228	03/02/2017	Cape Hallett Canyon	750	*Inferiolabiata labiata* (Moseley, 1879)
GRC-02-108	07/01/2017	Iselin Bank	670	*Inferiolabiata labiata* (Moseley, 1879)
GRC-02-121	07/01/2017	Iselin Bank	670	*Inferiolabiata labiata* (Moseley, 1879)
GRC-02-125	07/01/2017	Iselin Bank	670	*Inferiolabiata labiata* (Moseley, 1879)
GRC-02-126	07/01/2017	Iselin Bank	670	*Inferiolabiata labiata* (Moseley, 1879)
GRC-02-115	07/01/2017	Iselin Bank	670	*Inferiolabiata labiata* (Moseley, 1879)

Table s. 2: list of all identified sponge samples with additionally information.

Station	Sample	Date	Latitude	Longitude	Depth (m)	Sponge species
GRC-02-223	A	07/01/2017	72° 16.1196' S 72° 15.7728' S	176° 36.2814' W 176° 35.5638' W	670	*Polymastia invaginata* Kirkpatrick, 1907
						Clathria sp.
						Clathria (Microciona) sp.
						Clathria (Clathria) paucispicula (Burton,1932)
						Clathria (Clathria) paucispicula (Burton,1932)
						Biemna chilensis Thiele, 1905
						Indeterminate
GRC-02-223	B	07/01/2017	72° 16.1196' S 72° 15.7728' S	176° 36.2814' W 176° 35.5638' W	670	*Myxilla (Myxilla) elongata* Topsent, 1916
						Tedania (Tedaniopsis) tantula (Kirkpatrick, 1907)
GRC-02-223	C	07/01/2017	72° 16.1196' S 72° 15.7728' S	176° 36.2814' W 176° 35.5638' W	670	*Clathria (Clathria) paucispicula* (Burton,1932)
						Clathria (Clathria) paucispicula (Burton,1932)
						Clathria (Clathria) paucispicula (Burton,1932)

GRC-02-223	D	07/01/2017	72° 16.1196' S 72° 15.7728' S	176° 36.2814' W 176° 35.5638' W	670	*Rhabdocalyptus australis* Topsent, 1901
						Lissodendoryx (Ectyodoryx) sp.
						Indeterminate
GRC-02-223	E	07/01/2017	72° 16.1196' S 72° 15.7728' S	176° 36.2814' W 176° 35.5638' W	670	*Asbetopluma (Asbestopluma)* sp.
						Clathria (Clathria) paucispicula (Burton,1932)
						Indeterminate
GRC-02-223	F	07/01/2017	72° 16.1196' S 72° 15.7728' S	176° 36.2814' W 176° 35.5638' W	670	*Iophon radiatum* (Topsent, 1901)
						Iophon radiatum (Topsent, 1901)
						Iophon radiatum (Topsent, 1901)
						Indeterminate
GRC-02-223	G	07/01/2017	72° 16.1196' S 72° 15.7728' S	176° 36.2814' W 176° 35.5638' W	670	*Isodictya setifera* (Topsent, 1901)
						Iophon radiatum (Topsent, 1901)
GRC-02-223	H	07/01/2017	72° 16.1196' S 72° 15.7728' S	176° 36.2814' W 176° 35.5638' W	670	Indeterminate
GRC-02-223	I	07/01/2017	72° 16.1196' S 72° 15.7728' S	176° 36.2814' W 176° 35.5638' W	670	*Iophon radiatum* (Topsent, 1901)

GRC-02-223	L	07/01/2017	72° 16.1196' S 72° 15.7728' S	176° 36.2814' W 176° 35.5638' W	670	*Iophon radiatum* (Topsent, 1901)
						Iophon radiatum (Topsent, 1901)
						Poecillastra compressa antarctica Koltun, 1964
GRC-02-223	M	07/01/2017	72° 16.1196' S 72° 15.7728' S	176° 36.2814' W 176° 35.5638' W	670	Indeterminate
GRC-02-223	N	07/01/2017	72° 16.1196' S 72° 15.7728' S	176° 36.2814' W 176° 35.5638' W	670	*Poecillastra compressa antarctica* Koltun, 1964
						Pseudosuberites sulcatus (Thiele, 1905)
						Indeterminate
						Haliclona cf. *virens* (Topsent, 1908)
GRC-02-223	O	07/01/2017	72° 16.1196' S 72° 15.7728' S	176° 36.2814' W 176° 35.5638' W	670	*Clathria (Clathria) paucispicula* (Burton,1932)
						Lissodendoryx (Lissodendoryx) complicata (Hansen, 1885) *sensu* Boury-Esnault & Van Beveren (1982)
GRC-02-223	P	07/01/2017	72° 16.1196' S 72° 15.7728' S	176° 36.2814' W 176° 35.5638' W	670	Indeterminate

GRC-02-223	Q	07/01/2017	72° 16.1196' S 72° 15.7728' S	176° 36.2814' W 176° 35.5638' W	670	*Artemisina plumosa* Hentschel, 1914
GRC-02-223	R	07/01/2017	72° 16.1196' S 72° 15.7728' S	176° 36.2814' W 176° 35.5638' W	670	*Polymastia invaginata* Kirkpatrick, 1907
						Indeterminate
GRC-02-223	S	07/01/2017	72° 16.1196' S 72° 15.7728' S	176° 36.2814' W 176° 35.5638' W	670	*Clathria (Clathria) paucispicula* (Burton,1932)
						Haliclona cf. *virens* (Topsent, 1908)
						Haliclona sp. 1
GRC-02-223	T	07/01/2017	72° 16.1196' S 72° 15.7728' S	176° 36.2814' W 176° 35.5638' W	670	*Clathrochone* cf. *clathroclada* (Lévi & Lévi, 1982)
GRC-02-223	AG	07/01/2017	72° 16.1196' S 72° 15.7728' S	176° 36.2814' W 176° 35.5638' W	670	*Iophon radiatum* (Topsent, 1901)
GRC-02-223	AH	07/01/2017	72° 16.1196' S 72° 15.7728' S	176° 36.2814' W 176° 35.5638' W	670	*Iophon radiatum* (Topsent, 1901)
						Iophon radiatum (Topsent, 1901)
						Mycale (Anomomycale) titubans (Schmidt, 1870) *sensu* Boury-Esnault & Van Beveren (1982)
GRC-02-223	AI	07/01/2017	72° 16.1196' S 72° 15.7728' S	176° 36.2814' W 176° 35.5638' W	670	Indeterminate

GRC-02-223	AL	07/01/2017	72° 16.1196' S 72° 15.7728' S	176° 36.2814' W 176° 35.5638' W	670	*Clathria (Clathria) paucispicula* (Burton,1932)
						Inflatella belli (Kirkpatrick, 1907)
						Lissodendoryx (Ectyodoryx) nobilis (Ridley & Dendy, 1886)
GRC-02-223	AM	07/01/2017	72° 16.1196' S 72° 15.7728' S	176° 36.2814' W 176° 35.5638' W	670	*Clathrochone* cf. *clathroclada* (Lévi & Lévi, 1982)
						Haliclona cf. *virens* (Topsent, 1908)
						Myxilla (Myxilla) elongata Topsent, 1916
						Amphilectus rugosus (Thiele, 1905)
						Iophon radiatum (Topsent, 1901)
						Iophon radiatum (Topsent, 1901)
GRC-02-223	AN	07/01/2017	72° 16.1196' S 72° 15.7728' S	176° 36.2814' W 176° 35.5638' W	670	*Artemisina plumosa* Hentschel, 1914
						Indeterminate
GRC-02-223	AO	07/01/2017	72° 16.1196' S	176° 36.2814' W	670	*Esperiopsis villosa* (Carter, 1874) *sensu*

			72° 15.7728' S	176° 35.5638' W		Koltun (1964)
						Indeterminate
GRC-02-223	AP	07/01/2017	72° 16.1196' S 72° 15.7728' S	176° 36.2814' W 176° 35.5638' W	670	*Haliclona* sp. 2
						Iophon radiatum (Topsent, 1901)
GRC-02-223	AQ	07/01/2017	72° 16.1196' S 72° 15.7728' S	176° 36.2814' W 176° 35.5638' W	670	*Clathrochone* cf. *clathroclada* (Lévi & Lévi, 1982)
						Indeterminate
						Iophon radiatum (Topsent, 1901)
						Poecillastra compressa antarctica Koltun, 1964
GRC-02-223	AR	07/01/2017	72° 16.1196' S 72° 15.7728' S	176° 36.2814' W 176° 35.5638' W	670	*Iophon abnormalis* Ridley & Dendy, 1886
						Iophon abnormalis Ridley & Dendy, 1886
GRC-02-223	AS	07/01/2017	72° 16.1196' S 72° 15.7728' S	176° 36.2814' W 176° 35.5638' W	670	*Haliclona (Gellius) rudis* (Topsent, 1901)
						Ideterminate
GRC-02-223	AT	07/01/2017	72° 16.1196' S 72° 15.7728' S	176° 36.2814' W 176° 35.5638' W	670	*Iophon radiatum* (Topsent, 1901)

						Ideterminate
GRC-02-223	AU	07/01/2017	72° 16.1196' S 72° 15.7728' S	176° 36.2814' W 176° 35.5638' W	670	*Polymastia invaginata* Kirkpatrick, 1907
						Indeterminate
						Mycale (Anomomycale) titubans (Schmidt, 1870) *sensu* Boury-Esnault & Van Beveren (1982)
						Clathrochone cf. *clathroclada* (Lévi & Lévi, 1982)
GRC-02-223	AV	07/01/2017	72° 16.1196' S 72° 15.7728' S	176° 36.2814' W 176° 35.5638' W	670	Indeterminae
						Iophon radiatum (Topsent, 1901)
						Iophon radiatum (Topsent, 1901)
						Esperiopsis villosa (Carter, 1874) *sensu* Koltun (1964)
						Esperiopsis villosa (Carter, 1874) *sensu* Koltun (1964)
GRC-02-223	AZ	07/01/2017	72° 16.1196' S 72° 15.7728' S	176° 36.2814' W 176° 35.5638' W	670	Indeterminate
GRC-02-223	BA	07/01/2017	72° 16.1196' S 72° 15.7728' S	176° 36.2814' W 176° 35.5638' W	670	Indeterminate

GRC-02-223	BB	07/01/2017	72° 16.1196' S 72° 15.7728' S	176° 36.2814' W 176° 35.5638' W	670	*Iophon radiatum* (Topsent, 1901)
						Iophon radiatum (Topsent, 1901)
						Indeterminate
						Indeterminate
						Clathria (Clathria) paucispicula (Burton,1932)
GRC-02-223	BC	07/01/2017	72° 16.1196' S 72° 15.7728' S	176° 36.2814' W 176° 35.5638' W	670	*Iophon radiatum* (Topsent, 1901)
						Iophon radiatum (Topsent, 1901)
						Artemisina plumosa Hentschel, 1914
						Artemisina plumosa Hentschel, 1914
GRC-02-223	BD	07/01/2017	72° 16.1196' S 72° 15.7728' S	176° 36.2814' W 176° 35.5638' W	670	Indeterminate
GRC-02-223	BE	07/01/2017	72° 16.1196' S 72° 15.7728' S	176° 36.2814' W 176° 35.5638' W	670	Indeterminate
GRC-02-223	BF	07/01/2017	72° 16.1196' S 72° 15.7728' S	176° 36.2814' W 176° 35.5638' W	670	*Clathrochone* cf. *clathroclada* (Lévi & Lévi, 1982)
						Indeterminate
						Myxilla (Myxilla) mollis Ridley & Dendy, 1886
						Clathria (Clathria) paucispicula

						(Burton,1932)
						Rhabdocalyptus australis Topsent, 1901
						Indeterminate
						Indeterminate
						Indeterminate
GRC-02-223	BG	07/01/2017	72° 16.1196' S 72° 15.7728' S	176° 36.2814' W 176° 35.5638' W	670	Indeterminate
GRC-02-223	BH	07/01/2017	72° 16.1196' S 72° 15.7728' S	176° 36.2814' W 176° 35.5638' W	670	Indeterminate
						Indeterminate
GRC-02-223	BI	07/01/2017	72° 16.1196' S 72° 15.7728' S	176° 36.2814' W 176° 35.5638' W	670	*Iophon radiatum* (Topsent, 1901)
GRC-02-223	BL	07/01/2017	72° 16.1196' S 72° 15.7728' S	176° 36.2814' W 176° 35.5638' W	670	*Clathrochone* cf. *clathroclada* (Lévi & Lévi, 1982)
GRC-02-223	BM	07/01/2017	72° 16.1196' S 72° 15.7728' S	176° 36.2814' W 176° 35.5638' W	670	Indeterminate
						Indeterminate
GRC-02-223	BN	07/01/2017	72° 16.1196' S 72° 15.7728' S	176° 36.2814' W 176° 35.5638' W	670	Indeterminate
						Indeterminate
						Haliclona cf. *virens* (Topsent, 1908)
GRC-02-223	BO	07/01/2017	72° 16.1196' S 72° 15.7728' S	176° 36.2814' W 176° 35.5638' W	670	*Polymastia invaginata* Kirkpatrick, 1907

GRC-02-223	BP	07/01/2017	72° 16.1196' S 72° 15.7728' S	176° 36.2814' W 176° 35.5638' W	670	*Crella (Crella) tubifex* (Hentschel, 1914)
						Crella (Crella) tubifex (Hentschel, 1914)
GRC-02-223	BQ	07/01/2017	72° 16.1196' S 72° 15.7728' S	176° 36.2814' W 176° 35.5638' W	670	Indeterminate
GRC-02-223	BR	07/01/2017	72° 16.1196' S 72° 15.7728' S	176° 36.2814' W 176° 35.5638' W	670	Indeterminate
GRC-02-223	BS	07/01/2017	72° 16.1196' S 72° 15.7728' S	176° 36.2814' W 176° 35.5638' W	670	*Iophon unicorne* Topsent, 1907
GRC-02-223	BT	07/01/2017	72° 16.1196' S 72° 15.7728' S	176° 36.2814' W 176° 35.5638' W	670	*Iophon radiatum* (Topsent, 1901)
GRC-02-223	BU	07/01/2017	72° 16.1196' S 72° 15.7728' S	176° 36.2814' W 176° 35.5638' W	670	*Iophon radiatum* (Topsent, 1901)
						Indeterminate
GRC-02-223	BV	07/01/2017	72° 16.1196' S 72° 15.7728' S	176° 36.2814' W 176° 35.5638' W	670	*Lissodendoryx (Lissodendoryx) styloderma* Hentschel, 1914
						Amphilectus rugosus (Thiele, 1905)
GRC-02-223	BZ	07/01/2017	72° 16.1196' S 72° 15.7728' S	176° 36.2814' W 176° 35.5638' W	670	Indeterminate
						Indeterminate

						Plicatellopsis fragilis Koltun, 1964
GRC-02-223	CA	07/01/2017	72° 16.1196' S 72° 15.7728' S	176° 36.2814' W 176° 35.5638' W	670	Indeterminate
						Lissodendoryx (Lissodendoryx) complicata (Hansen, 1885) *sensu* Boury-Esnault & Van Beveren (1982)
GRC-02-223	CB	07/01/2017	72° 16.1196' S 72° 15.7728' S	176° 36.2814' W 176° 35.5638' W	670	*Lissodendoryx (Lissodendoryx) complicata* (Hansen, 1885) *sensu* Boury-Esnault & Van Beveren (1982)
GRC-02-223	CC	07/01/2017	72° 16.1196' S 72° 15.7728' S	176° 36.2814' W 176° 35.5638' W	670	*Haliclona (Flagellia)* cf. *flagellifera* (Ridley & Dendy, 1886)
GRC-02-223	CD	07/01/2017	72° 16.1196' S 72° 15.7728' S	176° 36.2814' W 176° 35.5638' W	670	*Clathria (Clathria) paucispicula* (Burton,1932)
GRC-02-223	CE	07/01/2017	72° 16.1196' S 72° 15.7728' S	176° 36.2814' W 176° 35.5638' W	670	*Amphilectus rugosus* (Thiele, 1905)
GRC-02-114	CF	07/01/2017	72° 16.1196' S 72° 15.7728' S	176° 36.2814' W 176° 35.5638' W	670	Indeterminate
GRC-02-046	CH	07/01/2017	72° 16.1196' S 72° 15.7728' S	176° 36.2814' W 176° 35.5638' W	670	Indeterminate
						Indeterminate
						Indeterminate

GRC-02-046	CI	07/01/2017	72° 16.1196' S 72° 15.7728' S	176° 36.2814' W 176° 35.5638' W	670	Indeterminate
GRC-08-048	CL	07/01/2017	72° 16.1196' S 72° 15.7728' S	176° 36.2814' W 176° 35.5638' W	670	*Iophon radiatum* (Topsent, 1901)
GRC-08-065	CM	03/02/2017	71° 58.8666' S 71° 59.2512' S	172° 11.6298' E 172° 10.6020' E	750	*Clathria (Clathria) paucispicula* (Burton,1932)
						Myxilla (Myxilla) mollis Ridley & Dendy, 1886
						Mycale (Anomomycale) titubans (Schmidt, 1870) *sensu* Boury-Esnault & Van Beveren (1982)
GRC-08-048	CN	07/01/2017	72° 16.1196' S 72° 15.7728' S	176° 36.2814' W 176° 35.5638' W	670	*Iophon radiatum* (Topsent, 1901)
						Iophon radiatum (Topsent, 1901)
						Indeterminate
						Indeterminate
						Clathrochone cf. *clathroclada* (Lévi & Lévi, 1982)
GRC-08-077	CO	03/02/2017	71° 58.8666' S 71° 59.2512' S	172° 11.6298' E 172° 10.6020' E	750	*Iophon radiatum* (Topsent, 1901)
						Indeterminate

GRC-TR17-007	CP	09/02/2017	\ \	\ \	1022	*Tetilla coronida* Sollas, 1888
						Indeterminate
GRC-02-113	CQ	07/01/2017	72° 16.1196' S 72° 15.7728' S	176° 36.2814' W 176° 35.5638' W	670	*Clathrochone* cf. *clathroclada* (Lévi & Lévi, 1982)
						Clathrochone cf. *clathroclada* (Lévi & Lévi, 1982)
						Iophon radiatum (Topsent, 1901)
						Iophon radiatum (Topsent, 1901)
						Iophon radiatum (Topsent, 1901)
						Indeterminate
						Tedania (Tedaniopsis) oxeata Topsent, 1916
GRC-02-092	CR	07/01/2017	72° 16.1196' S 72° 15.7728' S	176° 36.2814' W 176° 35.5638' W	670	*Clathrochone* cf. *clathroclada* (Lévi & Lévi, 1982)
						Clathrochone cf. *clathroclada* (Lévi & Lévi, 1982).
						Clathrochone cf. *clathroclada* (Lévi & Lévi, 1982).
						Indeterminate
						Iophon radiatum (Topsent, 1901)

						Indeterminate
GRC-02-093	CS	07/01/2017	72° 16.1196' S 72° 15.7728' S	176° 36.2814' W 176° 35.5638' W	670	*Clathrochone* cf. *clathroclada* (Lévi & Lévi, 1982).
						Clathrochone cf. *clathroclada* (Lévi & Lévi, 1982).
						Clathrochone cf. *clathroclada* (Lévi & Lévi, 1982).
						Iophon radiatum (Topsent, 1901)
						Indeterminate
						Indeterminate
						Indeterminate
						Indeterminate
						Clathria (Clathria) paucispicula (Burton,1932)
						Clathria (Clathria) paucispicula (Burton,1932)
						Iophon radiatum (Topsent, 1901)
						Clathrochone cf. *clathroclada* (Lévi & Lévi, 1982)
						Biemna chilensis Thiele, 1905
GRC-02-133	CT	07/01/2017	72° 16.1196' S 72° 15.7728' S	176° 36.2814' W 176° 35.5638' W	670	*Clathria (Clathria) paucispicula* (Burton,1932)

						Polymastia invaginata Kirkpatrick, 1907
						Clathria (Clathria) paucispicula (Burton,1932)
GRC-02-091	CU	07/01/2017	72° 16.1196' S 72° 15.7728' S	176° 36.2814' W 176° 35.5638' W	670	*Clathria (Clathria) paucispicula* (Burton,1932)
						Clathrochone cf. *clathroclada* (Lévi & Lévi, 1982)
						Clathrochone cf. *clathroclada* (Lévi & Lévi, 1982)
						Clathrochone cf. *clathroclada* (Lévi & Lévi, 1982)
						Clathrochone cf. *clathroclada* (Lévi & Lévi, 1982)
						Clathrochone cf. *clathroclada* (Lévi & Lévi, 1982)
						Haliclona cf. *virens* (Topsent, 1908)
						Polymastia invaginata Kirkpatrick, 1907
						Tedania (Tedaniopsis) tantula (Kirkpatrick, 1907)

						Indeterminate
GRC-07-028	CV	31/01/2017	72° 23.0340' S 72° 23.3868' S	176° 06.1020' E 176° 06.2094' E	910	*Clathrochone* cf. *clathroclada* (Lévi & Lévi, 1982)
						Clathrochone cf. *clathroclada* (Lévi & Lévi, 1982)
						Clathrochone cf. *clathroclada* (Lévi & Lévi, 1982)
						Myxilla (Myxilla) mollis Ridley & Dendy, 1886
						Myxilla (Myxilla) mollis Ridley & Dendy, 1886
						Iophon radiatum (Topsent, 1901)
						Iophon radiatum (Topsent, 1901)
						Iophon radiatum (Topsent, 1901)
						Iophon radiatum (Topsent, 1901)
						Iophon radiatum (Topsent, 1901)
						Iophon radiatum (Topsent, 1901)
						Iophon radiatum (Topsent, 1901)
						Artemisina plumosa Hentschel, 1914

						Myxilla (Myxilla) mollis Ridley & Dendy, 1886
						Haliclona sp. 1
						Clathria (Microciona) sp. 2
						Clathria (Microciona) sp. 1
						Haliclona sp. 1
						Halichondria (Halichondria) cristata Sarà, 1978
GRC-08-023	CW	03/02/2017	71° 58.8666' S 71° 59.2512' S	172° 11.6298' E 172° 10.6020' E	750	*Iophon radiatum* (Topsent, 1901)
						Iophon radiatum (Topsent, 1901)
GRC-08-023	CX	03/02/2017	71° 58.8666' S 71° 59.2512' S	172° 11.6298' E 172° 10.6020' E	750	*Lissodendoryx (Lissodendoryx) styloderma* Hentschel, 1914
GRC-08-023	CY	03/02/2017	71° 58.8666' S 71° 59.2512' S	172° 11.6298' E 172° 10.6020' E	750	Indeterminate
						Myxilla (Myxilla) elongata Topsent, 1916
GRC-08-023	CZ	03/02/2017	71° 58.8666' S 71° 59.2512' S	172° 11.6298' E 172° 10.6020' E	750	*Iophon radiatum* (Topsent, 1901)
						Myxilla (Myxilla) mollis Ridley & Dendy, 1886
						Indeterminate

GRC-08-023	DA	03/02/2017	71° 58.8666' S 71° 59.2512' S	172° 11.6298' E 172° 10.6020' E	750	*Myxilla (Myxilla) mollis* Ridley & Dendy, 1886
						Indeterminate
						Halichondria (Halichondria) prostrata Thiele, 1905
GRC-08-023	DB	03/02/2017	71° 58.8666' S 71° 59.2512' S	172° 11.6298' E 172° 10.6020' E	750	Indeterminate
						Iophon radiatum (Topsent, 1901)
GRC-08-023	DC	03/02/2017	71° 58.8666' S 71° 59.2512' S	172° 11.6298' E 172° 10.6020' E	750	*Iophon unicorne* Topsent, 1907
GRC-08-023	DD	03/02/2017	71° 58.8666' S 71° 59.2512' S	172° 11.6298' E 172° 10.6020' E	750	*Iophon radiatum* (Topsent, 1901)
GRC-08-023	DD	03/02/2017	71° 58.8666' S 71° 59.2512' S	172° 11.6298' E 172° 10.6020' E	750	*Haliclona (Gellius) rudis* (Topsent, 1901)
						Haliclona (Gellius) rudis (Topsent, 1901)